

THE MU TRANSPOSONS OF ZEA MAYS AND THEIR USE IN DETERMINING
GENE FUNCTION: CELLULOSE SYNTHASE-LIKE D GENES IN
PLANT AND CELL DEVELOPMENT

By

CHARLES THOMAS HUNTER III

A DISSERTATION PRESENTED TO THE GRADUATE SCHOOL
OF THE UNIVERSITY OF FLORIDA IN PARTIAL FULFILLMENT
OF THE REQUIREMENTS FOR THE DEGREE OF
DOCTOR OF PHILOSOPHY

UNIVERSITY OF FLORIDA

2010

© 2010 Charles Thomas Hunter III

To my beautiful wife, Maggie, for her always-appreciated love, support, kindness and fascinating dinner-time conversations!

ACKNOWLEDGMENTS

I wholeheartedly thank my lab colleagues, past and present, for advice and friendship, especially Wayne Avigne, Brent O'Brien, Andrea Eveland, Li-Fen Huang, Christian Restrepo, Joe Collins, Maggie Paxson, Emeka Ibekwe, and Nana Ankumah. Additionally, I thank the founders of the UniformMu maize population, including Don McCarty, Karen Koch, Mark Settles, and Curt Hannah. I thank the members of my committee, which included John Davis, Don Huber, Karen Koch, Don McCarty, Gary Peter, and Wilfred Vermerris, all of whom have provided much-appreciated input and advice. I also acknowledge and thank the faculty and staff of the University of Florida Interdisciplinary Center for Biotechnology Research (ICBR), including Byung-Ho Kang, Bill Farmerie, Karen Kelley, Kim Backer-Kelley, Neal Benson, David Moraga, and Savita Shankir. My fullest appreciation also goes out to my co-authors, including Gary Peter, Don McCarty, and Anne Sylvester, with whom I look forward to continued collaborations. I acknowledge and thank Bob Meeley for providing access to the Pioneer Trait Utility System in Corn (TUSC) maize population, as well as a wonderful opportunity to experience working at Pioneer Hi-Bred International. I call special recognition to work done cooperatively with Christian Restrepo and Christy Gault, who contributed greatly to the characterizations of Mu transposons presented here. I acknowledge Sue Latshaw, Andrea Eveland, and Christain Restrepo for their invaluable help in developing and assisting in the 454-based sequencing experiments conducted in this work. I express my deepest appreciation for my family, who have always given me their love and support, including my parents, Ruthie, Charlie, Shannon, and Wayne, my brother and his wife, David and Keri Anne, and my wonderful bride, Maggie. Finally, I

want to thank my advisor, Karen Koch, for years of encouragement and motivation, and for being an excellent scientific mentor.

TABLE OF CONTENTS

	<u>page</u>
ACKNOWLEDGMENTS.....	4
LIST OF TABLES.....	9
LIST OF FIGURES.....	10
ABSTRACT	12
CHAPTER	
1 INTRODUCTION	14
2 IDENTIFICATION AND CHARACTERIZATION OF THE MU TRANSPOSONS IN VARIOUS MAIZE INBREDS AND THEIR TEOSINTE ANCESTORS	19
Introduction	19
Results.....	25
Mu Insertions Identified Bioinformatically in the B73 Genome.....	25
Phylogenetic Relationships between the B73 Mu Transposons.....	26
The B73 Inbred Contains some MuDR-like Sequences	26
Mu-anchored Sequencing to Identify Mu Insert Locations in Maize and Teosinte Inbreds	27
Comparative Analysis of Mu Elements and Insert Sites in Maize and Teosinte	29
Discussion	29
Bioinformatic Analysis of B73 Reveals Diversity	29
Homomorphic Versus Heteromorphic Mu Elements.....	31
Some Mu10 Elements Have Full-length Putative Transposase Sequences....	33
Relationships Between Zea Inbreds are Highlighted by Mu Element Mapping	34
Methods.....	36
Bioinformatic Identification of Mu Elements in the B73 Maize Genome	36
Phylogenetic Analysis of B73 Mu-TIRs	37
Mu-flank-anchored 454 Library Construction.....	37
Sequence Annotation and Alignment	40
Accession Numbers	41
3 ANALYSIS OF THE CELLULOSE SYNTHASE-LIKE D GENE FAMILY IN MAIZE.....	54
Introduction	54
Results.....	57
Bioinformatic Analyses of the Cs/D Genes from Maize, Rice, and Arabidopsis	57

Expression Profiles of the Maize <i>Cs/D</i> Genes	61
Reverse Genetic Screens for <i>cs/d</i> Mutants	62
Analysis of <i>cs/d5</i> Mutants	63
Root-hair Transcriptome Profiling	63
Discussion	64
The <i>CSLD</i> Genes are Highly-conserved Among Diverse Species	64
Conservation of Developmental Roles are Indicated by Phenotypic Similarities Across Taxa	65
Specificity of Expression Argues for Strictly-defined Roles for <i>Cs/D</i> Genes	66
Functional <i>Cs/D5</i> is Required for Maize Root-hair Elongation	67
Methods	70
Bioinformatic Analyses of <i>Cs/D</i> Genes from Maize, Rice, and Arabidopsis	70
Phylogenetic Analyses	70
Real-Time RT-PCR	71
Reverse Genetic Screening	72
Growth Conditions for <i>cs/d5</i> Mutant Analyses	72
Fixation and Sectioning	72
Scanning Electron Microscopy	73
Isolation of Root Hair mRNA	74
Three-prime Anchored 454 Sequencing	75
Analysis of 454-generated Sequence Data	76
Accession Numbers	76
4 MUTATIONS OF <i>CELLULOSE SYNTHASE-LIKE D1</i> DISRUPT CELL DIVISION AND LEAD TO A <i>NARROW-LEAF WARTY</i> PHENOTYPE IN MAIZE ...	85
Introduction	85
Results	87
An Allelic Series of <i>cs/d1</i> Mutants in Maize Enabled Functional Analysis	87
Plant Dry Weight and Organ Width are Reduced in <i>cs/d1</i> Mutants	87
Epidermal Cells Balloon into Warts on <i>cs/d1</i> Mutants	88
Cells of <i>cs/d1</i> Mutant Leaves are Larger, but Fewer in Number	89
Stalks of <i>cs/d1</i> Mutants Contain Altered Vascular Bundle Number and Cell Wall Properties	91
Cell Wall Sugar Components were not Detectably Altered by Loss of <i>Cs/D1</i> Function	91
Levels of Maize <i>Cs/D1</i> mRNA are Greatest in Regions of Active Cell Division	92
Multiple Cell Division Defects are Evident in <i>cs/d1</i> mutant Epidermis.	93
Discussion	94
The <i>CSLD1</i> Enzyme Appears to Affect a Mechanism Other than Tip-growth ..	94
The Maize <i>Cs/D1</i> Gene is Essential for Normal Plant Dry Weight and Organ Width	95
Warty Cells Represent Distinctive and Informative Features of Maize <i>cs/d1</i> Mutants	96
Larger, Non-warty Epidermal Cells Suggest a Limitation in Cell Division	97

Cell Walls of the <i>csld1</i> Mutant are Thinner and More Dense, but of Normal Composition	97
Maize <i>Cs/D1</i> has a Role in Plant Cell Division	99
Broader Perspectives	101
Methods	103
Identification of <i>csld1</i> Mutants	103
Overall Phenotypic Analyses and Size Measurements	104
Cell Volume Estimates	105
Epidermal Impressions and Non-warty Cell Size Determination	105
Tissue Fixation and Sectioning.....	105
Scanning Electron Microscopy	106
Phloroglucinol Staining and Stalk Measurements	107
High-resolution X-ray Micro Computed Tomography Analysis	107
Epidermal Isolation.....	108
Cell Wall Composition Analysis.....	108
Real Time Quantitative RT-PCR	109
Propidium Iodide Staining.....	110
Flow Cytometry	110
 5 CONCLUSIONS AND FUTURE DIRECTIONS	 128
APPENDIX	131
LIST OF REFERENCES	168
BIOGRAPHICAL SKETCH.....	181

LIST OF TABLES

<u>Table</u>		<u>page</u>
2-1	Bioinformatically-identified Mu elements in B73	42
2-2	Classification of canonical B73 Mu insertions.....	43
2-3	Mu elements identified by Mu-flank sequencing in three maize inbreds.....	44
2-4	Mu elements identified by Mu-flank sequencing in five teosinte inbreds	45
2-5	Primers used for 454-based Mu-flank sequencing.	46
3-1	Three prime-anchored 454-sequencing transcript profiles.	77
3-2	PCR primers utilized in Chapter 3.	77
4-1	Cell wall composition of whole-leaf blades and epidermal peels from <i>csld1</i> mutant and non-mutant plants.	112

LIST OF FIGURES

<u>Figure</u>	<u>page</u>
2-1 Example of a sequential mining track of the B73 genome.....	47
2-2 Neighbor-joining tree of 299 B73 Mu Terminal Inverted Repeats.....	48
2-3 Comparison between MuDR and a Mu10 (Mu4K) element from the B73 maize inbred.....	49
2-4 Estimated proportions of each Mu class in three maize inbreds and teosinte derived from the Balsas and Jalisco regions of Mexico.....	50
2-5 Approximate map sites for Mu insertions in three maize inbreds.....	51
2-6 Approximate map sites for Mu insertions in five teosinte inbreds.....	52
2-7 Diagrammatic representation of Mu-flank 454-sequencing library preparation.....	53
3-1 <i>Cellulose synthase-like D (CslD)</i> genes from Arabidopsis, maize, and rice.....	78
3-2 Cellulose synthase-like D proteins from Arabidopsis, maize, and rice.....	79
3-3 Protein sequence alignment and analysis of conserved motifs.....	80
3-4 Comparison of mutant phenotypes to CSLD protein phylogeny.....	81
3-5 Quantitative RT-PCR showing mRNA levels of the maize <i>CslD</i> genes.....	82
3-6 The root hair phenotype caused by mutation of <i>CslD5</i>	83
3-7 Transcript profiles of maize root hairs.....	84
4-1 Gene diagram of <i>Zm-CslD1</i> and location of each of the Mu insertions identified.....	113
4-2 Morphology and dry weight of the <i>cslD1-1</i> mutant.....	114
4-3 The narrow-leaf phenotype of <i>cslD1-1</i> mutant plants.....	115
4-4 Leaf blade curling in <i>cslD1</i> mutants.....	116
4-5 The warty phenotype of <i>cslD1</i> mutant leaf blades.....	117
4-6 SEM of <i>cslD1</i> mutant and wildtype leaves.....	118
4-7 Size estimates for epidermal cells of inter-lesion regions on <i>cslD1</i> mutant and non-mutant leaf blades.....	119

4-8	Internal structure of <i>csld1</i> mutant and non-mutant leaf blades.....	120
4-9	Internal structure of <i>csld1</i> mutant and non-mutant stems.....	121
4-10	High-resolution X-ray micro computed tomography analysis of <i>csld1</i> and wildtype stalks	122
4-11	Levels of Zm- <i>CsID1</i> mRNA in diverse tissues from wildtype plants of the W22 inbred.	123
4-12	Mature <i>csld1</i> mutant and non-mutant epidermis revealed apparent defects in cell division.	124
4-13	Confocal images showing defects early in development of <i>csld1</i> mutant leaf epidermis.....	125
4-14	Nuclei of immature <i>csld1</i> mutant and non-mutant epidermis.....	126
4-15	Isolation of maize leaf epidermis	127

Abstract of Dissertation Presented to the Graduate School
of the University of Florida in Partial Fulfillment of the
Requirements for the Degree of Doctor of Philosophy

THE MU TRANSPOSONS OF ZEA MAYS AND THEIR USE IN DETERMINING
GENE FUNCTION: CELLULOSE SYNTHASE-LIKE D GENES IN
PLANT AND CELL DEVELOPMENT

By

Charles Thomas Hunter III

December 2010

Chair: Karen Koch

Major: Plant Molecular and Cellular Biology

The two-fold goal of work presented here was, first, to test hypotheses for biological roles of the enigmatic *Cellulose Synthase-Like D (CslD)* gene family, and second, to test key aspects of a global resource for such research by examining the extent, diversity, and evolution of the maize Mutator (Mu) transposable elements. The Mu transposons comprise one of the most active mutagenic systems in plant biology, often inserting into genic regions, where they disrupt gene function. Not only is the Mu system a powerful evolutionary force, but also a valuable tool for defining biological roles of genes. Work here reveals new aspects of Mu transposon evolution and behavior by defining positions and relatedness of Mu elements in inbreds of both maize and its wild ancestor, teosinte. Results also demonstrate the diversity within both maize and teosinte, and will aid interpretations of future genetic studies. The surprisingly diverse and numerous Mu12-like elements identified here will also aid expansion of maize functional genetic resources such as that of the UniformMu maize population, used here to investigate the *CslD* gene family of maize. The *CslD* genes comprise one

of the few subfamilies of the Cellulose Synthase superfamily for which biochemical activity remains unclear. The CSLD proteins have domains characteristic of β -linked, cell-wall polysaccharide synthases, and are expected to produce a cell-wall structural component such as cellulose or a hemicellulose backbone. Plants with Mu transposon insertions in *CsID5* were deficient in root hair elongation, indicating a role in tip-growing cells. Plants with insertions in *CsID1* had pleiotropic phenotypes that arose from defective cell division during leaf development. This was evident in fewer cells per leaf and defects in cell size and shape at the earliest stages of leaf development. Cell files were disrupted, cell shapes and sizes were abnormal, and cross-walls between newly-divided cells were incomplete. Collectively, these data define a previously unexpected role for a cell-wall biosynthetic gene, *CsID1*, in cell division, where its contribution involves some aspect of cell plate formation, a process fundamental to all of plant biology.

CHAPTER 1 INTRODUCTION

Cell walls provide protection and structural support for whole plants and individual cells. It is through the modification and biosynthesis of cell walls that plant cells grow and their ultimate shapes are determined. Cell walls are also critically important for many aspects of human life, from nutrition to raw materials and industrial feedstocks. They represent the most abundant renewable resource on the planet (Pauly and Keegstra, 2008), and have received much recent attention as sources of transportation fuel in the form of cellulosic ethanol (reviewed by Schubert, 2006 and Sticklen, 2008). Despite their central importance to plant biology and human needs, the manner in which plant cell walls are synthesized and regulated remains poorly understood.

In all plant cell walls, cellulose is the major load-bearing molecule. It is composed of linear β -(1,4)-linked D-glucan chains, and is produced at the plasma membrane via multi-subunit protein complexes called rosettes (Kimura et al., 1999; Delmer, 1999). Within rosettes, Cellulose Synthase (CESA) proteins operate as processive glycosyl transferases that catalyze formation of individual cellulose glucan chains (Pear et al., 1996; Arioli et al., 1998). Collective action of CESA proteins as subunits of multi-protein complexes (rosettes) result in large multi-chain cellulose microfibrils. These cellulose microfibrils are embedded in a matrix of crosslinking hemicelluloses (non-cellulosic polysaccharides composed of diverse other sugars), pectins, and cell-wall proteins (McCann et al., 1990; Carpita and Gibeaut, 1993; McCann and Roberts, 1994; Willats et al., 2001).

Hemicelluloses include the glucans, xylans, and mannans. The various forms of these polysaccharides are made up of at least fourteen different monosaccharides

joined by diverse glycosidic bonds (Scheible and Pauly, 2004). Hemicelluloses are typically highly substituted with various sugar sidechains, potentially associated with a multitude of biological functions yet to be identified (Coutinho et al, 2003). Assembly of these hemicelluloses requires a massive host of enzymes (Sheible and Pauly, 2004; Coutinho et al., 2003). Resulting structures indicate that any of them could interact with cellulose via non-covalent bonds, and they are thus considered likely modulators of cell wall structural properties (Carpita, 1996; Cosgrove, 2005). Hemicelluloses are normally produced in the Golgi apparatus (Delmer and Stone, 1988). In addition to their potential roles in moderating cell wall properties and growth dynamics, hemicelluloses can also serve as energy storage molecules, and commonly do so in developing seeds of diverse species. For example, nasturtium seeds store xyloglucan (Edwards et al., 1985), and galactomannans are common in legume seeds like guar and fenugreek (Reid, 1993; Dhugga et al., 2004). Finally, hemicelluloses, or fragments derived from them, can play major roles in intercellular signaling and in regulating responses to external stimuli (McDougall and Fry, 1990; Takeda et al., 2002; Pilling and Höfte, 2003).

Cell wall composition can vary markedly among plant species and between different tissues in a single plant (Popper and Fry, 2003; Lynch and Staehelin, 1995). One major taxonomic division within flowering plants lies between the commelenoid monocots (including maize, other grasses, bromeliads, and gingers), and non-commelonoid monocots (lilies, orchids, and most others). Commelenoids have a distinctive Type II cell wall, whereas other flowering plants have Type I cell walls (Harris and Hartley, 1980; Carpita and Gibeaut, 1993). This difference is characterized by major qualitative contrasts between the two types of primary cell wall (Carpita, 1996). In

Type I cell walls, the major polymer that interlinks cellulose microfibrils is xyloglucan (Hayashi et al., 1989; Redgwell and Selvendran, 1986), whereas in Type II cell walls, this role is filled by feruloylated glucuronoarabinoxylans (GAX) (Gubler et al., 1985; Carpita, 1996). Also, the Type I cell walls of cereals and other grasses (poaceae) contain abundant (1,3),(1,4) mixed-linkage β -D-glucans (Carpita, 1996; Smith and Harris, 1999), hypothesized to aid wall loosening during cell elongation by interacting with, and influencing properties of GAX molecules (Buckeridge et al., 2004). In addition, Type I cell-wall structure includes diverse and abundant pectins (Jarvis et al., 1988; Jarvis, 1994), compared to Type II cell walls, which instead, feature prominent phenolics such as hydroxycinnamates (Harris and Hartley, 1980; Iiyama et al., 1990; Rudall and Caddick, 1994).

Major qualitative differences in cell wall composition are also commonly observed between even closely related plant species. For instance, the relative proportions of cellulose, hemicelluloses, and lignin differ dramatically between rice straw and wheat straw (Lynd et al., 1999; Jin and Chen, 2007; Pauly and Keegstra, 2008). Additionally, cell wall composition can change radically during growth of individual tissues. In maize coleoptiles, for example, mixed-linkage glucans can accumulate to high levels during elongation (up to a third of total hemicelluloses), then drop to less than detectable quantities as the tissue matures (Meier and Reid, 1982; Carpita, 1984; Gibeaut and Carpita, 1993; Kim et al., 2000; Carpita et al., 2001; Derbyshire et al., 2007). Indeed, wall composition can vary around a single cell, such as in trichoblasts in *Arabidopsis* roots, where distinct cell-wall microdomains lead to specific areas with unique properties (Freshour et al., 1996). The wide range of plant cell wall compositions, growth-rates,

and chemical properties reveal the complex and highly-regulated nature of their biosynthesis (Zhong and Ye, 2007). With major differences between diverse cell walls, more than a single model species will be needed to fully elucidate the biosynthesis and function of this important plant cell component.

In addition to its position as one of the world's most agriculturally-important crop species, maize provides an excellent model species for genetic studies. Its genome is essentially diploid, its generation time is relatively short, the male and female flowers are easily isolated, and the large seeds are amenable to long-term storage. The amount of diversity represented within the various maize lines is extensive, and has been instrumental to developing the productivity and versatility of modern domesticated varieties (Duvick, 2002; Wei et al., 2007; Gore et al., 2009; Springer et al., 2009; Schnable et al., 2009). Despite the large size of its genome (approximately 2.3 gigabases with over 32,000 genes [Schnable et al., 2009]), genetic studies in maize have proven successful (McCarty et al., 1989; McCarty et al., 2005; McCarty and Meeley, 2009). The availability of numerous genetic resources, including the large Activator populations (Kolkman et al., 2005; Bai et al., 2007), the TILLING project (Targeting Induced Local Lesions IN Genomes) (Weil and Monde, 2007), the mapped recombinant inbred lines like the Intermated B73 x Mo17 (IBM) population (Lee et al., 2002), the Nested Association Mapping (NAM) lines (Yu et al., 2008), and various Mutator-based insertional mutation collections (see below), make maize an attractive species for genetic studies and a good candidate for a model species in the economically-important grasses.

Transposon mutagenesis in maize has been an invaluable tool for elucidating gene function, allowing roles for genes of interest to be examined individually in loss-of-function mutants (Walbot, 2000; Carpita and McCann, 2002; Brutnell, 2002; McCarty et al., 2005; Settles et al., 2007). Transposable elements (TEs) are DNA sequences that can physically change positions within the genome, or replicate themselves (and other TEs), generating copies for insertion elsewhere (Chandler, 1992). All together, transposon-derived sequences make up a large portion of most eukaryotic genomes, comprising about 85% of the maize genome (Schnable et al., 2009). Transposable elements are also a major driving force of genome restructuring and evolution (Wessler, 2001). When a TE inserts into or near a region of DNA that codes for an RNA, the sequence disruption typically (but not always) leads to loss of that RNA's function (Chandler, 1992), allowing researchers to elucidate gene functions by observing plants in which single gene disruptions have occurred (Brutnell, 2002). Transposon mutagenesis provides an avenue for dissecting complex and poorly-understood biological processes, such as the biosynthesis and regulation of plant cell walls, on a gene-by-gene basis.

CHAPTER 2 IDENTIFICATION AND CHARACTERIZATION OF THE MU TRANSPOSONS IN VARIOUS MAIZE INBREDS AND THEIR TEOSINTE ANCESTORS

Introduction

Transposons were discovered in the 1940s by Barbara McClintock, who's studies in maize first defined the concept of small genetic "elements" that could physically move (or transpose) within a genome (McClintock, 1947). These transposons could excise from one location and re-insert essentially anywhere in the DNA of an organism, leading to them being coined 'jumping genes' by the popular press. Transposons can also replicate during transposition and often lead to natural mutations when they insert into otherwise functional genes.

Following discovery of transposons, the Robertson's Mutator (Mu) transposable elements were identified as a particularly interesting system with high transposition rates that often led to unstable mutations (Robertson, 1978). Since then, Mu elements have become perhaps the most widely-utilized tool for genetic studies in maize (McCarty et al., 1989; McCarty et al., 2005; Settles et al., 2007). These elements make up a large, diverse family, characterized by highly-conserved, terminal inverted repeat (TIR) sequences about 215 nucleotides long, positioned at each termini and oriented in opposite directions (Brutnell, 2002). The TIR sequences are critical for transposon functionality, as they contain the binding sites for the transposase enzyme that catalyzes transposition (Raizada and Walbot, 2000; Lisch, 2002). When a Mu transposon inserts into a given site, a 9-bp target-site duplication (TSD) occurs, and when a Mu excises, it typically leaves this 9-bp TSD "footprint" (Barker et al., 1984; Schnable et al., 1989; Creese et al., 1995).

The transposase enzyme is coded for by genes contained in the autonomous Mu element in maize, MuDR, which, in addition to its TIRs, contains two genes, *mudrA* and *mudrB*, which code for enzymes MURA and MURB, thought to function together as a transposase (Chomet et al., 1991; Lisch, 2002). This transposase is considered to be responsible for the transposition of both autonomous and nonautonomous Mu elements. Nonautonomous Mu elements typically far outnumber autonomous ones (Dietrich et al., 2002; Liu et al., 2009). Nonautonomous elements contain conserved TIRs, but their internal sequences are typically highly diverse, non-functional fragments, apparently derived from captured host sequences (Lisch, 2002). The wide variety of Mu elements in maize have been grouped into 12 classes (Mu1 through Mu12) based on order of discovery and sequence similarity (Dietrich et al., 2002). The class originally designated as Mu9 is now known to include the autonomous MuDR element with its functional transposase-encoding genes (Hershberger et al., 1991; Walbot and Rudenko, 2002;). Previous data indicated that Mu's 1-9 represented the majority of transposition activity (Dietrich et al., 2002; Liu et al., 2009), and these have classically been used in transposon-tagging studies. The Mu1-9 classes also all have similar enough TIR sequences to be amenable to a single set of molecular tools (such as PCR primers), unlike the Mu10 and Mu12 classes.

The numbers and locations of Mu elements can vary widely among maize lines, changing with MuDR activity and genetic background. However, previous estimates have suggested around 50-100 Mu elements in stable maize inbreds (Liu et al., 2009). Mu elements have a high rate of forward mutation when an active MuDR is present, and commonly occur in very high copy numbers in those lines (Brutnell, 2002). Indeed, the

Mu transposons are the most active of all DNA transposons currently known in plants (Alleman and Freeling, 1986; Lisch, 2002). Mu transposons exhibit a trans-genetic mode of action (Lisch et al., 1995; Settles et al., 2004), unlike other TEs (such as the Ac/Ds system) which show tendencies for transposition into linked site (Brutnell, 2002). Mutator elements do, however, preferentially insert into genic sequences (Cresse et al., 1995; Fernandes et al., 2004; Settles et al., 2004; Liu et al., 2009; Vollbrecht et al., 2010), and typically into 5'-regions of genes (Dietrich et al., 2002; Liu et al., 2009). The prevalence of inserts in these targets increases the likelihood of loss-of-function mutations. Mutator transposons reportedly also show some degree of sequence-dependent preference for insertion sites (Cresse et al., 1995; Dietrich et al., 2002), although these elements are generally regarded as having the potential to insert anywhere in the genome, regardless of their starting positions.

These characteristics make Mu transposons ideal for genetic resources aimed at identifying a broad array of unique insertion sites. Several large-scale mutagenesis programs have successfully employed Mutator to identify transposon-induced mutations in genes of maize. The most prominent include the Trait Utility System in Corn (TUSC) program developed at Pioneer Hi-Bred International, Inc (Bensen et al., 1995; Meeley and Briggs, 1995; McCarty and Meeley, 2009), the Maize Targeted Mutagenesis (MTM) effort, at Cold Spring Harbor Laboratories (May et al., 2003; Slotkin et al., 2003), the RescueMu resource developed at Stanford University (Walbot, 2000; Raizada et al., 2001), and the UniformMu population developed at the University of Florida (Yong et al., 2005; McCarty et al., 2005; Settles et al., 2007).

The UniformMu population (University of Florida) was generated by introgressing a Mutator-active line (Robertson's Mutator with active MuDRs and a *bronze1-mutable* [*bz1-mum9*] color marker) into the isogenic, W22 inbred line (McCarty et al., 2005). Presence of the *bz1-mum9* gene results in a spotted aleurone for MuDR-active seeds, providing an easily selectable marker for MuDR activity (Chomet et al., 1991). Repeated backcrosses of UniformMu plants to their W22, wildtype parents allows the population to be maintained with a highly uniform background and a steady mutation frequency. This strategy also prevents build-up of parental Mu insertions to an undesirable level and helps assure that new mutations comprise a significant portion of the total Mu inserts in each generation (McCarty et al., 2005). A database of detailed pedigrees for thousands of lines also allows researchers to trace the ancestry of families of interest. Together, these result in the UniformMu population being ideal for genetic studies, with i) a high and steady transposition rate, ii) a relatively low number of mutations per line, iii) a uniform background for phenotypic comparisons, iv) a traceable pedigree for each plant, and v) an easily selectable marker for MuDR activity. Nonheritable, somatic transpositions are avoided by exclusively selecting stable, non-mutagenic seeds that lack an active MuDR transposase. These "Mu-off" kernels are identified by their bronze kernels not displaying a spotted aleurone and are used in reverse genetic projects.

Release of the maize genome (B73 inbred) (Schnable et al., 2009), allowed the use of the highly-conserved TIR sequences from Mu elements to be identified bioinformatically (reported here). Additionally, PCR primers were designed that anneal to the highly-conserved TIR sequences and extend outward from either end of a given

Mu element. This approach has previously been widely successful in identifying gene mutation sites via either forward genetic screens (using non-specific, degenerate primers) (Settles et al., 2004), or reverse genetic screens (using gene-specific primers) (Bensen et al., 1995; Meeley and Briggs, 1995; Penning et al., 2009; McCarty and Meeley, 2009). More recently, sequencing approaches have become feasible, with the advent of cost-effective, high-throughput sequencing technologies (from 454 [Margulies et al., 2005], to Illumina [www.illumina.com] and Solid [Smith et al., 2010]).

Transposon insertion sites can be sequenced (again using TIR-specific and random primers) in large numbers of mutants from mutagenic populations such as UniformMu (McCarty et al., 2005). It is now possible, by taking advantage of the properties and behavior of Mu transposons, to generate resources comparable to the highly-successful, T-DNA insertional mutant lines for Arabidopsis. The latter have provided an invaluable resource for genetic and functional analyses in that model species (Alonso et al., 2003).

Domestication of maize began approximately 10,000 years ago, and began the divergence of this crop species from its wild ancestor, teosinte (reviewed by Doebley, 2004). Data indicate that the origin of current-day maize traces back to a South-Central region of Mexico, the Balsas River region, home of the *parviglumis* subspecies of teosinte (Matsuoka et al., 2002; Fukunaga et al., 2005). Doebley and coworkers (Iowa State University), have isolated varieties of *teosinte parviglumis* from both Balsas and Jalisco regions and used these to generate a number of teosinte inbred lines (TIL). Five of them, designated TIL-1, TIL-11, TIL-14, TIL-15, and TIL-17 have been used in the

present study. The TIL-1, TIL-15, and TIL-17 inbreds originated from the Balsas region, whereas TIL-11 and TIL-14 originated from the Jalisco region.

Maize breeders have developed elite inbreds as powerful tools to create commercial hybrids based on maximal “combining ability” of the parents. The resulting heterosis, or hybrid vigor, is fundamental to the yield potential achieved for maize, and for the uniformity within crop stands (reviewed by Lippman and Zamir, 2007; Springer and Stupar, 2007). Maize inbreds have thus been widely studied from applied to basic levels, with classic lines including B73 (Iowa), Mo17 (Missouri), and W22 (Wisconsin).

By indentifying the Mu transposons from various maize inbreds, differences between the inbreds can be highlighted, as well as their relatedness to one another. The contribution of Mu transposons to diversity between maize inbreds and between maize and teosinte has potential to be large given their elevated activity in some lines, their high affinity for genic sequences, their capacity for gene disruption, and their abundance. Here, the location and classification of the majority of Mu transposons in B73, W22, Mo17, as well as five inbred teosinte lines, derived from two distinct regions of Mexico, are reported. In addition to the most commonly-studied “canonical” Mu elements (Mu1-Mu9), the Mu10, Mu11, and Mu12 elements have been identified and mapped to the B73 reference genome. Interestingly, Mu12-like elements comprised the majority of all Mu elements, and represent a diverse family of Mu transposons with a previously-unrecognized variability and abundance in diverse maize and teosinte inbreds.

The original convention of classifying Mu elements as Mu1-Mu12 based on sequence identity has become challenging in the face of the extensive diversity among

Mu elements identified in the B73 genome. Full-length sequences of the 179 Mu elements identified here showed that the most of them did not match any of the previously-described Mu classes, especially when considering the Mu10, Mu11, and Mu12 groups. We suggest here, based on abundance and diversity of internal sequence for these elements, that the Mu10s, Mu11s, and Mu12s each comprise entire classes of elements separate from the Mu1-9 group. These analyses thus allow Mu elements to be grouped into one of four Mu subfamilies based on their distinct TIR sequences. The “canonical” Mu’s include Mu1-Mu9 (and others with highly-similar TIR sequences), the Mu10 and Mu12 groups refer to elements with TIR sequences most closely matching the previously-described Mu10 and Mu12 TIRs reported by Dietrich et al.(2002), and the Mu11 group includes inserts with one TIR being similar Mu10 and the other TIR being similar to the canonicals.

Results

Mu Insertions Identified Bioinformatically in the B73 Genome

To explore and capture the diverse sequences of Mu transposons in the B73 inbred, its genome (version 2, release 4a.53) (maizesequence.org) was examined via sequential BLAST analyses using the terminal 150 bp of TIR sequences, first from previously-identified Mu elements, then using the most divergent Mu sequences obtained from prior analyses (Fig. 2-1). Each new TIR identified this way was used to build a Mu-TIR database that included genome location and Mu sequence, and which was used to select the most divergent TIRs as queries for each additional BLAST analysis. Novel TIR sequences continued to be identified until searches yielded no unique results. Using this approach, 300 TIR sequences were identified in the B73 genome, corresponding to 179 unique Mu insertions (Table 1). Of these, 25 were

canonical Mu's (Mu1-Mu9), 17 were classified as Mu10's, 10 were classified as Mu11's, and 127 were classified as Mu12's (Table 1). Two distinct, oppositely-oriented TIRs were identified for only 76.25% of these elements, suggesting either the degradation of TIR sequence through mutation (and thus some TIRs not being recognized in BLAST-based searches) or the absence of some TIRs from the current genome due to gaps or anomalous arrangements in the B73 genome (assembly in progress).

Phylogenetic Relationships between the B73 Mu Transposons

Phylogenetic analyses using 150 bp of each TIR sequence identified through BLAST analysis of the B73 genome revealed the diversity of Mu elements (Fig. 2-2). As expected, the distinct classes of Mu elements grouped into mutually-exclusive groups according to their TIRs, with the canonical Mu's (1-9), Mu10's, and Mu12's each occupying their own positions in the phylogenetic tree (Fig. 2-2), and with Mu11's grouping with both the canonicals and Mu10s. Often, the two arms of a single Mu insert had divergent sequences and thus grouped in different sub-clades (Fig. 2-2). This degree of asymmetry was counter to expectations, and is thought to be atypical of transposons (Brutnell, 2002; Lisch, 2002). These elements with divergent TIRs have been termed "heteromorphic" Mu elements, of which there appear to be at least five independent groups in B73, including the Mu11s.

The B73 Inbred Contains some MuDR-like Sequences

Being a stable inbred line, B73 is not expected to contain the autonomous MuDR transposase, and no exact matches to the published MuDR sequence were detected in our analyses (Table 2-2). However, some of the Mu elements in B73 have very high similarity to MuDR and are likely MuDR derivatives. None of these MuDR-like, canonical Mu's appear to have retained the capacity to encode functional proteins since

their putative *mudra* and *mudrb* coding sequences included mutations that would lead to premature stop codons or contained large deletions.

Interestingly, many of the Mu10 elements identified in B73 had internal sequence very similar to MuDR, but divergent TIRs. Although most of the *mudra* and *mudrb* coding sequences of these Mu10s were disrupted, at least one appeared to be intact (Fig. 2-3). This Mu10, designated Mu4K in these analyses, included full-length sequences apparently capable of encoding both MURA-like and MURB-like proteins (Fig. 2-3). Normal intron-exon borders were intact and, if processed, would lead to translation of proteins highly similar to MURA and MURB (Fig. 2-3). These putative proteins would be 82% and 79% identical at the amino acid level to MURA and MURB, respectively (Fig. 2-3).

Mu-anchored Sequencing to Identify Mu Insert Locations in Maize and Teosinte Inbreds

Over 43,000 reads were obtained from 454-based sequencing of thirty independent libraries, each constructed using anchor primers to one of the three classes of Mu elements (canonicals, Mu10s, and Mu12s) in one of the ten *Zea mays* inbreds examined (3 maize and 5 teosinte) (Appendix A). From the resulting reads, 15,348 Mu insert sites were identified by aligning Mu-flanking sequences with the B73 genome. Among these mapped inserts, two flanks were identified for between 20-50% for most libraries, thus we estimate that these data represents an average of approximately 25-60% coverage of the total Mu inserts in these inbreds. Complete appraisal of the Mu inserts by these methods is not currently feasible due to degeneration of TIR sequence and PCR-based variation, though deeper sequencing will provide greater coverage.

Results from Mu-TIR-anchored sequencing of the three maize inbreds (B73, Mo17, and W22) are summarized in Table 2-3, and those from the five teosinte lines are summarized in Table 2-4. All reads from each library were mapped to the B73 reference genome as noted above. Of the current-day maize Inbreds, Mo17 contained the highest numbers of all three classes of Mu transposons (Table 2-3). For the five teosinte inbred lines, the results were more variable, with TIL-11 having the most canonical Mu's and TIL-17 having the most Mu12-like elements (Table 2-4). Reads that originated from opposite arms of the same Mu insertion (one from each TIR) were determined as such by examining their proximity on the reference genome and by the presence of matching 9-bp target-site duplications (TSDs). The number of inserts for which two flanking sequences were recovered from each library was subtracted from the number of uniquely-mapping reads to obtain the total number of Mu elements identified from each library (Tables 2-3, 2-4, column 4). In order to estimate the coverage from each of these libraries, the percentage of elements identified with both flanks was divided by that for which both arms were detectable in the B73 genome using bioinformatic approaches (Tables 2-3, 2-4). Each Mu class was treated separately. The rough estimates of Mu inserts from each class in a given inbred (Tables 2-3, 2-4, column 8) is based on BLAST-analysis alone, and thus represents a general approximation.

Expression of these estimates as proportions of the total Mu presence from each Mu class showed remarkable consistency between inbreds (Fig. 2-4). With the exception of the teosinte lines derived from the Jalisco region (TIL-11 and TIL-14), the canonical Mu elements are estimated to make up between 12 - 15%, while Mu12-like

elements account for between 75 - 82% of the total Mu's. Jalisco-derived teosinte lines had a higher proportion of canonical Mu's at the expense of Mu12s (Fig. 2-4). The B73 maize inbred appears to contain a higher proportion of Mu10 elements than any other group, with around 13% of its total Mu elements being classified as Mu10-like (Fig. 2-4).

Comparative Analysis of Mu Elements and Insert Sites in Maize and Teosinte

A number of observations can be made by diagramming each Mu insert from the three maize inbreds (Fig. 2-5) and the five teosinte lines (Fig. 2-6) onto the B73 physical map. First, the Mu elements were not distributed in a completely random manner throughout the genome. Distinct areas of some chromosomes were devoid of detectable Mu elements, whereas other areas had a relative overabundance. The latter were typically near the ends of chromosomes (Figs. 2-5; 2-6). However, patterns of Mu-insert distribution vary greatly among the inbreds (Figs. 2-5; 2-6). Additionally, there was no obvious pattern of any two of the maize inbreds sharing more Mu inserts than the other. No immediate inter-relational patterns are thus indicated by these data for the three maize lines. Finally, some classes of Mu elements tended to group together in some areas (Figs. 2-5; 2-6). Importantly, the large majority of Mu elements detected in this study appear to be unique to a single inbred (Figs. 2-5; 2-6).

Discussion

Bioinformatic Analysis of B73 Reveals Diversity

Previous estimates for the number of "background" Mu inserts in inbred maize lines were between 20 and 50 (Liu et al., 2009). Until recently, such approximations were based on canonical Mu's (1-9) alone, and even when Mu's 10-12 were identified (Dietrich et al., 2002), the extent of their abundance was not recognized. Here we show that the total number of Mu elements in B73 is closer to 200, and that some inbred

teosinte lines may have closer to 500 (Tables 2-1, 2-3, 2-4). The majority of Mu transposon sequences in all the maize and teosinte inbreds tested here are Mu12-like elements. This abundance is intriguing when considering how little these elements have been utilized in gene tagging experiments. One possibility is that Mu12 elements could be have limited activity in current mutagenic maize lines (such as the UniformMu population). Alternatively, their activity may have gone undetected thus far due to a lack in tools for their detection. Primers designed based on flanking sequences from the canonical Mu's would be unlikely to anneal to TIR sequences from a Mu10 or Mu12 element.

Several factors could contribute to the presence of Mu sequences in the maize genome that did not have two readily-identifiable, oppositely-oriented TIR sequences (23%) (Table 2-1). First, despite being close to completion, the B73 genome is not yet fully assembled (Schnable et al., 2009). Gaps remain where sections have not yet been positioned and oriented, and large sections of DNA may not yet be correctly arranged. A number of the Mu sequences examined here terminate at gap sites, providing the likelihood that some of the single-armed Mu sequences here might actually have an unrecognized complement TIR elsewhere in the dataset. Others will likely be completed as the genome sequence becomes more refined. Actually, the repetitive nature of internal Mu-element sequences may complicate their arrangement during genome assembly and/or lead to gaps in the sequence, a scenario that seems likely given the disproportionate number of elements that terminate in gaps. Assembly of repetitive DNA sequence has long plagued genome sequencing projects (International Human Genome Sequencing Consortium, 2001), and Mu elements might be a

contributing factor of that in maize. Alternatively, Mu elements with a single detectable TIR might have lost all or part of one arm due to deletion or translocation events, or through the accumulation of enough small mutations over time to compromise recognition by BLAST using queries of 150-bp TIR sequences. Further decrease to the threshold of BLAST e-value cutoffs used here might reveal some additional TIRs, but these would be difficult to distinguish from non-Mu-derived DNA sequence.

Homomorphic Versus Heteromorphic Mu Elements

Heteromorphic elements (those with divergent TIRs) may reveal important clues about Mu transposon evolution and behavior. The Mu11 elements were first described as having one TIR similar to a canonical Mu and one TIR like that of a Mu10 (Dietrich et al., 2002). Ten such Mu11's were identified in the B73 genome by BLAST analyses (Table 2-1). Additional Mu's that are currently represented by one-armed sequences may also belong to this class. The mechanism by which such Mu elements might arise, with two very different arms, deserves some discussion. It seems almost certain that for a Mu11, one arm originated from a canonical Mu while the other arose from a Mu10. One possibility is that a transposase attached to distal arms of two, physically-close, but unrelated Mu elements, starting the amplification of hybrid Mu element, the progenitor of the Mu11 class. Alternatively, the insertion of a Mu10 inside of a canonical Mu (or vice-versa) could lead to the formation of a hybrid Mu11-like element. A similar mechanism could possibly have given rise to some of the Mu12 elements that contain two very distinct arms (connected by red, dashed lines in Figure 2-2). However, it is also possible that one arm (or both) simply accumulated changes independently of the other, but maintained transposase recognition sites, and thus activity. If so, the evolving, but still-functional arm would continue to be amplified, and thus give rise to groups of

elements with two different arms. Such arms would group in separate clades in phylogenetic analyses, as observed in Figure 2-2. Heteromorphic Mu's do not necessarily lose their potential to transpose, as multiple instances of heteromorphic Mu amplification are evident by replicated inserts seen in the phylogenetic analyses (parallel dashed lines in Fig. 2-2). At least five independent groups of heteromorphic Mu's have arisen in the Mutator system.

There were also a number of Mu elements for which both TIR sequences were essentially identical, differing by as few as 3 base-pair changes (Fig. 2-2). These elements may represent relatively recent TIR duplication events, as left and right arms have not accumulated mutations since their origination. Therefore, the extent of similarity between arms does not seem related to time since insertion of the element into its current site, but time since a single arm was replicated to make a completely homomorphic element. A mechanism for doing so need not be common, but should allow a single TIR sequence to be duplicated, such that the resulting Mu element have identical left and right arms, oriented in opposite directions. No such pathway is currently known, but during replicative transposition a Mu element is copied before its insertion elsewhere (Shapiro, 1979). During this process, one TIR might possibly be replicated twice, creating a new Mu element with identical TIRs. Notably, for insertions with near-identical TIRs (such as the Mu12 insertion, Mu9K, in this analysis) the homology between the arms is limited to the TIRs (data not shown), and does not extend into internal sequence. This observation indicates that the TIRs in particular are replicated to generate a new homomorphic Mu element, and not larger portions of the transposon.

Some Mu10 Elements Have Full-length Putative Transposase Sequences

The possibility that some Mu10 elements might encode functional transposases is indicated by the high degree of predicted amino acid sequence similarity between putative coding regions of the Mu10 element, Mu4K, and the MURA and MURB proteins of the MuDR transposase (Fig. 2-3). One possibility is that these Mu10 elements function in a similar manner and on similar targets as MuDR, but have remained undetected and uncharacterized because of differences in activity and/or sequence. Alternatively, Mu10 and MuDR elements might have diverged enough to have distinct targets, either mutually-exclusive or overlapping. The autonomous MuDR has been associated with transposition of canonical Mu elements (Mu1-9) (Chomet et al., 1991), but its effects on the more divergent Mu's (10-12) have received little previous attention, and are unknown. Involvement of another transposase is possible, particularly given the presence of the Mu10s, and the divergent sequence of Mu10 and Mu12 TIRs (and transposase binding sites). Either MuDRs, Mu10s, or both could be responsible for transposition of the divergent Mu classes, including the Mu10s, Mu11s, and/or Mu12s. It is also possible that Mu10 elements may be non-functional derivatives of MuDR that have not yet diverged in significant ways. However, as the TIR sequences of MuDRs and Mu10s have accumulated many changes, but the putative coding sequences have maintained homology, their being non-functional derivatives seems unlikely. The observation that predicted protein sequence is more similar than the nucleotide sequence between MuDR and Mu4K suggests selection pressure to maintain protein function (Miyata et al., 1980). Selective pressures that might favor an active transposase are hotly debated (Kidwell and Lisch, 2000; Okamoto and Hirochika, 2001; Rebollo et al., 2010).

Relationships Between Zea Inbreds are Highlighted by Mu Element Mapping

While the overall ratios of Mu classes were similar for the inbreds tested here (Fig. 2-4), comparisons of insert locations and overall abundance in each of the maize and teosinte inbreds demonstrated some striking differences between them. First, the greater variation between Mu insert sites in teosinte lines than between the maize inbreds is consistent with the greater diversity of teosinte overall (Fukunaga et al., 2005) (compare Tables 2-3 and 2-4). Only about 10% of the Mu elements detected in the five teosinte inbreds were present in more than one line, as opposed to around 30% for the maize lines. Also, some of the teosinte lines, specifically TIL-15 and TIL-17 from the Balsas region, have abundant Mu's, estimated at over 600 insertions each. In addition, the TIL-11 teosinte line contains approximately twice the number of canonical Mu elements as any of the other maize or teosinte inbreds tested, indicating a higher activity for this particular class in that line (Table 2-4, Fig. 2-6; Fig. 2-4). Some inbreds had areas of especially high insert abundance, such as TIL-17 having 27 unique inserts on the short arm of chromosome 10 (covering 58 million nucleotides), that seem to suggest location-specific differences in insert activity between lines (Fig. 2-6). It is possible that the various inbreds have different chromatin structure and/or other DNA changes that could influence insertion frequency and insert site preference.

Other patterns of Mu insert location were common among all inbreds tested. Certain regions of chromosomes 2, 5, 6, and 9 had high numbers of transposons within relatively small areas in teosinte and maize inbreds (Figs. 2-5, 2-6). Also apparent was a relative abundance of Mu elements at the ends of chromosomes and their relative scarcity near centromeres in both teosinte and modern-day maize inbreds. Additionally, large areas of chromosomes lacking Mu inserts, together with frequent clusters of Mu

elements, strongly indicated that insertion sites were non-random. It is likely that physical characteristics of the DNA, like chromatin structure or DNA modification, influence the likelihood of Mu transposon insertion in a particular site, with more genic regions being less tightly organized and thus better candidates for Mu insertion, as has previously been suggested (Liu et al., 2009; Vollbrecht et al., 2010). This scenario is supported by data shown here, as well as observations that Mu elements target the five-prime regions of genes (Dietrich et al., 2002; Liu et al., 2009). This pattern seems to extend from canonical Mu's to the Mu10 and Mu12 elements (Figs. 2-5; 2-6).

Also apparent were chromosomal regions that appeared to preferentially accumulate insertions of certain classes. For instance, despite Mu10 elements being less abundant than the canonicals or Mu12s, regions on the short arms of chromosomes 2 and 5 contained multiple Mu10 elements within relatively small areas (Fig. 2-5). Other regions contained unusually high numbers of canonical Mu elements or Mu12s, possibly reflecting differences between the Mu classes in their insertion-site preferences. What the underlying causes of these differences might be remains to be determined.

Many of the Mu elements identified here were present in both maize and teosinte (stars in Figs. 2-5, 2-6), and presumably represent ancient insertion events that have been propagated since before the divergence of teosinte and modern maize. Alternatively, these Mu elements could theoretically be independent insertion events in the same exact location, as has been reported, albeit rarely, in other cases (Dietrich et al., 2002). We consider the former suggestion, that of their being ancient insertion events, to be more likely, as the classification of shared Mu's is typically consistent (a

Mu12 insert in teosinte matches a Mu12 insert in maize). While these elements were found throughout the genome, the dispersal pattern was uneven, with small clusters of two or more shared Mu's occurring regularly (Figs. 2-5, 2-6). In particular, regions of chromosome 2 short arm, and chromosomes 4 and 5 long arms had groups of 4 or more Mu elements that appear to be ancient in origin and to have been inherited together. Other regions, such as the short arm of chromosome 4 and the majority of chromosomes 3, 8, and 10 have very few shared Mu elements between teosinte and maize. Interestingly, the Mu elements shared between these subspecies were not over-represented by a certain class of Mu. There were specific canonicals, Mu10s, Mu11s, and Mu12s present in both modern maize and teosinte, in approximately the same ratio as their overall abundance. We had speculated that the large Mu12 class may represent more ancient insertions, but based on these data, that does not necessarily appear to be the case.

Methods

Bioinformatic Identification of Mu Elements in the B73 Maize Genome

As diagramed in Fig. 2-1, mining of the B73 reference genome (version 2, release 4a.53) (maizesequence.org) was conducted by repeated BLAST analyses, starting with a single Mu TIR from each class of Mu transposons, (canonicals, Mu10s, and Mu12s). Individual returns from each BLAST output (cut-off at $10e^{-6}$) were annotated and deposited in a database. They were named based on chromosome, then order of discovery (as in Mu1A for the first transposon identified on chromosome 1). This process was repeated, using more divergent Mu TIR sequences, until no additional unique transposons were identified. Genomic sequences surrounding each Mu were then individually analyzed to match paired TIRs (opposite arms from the same element)

based on 9-bp target-site duplications. Matching arms were given a common name and arbitrarily designated left or right arm (as in Mu1AL for the left arm of the first transposon identified on chromosome 1).

Phylogenetic Analysis of B73 Mu-TIRs

For each bioinformatically-identified TIR in the B73 reference genome, the terminal 150 bp were trimmed, oriented in the same 5`-to-3` direction, and arranged with their terminal bases oriented 5` (as in 5`-GAGATAA-3`). The 299 TIRs (one was omitted due to truncation by a gap in the reference genome) were aligned using ClustalW (Larkin et al., 2007). A neighbor-joining tree was created with MEGA4 (Tamura et al., 2007) using the pairwise deletion option and 1,000 bootstrap repetitions.

Mu-flank-anchored 454 Library Construction

DNA from each maize and teosinte inbred (B73, Mo17, W22, TIL-1, TIL-11, TIL-14, TIL-15, and TIL-17) was randomly sheared and ligated to biotinylated amplicon-B (bioTEG0-ampB) adaptors. Approximately 5 µg of DNA was bound to 50 µL of Streptavidin beads (Dynal, product # 653.05) and immobilized using a magnetic rack (Applied Biosystems, Lot # 0804015). Beads were washed 4 times with 100 µL of washing buffer #1 (10mM Tris-HCl [pH 7.5], 1 mM EDTA [pH 8.0]), and removed from the rack between each wash. The second washes were conducted at 37°C for 5 min. The final washes were transferred to 0.2-mL PCR tubes, where buffer was removed from beads immobilized on a magnetic stand-96 (Applied Biosystems, Lot # 0903014). For primer extension 1 (Fig. 2-7), the following was added for each reaction: 0.33 µL of 10 pmol/ul TIR primer (TIR6 for canonical Mu elements, primer 10.1 for Mu10s, and primer 12.1 for Mu12s, see Table 2-5) (10 pmol/ul), 10 µL 10X NEB ThermoPol buffer (1X = 10mM KCl, 20 mM Tris-HCl [pH 8.8 at 25°C], 10 mM NH₄2SO₄, 2 mM MgSO₄,

0.1% Triton X-100 [Sigma Lot # MKBD6639V]), 2 μ L dNTPs (10 mM), 85 μ L HPLC-grade water, and 2 μ L Vent DNA Polymerase (NEB M0257S 2 units/ μ L). Each reaction tube received 100 μ L of this master mix, and were transferred to a thermocycler. The primer extension 1 reaction differed for canonicals (80°C, 2 min; 72°C, 10 min; -1°C/min to 67°C; 67°C, 10 min; 70°C, 6 min), and Mu10s and Mu12s (80°C, 2 min; 70°C, 10 min; -1°C/min to 65°C, 65°C, 10 min; 70°C, 6 min). To stop the reaction, 1 μ L 0.5 M EDTA (pH 8.0) was added. Tubes were gently vortexed and beads were transferred to the original 1.5-mL tubes. Beads were rinsed 4 times with washing buffer #1, with the second wash at 37°C for 5 min. After the last wash was removed, 125 μ L of melt solution (100 mM NaCl, 125 mM NaOH) was added and tubes were incubated on a slow shaker for 10 min to elute the newly synthesized strand. Beads were immobilized and supernatant was transferred to acidified PBI buffer (Qiagen, 625 μ L PBI with 4.5 μ L 20% fresh aqueous acetic acid). Single-stranded DNA was concentrated and de-salted using MinElute PCR purification kit columns (Qiagen Cat # 28704), before elution with 20 μ L of 55°C EB buffer. Beads (containing original DNA) were washed as before and stored at 4°C.

Products from primer extension 1 were then PCR amplified using a 2-step PCR protocol. The following reagents were used for a single reaction: 6 μ L 10X PCR Enhancer (Invitrogen Cat # 11495-017), 2 μ L 10X PCR amp buffer, 1.5 μ L 100 mM MgSO₄, 0.5 μ L 10 mM dNTP, 0.8 μ L 10 μ M bioTEG0-ampB primer, 0.8 μ L 10 μ M Mu primer (TIR 8 for canonicals, 10.1 for Mu10s, 12.1 for Mu12s), 0.2 μ L 10 units/ μ L Taq, and 7.9 μ L HPLC-grade water. The 2-step PCR thermocycler settings were: 96°C, 3

min; [96°C, 30s; 60°C, 45s; 72°C, 90s] 9 cycles; [96°C, 30s; 54°C, 30s; 72°C, 90s] 31 cycles; 72°C, 5 min.

The amplified PCR products were then optimized for the desired size as follows. Portions of the amplified libraries (85 µL) were added to 59.5 µL SPRI bead slurry. Solutions were vortexed and incubated at 25°C for 5 min. Beads were immobilized for 15 min and liquid was removed. While tubes remained on the magnet rack, beads were washed 2 times with 200 µL 70% EtOH. After the wash was removed, beads (on rack) were placed in a 37°C incubator for 30 min to allow EtOH evaporation. Size-selected, double-stranded DNA was eluted with 50 µL 10 mM Tris (pH 7.5), 1 mM EDTA (pH 8.0).

Streptavidin beads were prepared for binding by washing twice with 100 µL of 1X B&W buffer (5 mM Tris-HCl [pH 7.5], 0.5 mM EDTA [pH 8.0], 1 M NaCl). Buffer was then added (50 µL of 2X B&W buffer [10 mM Tris-HCl (pH 7.5), 1 mM EDTA (pH 8.0), and 2 M NaCl], along with 50 µL of the size-selected PCR product. Tubes were vigorously shaken for 20 min at 25°C to bind beads. The beads were then immobilized and washed twice with 1X B&W, and twice with HPLC-grade water. The biotinylated strands were isolated by adding 125 µL melt solution and shaking for 10 min at 25°C. Beads were again immobilized and the eluted strands were removed (purified and retained for validation analyses). Beads were washed twice with 200 µL HPLC-grade water, twice with 100 µL washing buffer 2 (100 mM Tris-HCl [pH 7.5], 0.5 mM EDTA [pH 8.0]), and twice with washing buffer 1. The second wash was done at 37°C for 5 min. Prepared streptavidin beads were then resuspended in 50 µL of washing buffer 1.

For primer extension 2, beads (50 µL) were transferred to 0.2-mL PCR tubes, immobilized, and solution was removed. The following was added to each tube: 5 µL 10

pmol/uL sequencing primer (specific for each reaction, see Table 2-5), 10 μ L 10X ThermoPol Buffer (NEB), 2 μ L 10 mM dNTP, 81 μ L HPLC-grade water. Tubes were transferred to a thermocycler and subjected to the following: 80°C, 2 min; 61°C, 10 min; -1°C/min to 51°C; 51°C, 30 min. Reactions were initiated by adding 5 μ L Vent DNA Polymerase (NEB Cat # M0257S) and mixing the solution by gentle pipetting. Temperature was raised to 70°C for 6 min, and 1 μ L 0.5 uM EDTA (pH 8.0) was added to stop the reaction. Tubes were gently vortexed and beads were transferred to new, 1.5-mL tubes. Beads were again immobilized and rinsed 4 times with washing buffer 1, with the second was at 37°C for 5 min. The last rinse was removed before adding 125 uL wash solution. Tubes were incubated at 25°C for 10 min while shaking. Beads were immobilized and newly-synthesized DNA strands (with A- and B-adaptors) were eluted, purified, and concentrated in a final volume of 20 μ L using a PCR purification kit (Qiagen Cat # 28704). Single-stranded DNA templates were then sequenced on a 454 GS-20 (Roche Biosciences, Indianapolis, IN) as per Margulies et al., (2005).

Sequence Annotation and Alignment

Sequences from 454 runs were trimmed and compiled using custom, Java-based programs (courtesy of Don McCarty). Each sequence was surveyed for correct, 4-base keycodes to assign sub-libraries of origin and to check for sequencing errors (bar-codes included a checksum code). They were each independently used as queries against the B73 reference genome in BLAST analyses in order to map them to specific chromosomal locations. Databases for each inbred and Mu class were assembled based on these BLAST results. Repetitive sequences were discarded. Insertions mapping within close proximity were examined for matching 9-bp target-site duplications and scored as single insertions for the final analyses.

Accession Numbers

Mu1, X00913.1; Mu1.7, Y00603.1; Mu3, U19613.1; Mu4, X14224.1; Mu5, X14225.1; Mu7, X15872.1; Mu8, X53604.1; Mu9 (MuDR), M76978.1.

Table 2-1. Bioinformatically-identified Mu elements in B73

Mu Class	# TIRs detected	# Mu elements	% with both arms
Mu (1-9)	44	25	76%
Mu 10	28	17	65%
Mu 11	20	10	100%
Mu 12	208	127	64%
Total	300	179	76.25%

Numbers of Mu elements from each class detected by BLAST searches of the B73 genome using 150 bp terminal inverted repeat (TIR) sequences. The TIRs were manually curated to determine whether they belonged to the same Mu element based on their relative genomic locations and by matching 9-bp duplications of insert site DNA. *Note that a Mu 11 element with only one arm would be classified with either the Mu10s or the canonicals (Mu1-9) because the Mu11s have heteromorphic TIRs (one like the Mu10s and one like the canonicals).

Table 2-2. Classification of canonical B73 Mu insertions.

Insert	Length	Class	% Identity	e-value	Score
Mu1	1376	Mu1	100	0.0	1990
Mu1.7	1745	Mu1.7	100	0.0	2825
Mu3	1824	Mu3	100	0.0	2944
Mu4	2015	Mu4	100	0.0	3947
Mu5	1320	Mu5	100	0.0	2617
Mu7	2199	Mu7	100	0.0	4359
Mu8	1410	Mu8	100	0.0	2795
Mu9 (MuDR)	4942	Mu9	100	0.0	6445
1B	2018	Mu4	99.85	0.0	3905
1C	4805	Mu9	94.82	0.0	2761
2A	4864	Mu9	94.32	0.0	3406
2B	1891	Mu4	91.79	1e-071	260
2C	1890	Mu4	91.79	1e-071	260
2D	1914	Mu4	92.31	6e-074	268
3A	3578	Mu9	94.21	0.0	2072
4B	2018	Mu4	99.70	0.0	3881
5A	1498	Mu9	91.93	0.0	1292
6A	1321	Mu5	99.92	0.0	2603
7B	1134	Mu7	95.57	0.0	1047
7C	2199	Mu7	99.59	0.0	4270
8A	2037	Mu4	92.34	3e-085	305
8B	1621	Mu7	97.26	8e-110	387
9A	1955	Mu7	97.26	1e-109	387
10A	10830	Mu3	98.47	0.0	1850
UNKA	1955	Mu9	93.38	0.0	1984
UNKB	2078	Mu4	92.79	1e-087	313

To assign the canonical Mu elements identified in the B73 genome to a specific class, each of those for which the entire sequence was available were compared to the eight previously-published Mu elements in a BLAST-based analysis. The upper portion of this table shows the results using the eight published Mu elements, and should be referred to in comparing BLAST scores to those of the individual B73 elements below. Of the 18 full-length canonical Mu elements identified in B73, the majority of them were most similar to Mu4, Mu7, and Mu9. None were most similar to Mu1.7 or Mu8.

Table 2-3. Mu elements identified by Mu-flank sequencing in three maize inbreds

Inbred	Mu class	Mapped reads	# both flanks	# Mu's	% both flanks	Expected %	Estimated coverage	Estimated # of Mu's
B73	(1-9)	43	15	28	53.6%	76%	70.5%	40
B73	10	17	3	14	21.4%	65%	33.0%	42
B73	12	128	27	101	26.7%	64%	41.8%	242
Mo17	(1-9)	64	23	41	56.1%	76%	73.8%	56
Mo17	10	25	7	18	38.9%	65%	59.8%	30
Mo17	12	150	26	124	21.0%	64%	32.8%	378
W22	(1-9)	53	19	34	55.9%	76%	73.5%	46
W22	10	13	4	9	44.4%	65%	68.4%	13
W22	12	115	22	93	23.7%	64%	37.0%	251

Mu inserts in three maize inbreds were identified through 454-based Mu-flank sequencing. Each inbred and Mu class combination was sequenced with a unique key code to determine their library of origin. Mapped reads were unique TIR-flanking sequences that mapped to specific sites on the B73 genome. The number of these that had both flanks were determined by location on B73 the reference genome and by sequenced target-site duplications. Expected percentages with both flanks was based on bioinformatic results of BLAST analyses on the B73 genomic sequence, and was used in calculating the estimated coverage for each library. Estimated number of Mu's was calculated by dividing the number of Mu's detected by the percent coverage, and refers to the total number of Mu elements of each class that would be expected by these calculations, and can be considered a rough estimate only.

Table 2-4. Mu elements identified by Mu-flank sequencing in five teosinte inbreds

Inbred	Mu class	Mapped reads	# both flanks	# Mu's	% both flanks	Expected %	Estimated coverage	Estimated # of Mu's
TIL-1	(1-9)	45	12	33	36.4%	76%	47.8%	69
TIL-1	10	13	5	8	62.5%	65%	96.2%	8
TIL-1	12	86	9	77	11.7%	64%	18.2%	422
TIL-15	(1-9)	41	7	34	20.6%	76%	27.1%	126
TIL-15	10	15	2	13	15.4%	65%	23.7%	55
TIL-15	12	169	25	144	17.4%	64%	27.1%	531
TIL-17	(1-9)	55	15	40	37.5%	76%	49.3%	81
TIL-17	10	33	8	25	32.0%	65%	49.2%	51
TIL-17	12	215	30	185	16.2%	64%	25.3%	730
TIL-11	(1-9)	68	21	47	44.7%	76%	58.8%	80
TIL-11	10	3	0	3	0%	65%	N/A	N/A
TIL-11	12	61	11	50	22.0%	64%	34.4%	145
TIL-14	(1-9)	75	20	55	36.4%	76%	47.8%	115
TIL-14	10	26	10	16	62.5%	65%	96.2%	17
TIL-14	12	71	8	63	12.7%	64%	19.8%	318

Mu inserts in five teosinte inbreds were identified through 454-based Mu-flank sequencing. Each inbred and Mu class combination was sequenced with a unique key code to determine their library of origin. Mapped reads were unique TIR-flanking sequences that mapped to specific sites on the B73 genome. The number of these that had both flanks were determined by location on B73 the reference genome and by sequenced target-site duplications. Expected percentages with both flanks was based on bioinformatic results of BLAST analyses on the B73 genomic sequence, and was used in calculating the estimated coverage for each library. Estimated number of Mu's was calculated by dividing the number of Mu's detected by the percent coverage, and refers to the total number of Mu elements of each class that would be expected by these calculations, and can be considered a rough estimate only.

Table 2-5. Primers used for 454-based Mu-flank sequencing.

Name	Primer sequence
TIR6	AGAGAAGCCAACGCCAWCGCCTCYATTTTCGTC
TIR8	CGCCTCCATTTTCGTCTGAATCCCCTS, CGCCTCCATTTTCGTCTGAATCCSCTT, SGCCTCCATTTTCGTCTGAATCCCKT, CGCCTCCATTTTCGTCTGAATCACCTC
Mu-direct	CBCTCTTCKTCYATAATGGCAAT
12.1	YATTTTCGTYGAARCCGCAAYCCGTCGTGTTTC
12-direct	CCGTCGTRTTTCATAATRBCAAA
10.1	SCAACGCCTCCRWTTYDTCGAAACCGYKTCTC
10-direct	CTCTBDTGTTTTYATAATGGCAAT

Primers TIR6, TIR8, and Mu-direct were used to amplify canonical Mu elements, while 12.1 and 12-direct were used to amplify Mu12 elements, and 10.1 and 10-direct were used to amplify Mu10 elements. Sequencing primers included a 4-base bar code unique for each library to allow assignment of each read. Code: A (Adenine), C (Cytosine), G (Guanine), T (Thymine), R (Purine [A or G]), Y (Pyrimidine [C, T, or U]), M (C or A), K (T, U, or G), W (T, U, or A), S (C or G), B (C, T, U, or G), D (A, T, U, or G), H (A, T, U, or C), V (A, C, or G).

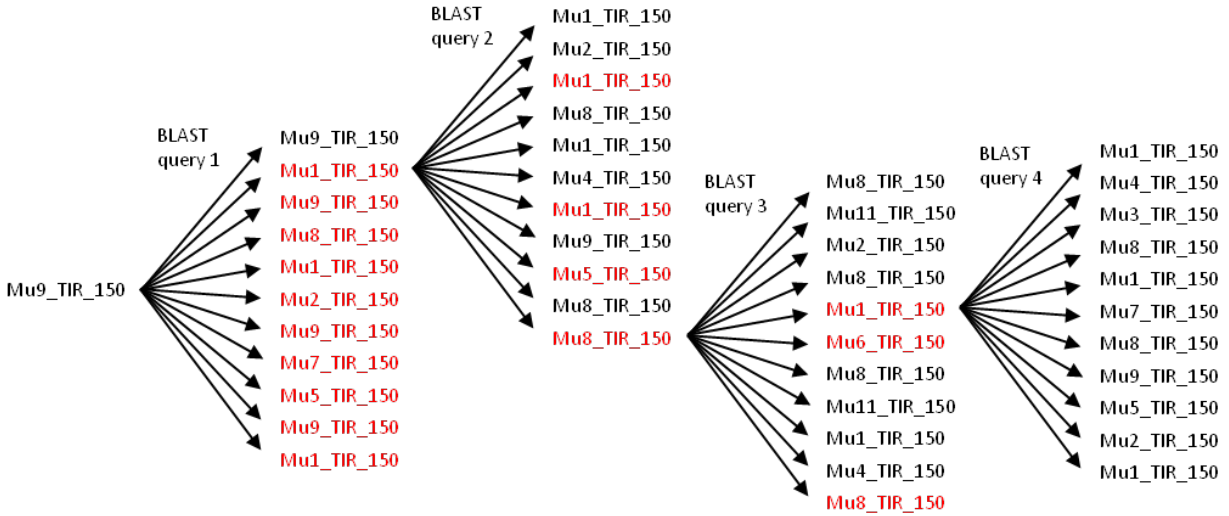


Figure 2-1. One example of a sequential mining track, diagramed here to show progression from an initial BLAST query using a single 150-bp TIR sequence to search the B73 genome. The first query typically returns multiple similar sequences, which are captured and cataloged in a database by genomic location. This initial query is followed by additional BLAST queries using 150 bp from the more divergent TIRs identified, and so on, until no new novel insertion sites are identified. This process was conducted using single initial queries from Mu9, Mu10, and Mu12 elements, and was successful in identifying 300 TIR sequences in the B73 genome. (Black = previously identified; Red = newly identified).

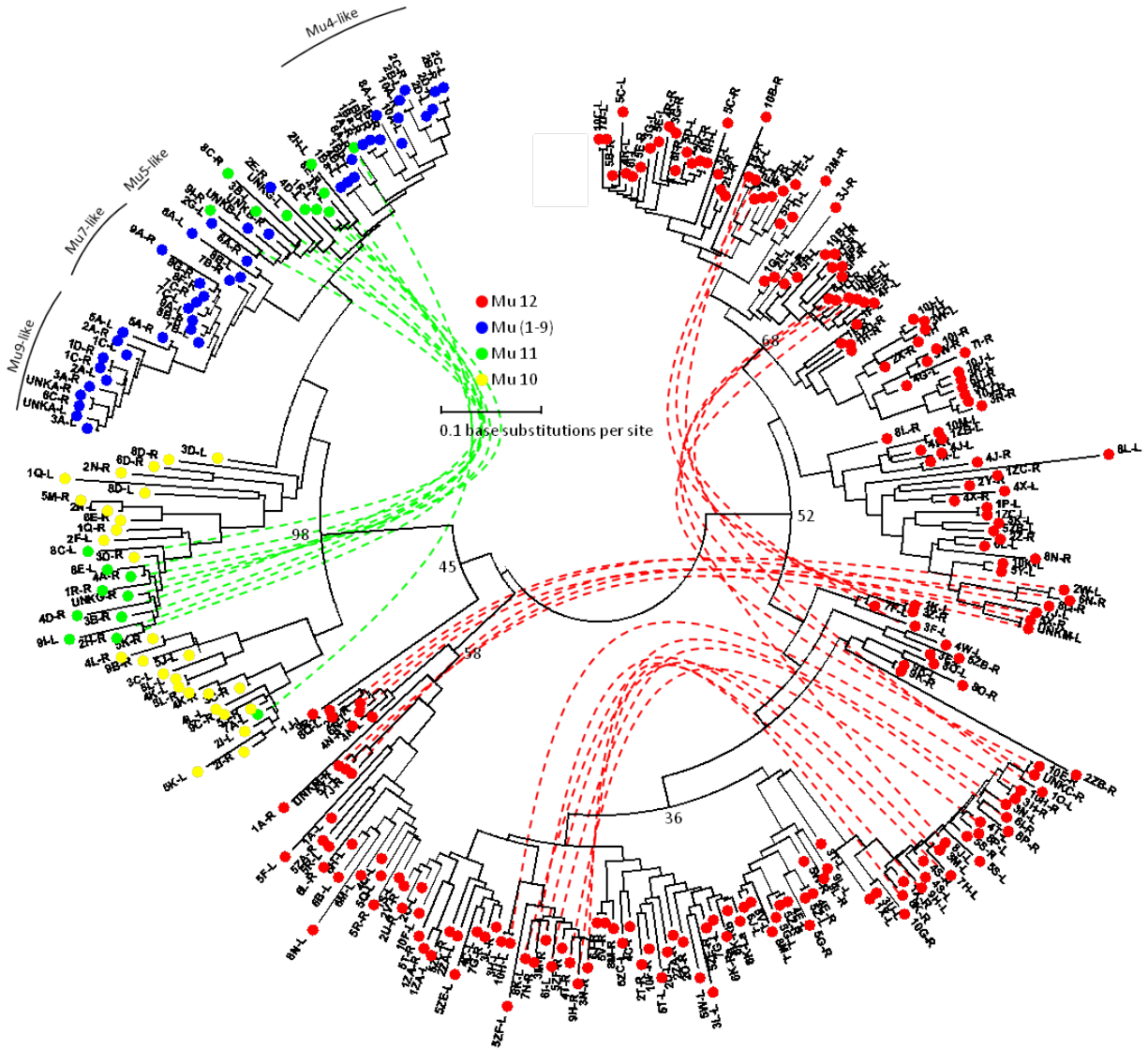


Figure 2-2. Neighbor-joining tree of 299, B73 Mu Terminal Inverted Repeats. The terminal 150 bases from each TIR of bioinformatically-identified B73 Mu transposons were trimmed, oriented in the same direction, and aligned using ClustalW. The phylogenetic tree was created in MEGA4, using 1,000 bootstrap replications with a pairwise deletion option. The canonical Mu elements are labeled based on the most closely-related, previously-described Mu element. Key bootstrap values are shown. Units are in number of base substitutions per site. Opposite arms of heteromorphous Mu elements are connected by dashed lines.

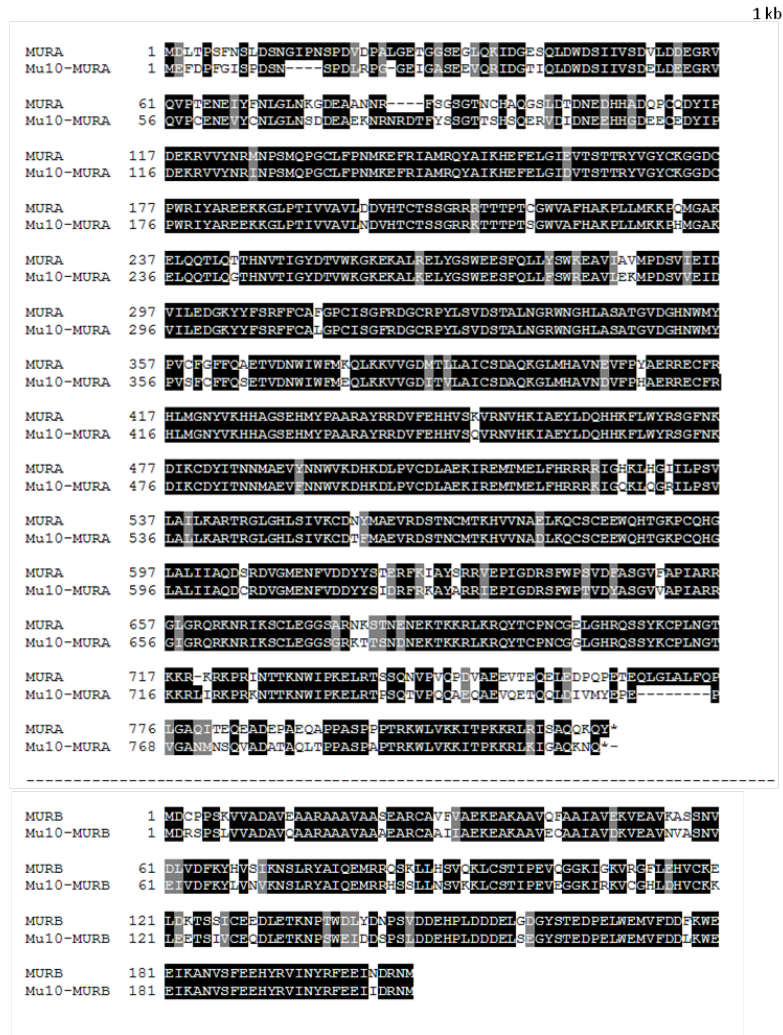
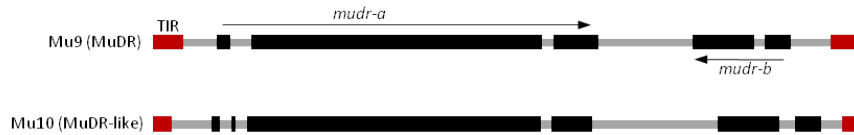


Figure 2-3. Comparison between MuDR and a Mu10 (Mu4K) element from the B73 maize inbred. The overall structure of MuDR and the MuDR-like element are diagrammed in the upper portion of the figure, with TIR sequences and putative coding regions of the *mudr-a* and *mudr-b* genes shown. The Mu10 element is the only apparent MuDR-like sequence in the B73 genome with an intact, uninterrupted sequence. Both *mudr-a* and *mudr-b* genes have potential to code for functional proteins, since they contain no mutations that would lead to premature stop codons (unlike the other MuDR-like sequences in B73). Below, protein alignments between MURA and MURB from MuDR (top) and the predicted analogous proteins from Mu10 MuDR-like element (bottom) reveal high sequence similarity (82% identical for MURA, 79% identical for MURB).

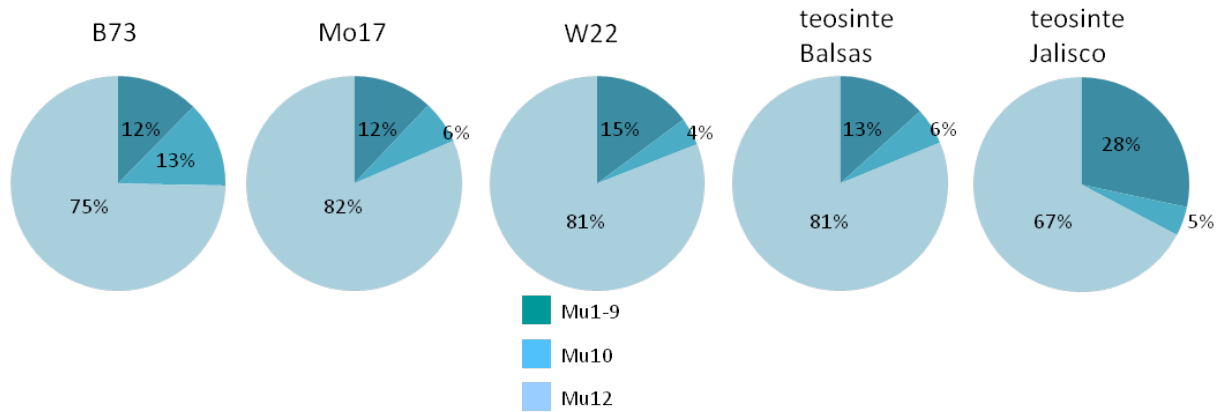


Figure 2-4. Estimated proportions of each Mu class in three maize inbreds and teosinte derived from the Balsas and Jalisco regions of Mexico. Estimates are based on extrapolations of 454-generated Mu-flank sequences summarized in Tables 2-3 and 2-4. Teosinte Balsas represents pooled data from teosinte inbred lines 1, 15, and 17. Teosinte Jalisco represents pooled data from teosinte inbred lines 11 and 14.

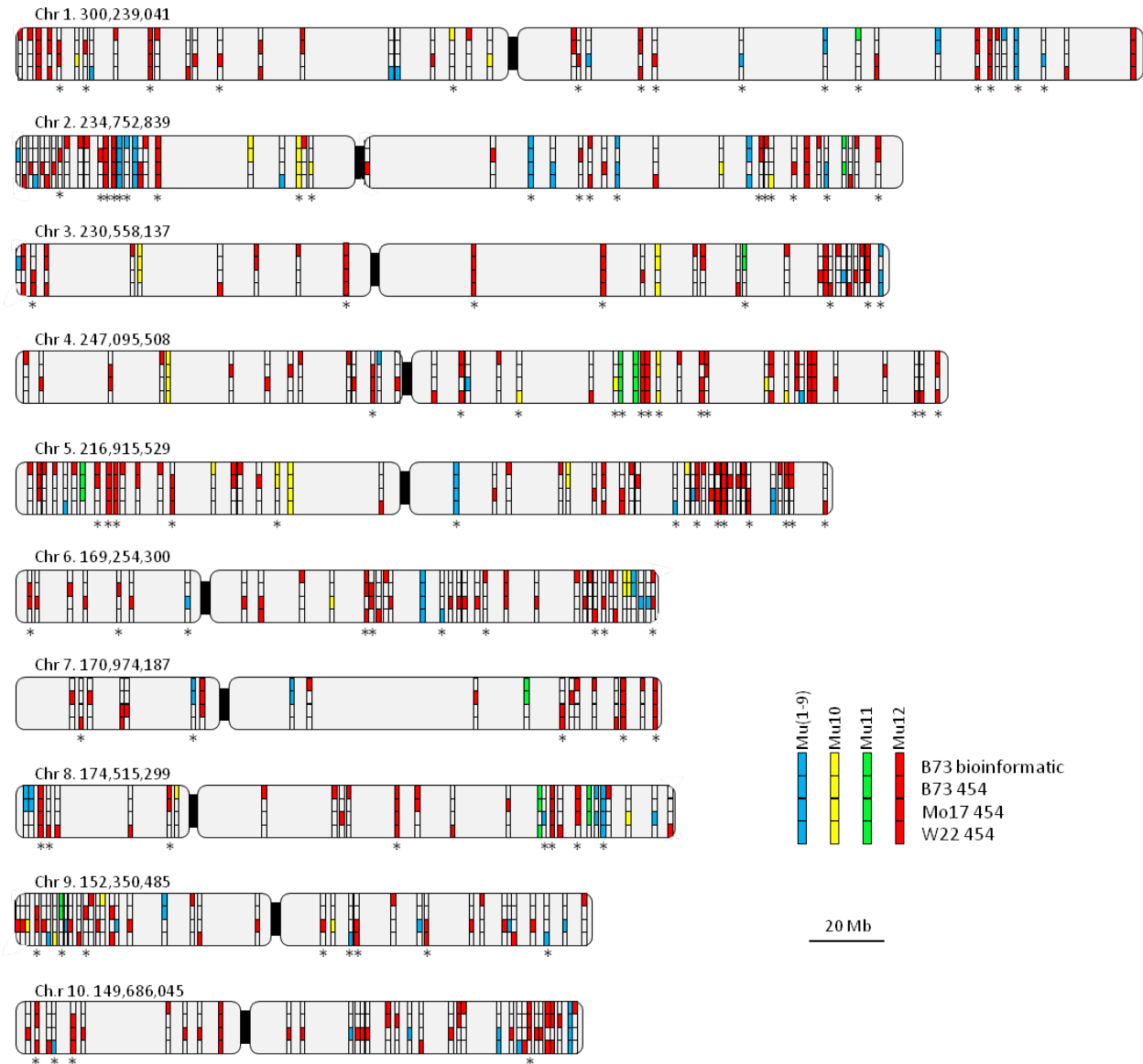


Figure 2-5. Approximate map sites for Mu insertions in three maize inbreds. Insertions were identified either through bioinformatic analysis of the B73 genome (top row), or through Mu-flank 454 sequencing of libraries from the three maize inbreds shown (B73, Mo17, W22 respectively positioned in rows 2, 3, and 4 of each vertical band on chromosomes). Positions on chromosomes are based on BLAST alignments of 454 flanking sequences to the B73 physical map, and are approximate. Above each chromosome diagram are total chromosome lengths (in bp). Inserts shared between at least one maize and one teosinte line are starred.

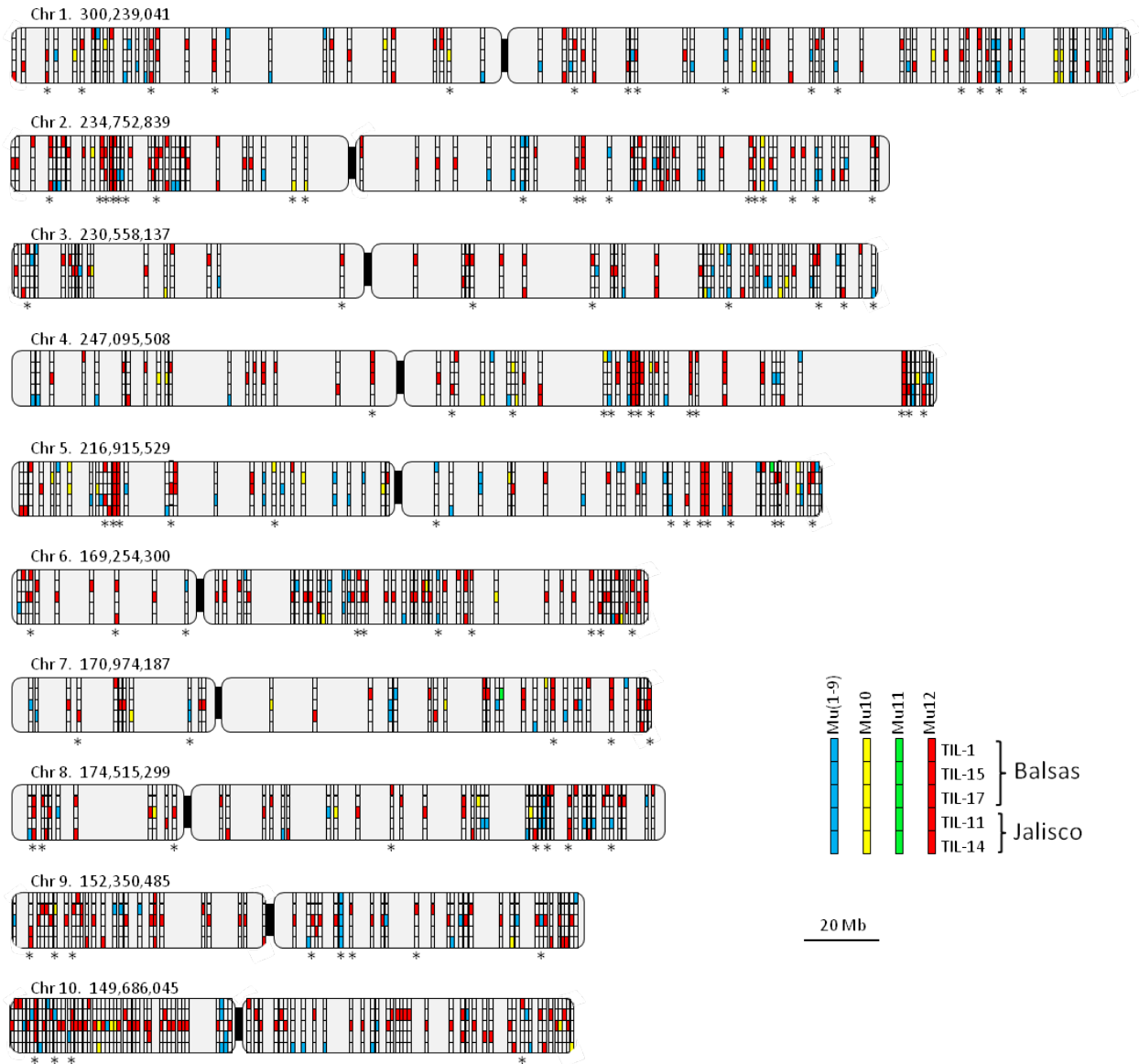


Figure 2-6. Approximate map sites for Mu insertions in five teosinte inbreds. Insertions were identified either through Mu-flank 454 sequencing of libraries from the five teosinte inbreds shown (TIL-1, TIL-15, TIL-17, TIL-11, and TIL-14), respectively positioned in rows 1-5 of each vertical band on chromosomes. Inbred lines 1, 15, and 17 originated from the Balsas region (top three rows), and inbred lines 11 and 14 originated from the Jalisco region (bottom two rows). Positions on chromosomes are based on BLAST alignments of 454 flanking sequences to the B73 physical map, and are approximate. Above each chromosome diagram are total chromosome lengths (in bp). Inserts shared between at least one maize and one teosinte line are starred.

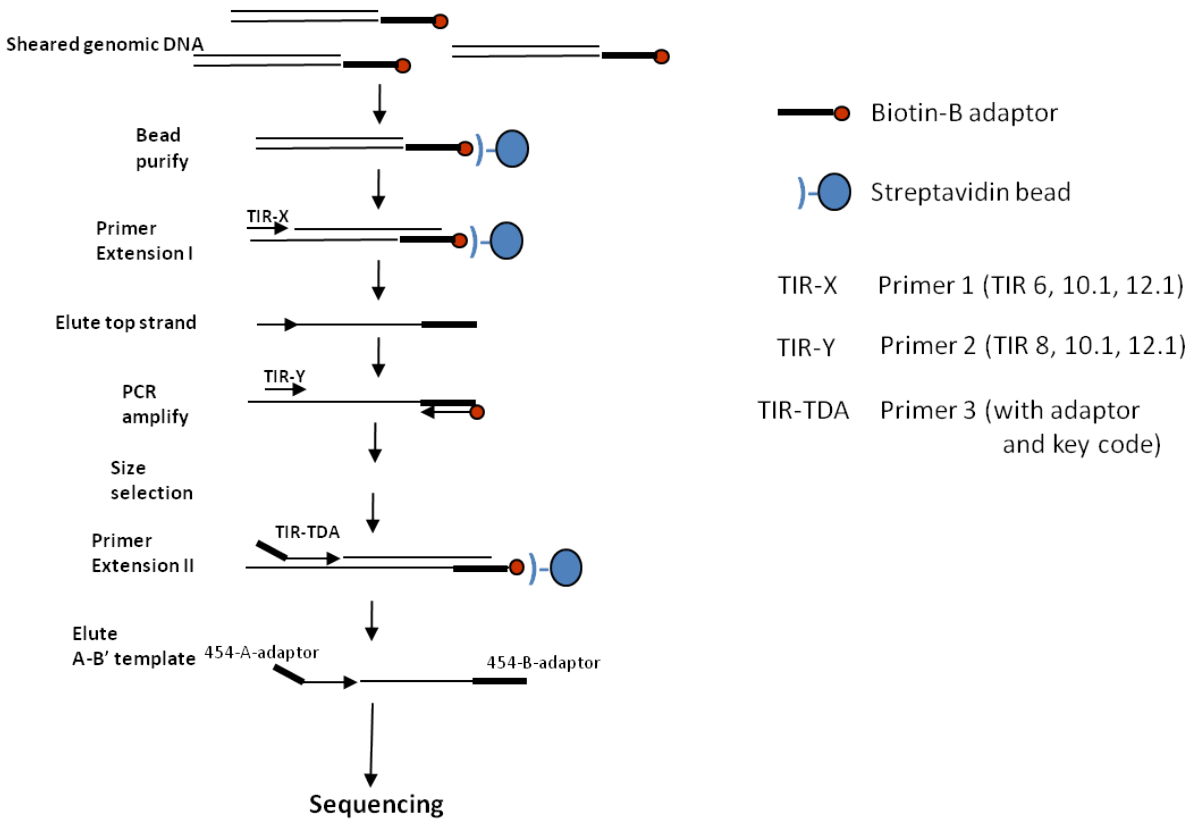


Figure 2-7. Diagrammatic representation of Mu-flank 454-sequencing library preparation. Sheared genomic DNA from inbred maize and teosinte lines was used to generate libraries with amplified canonical Mu's (Mu1-9), Mu10s, and Mu12s, separately. TDA primers contained library-specific key codes for assignment of each read to correct sub-libraries. See Table 2-5 for primer information.

CHAPTER 3 ANALYSIS OF THE CELLULOSE SYNTHASE-LIKE D GENE FAMILY IN MAIZE

Introduction

The ancient, highly-conserved *Cellulose Synthase-Like D (CslD)* genes encode enzymes required for specific cellular growth processes, yet whose biochemical and cellular functions remain elusive (Richmond and Somerville, 2000; 2001; Favery et al., 2001; Wang et al., 2001; Bernal et al., 2007; 2008; Yin et al., 2009). They form one of ten distinct subgroups in the Cellulose Synthase superfamily, defined by sequence similarity to Cellulose Synthases (CESAs) (Richmond and Somerville, 2000; Hazen et al., 2002; Farrokhi et al., 2006; Penning et al., 2009; Fincher, 2009). All members of the superfamily share characteristics of membrane-bound, processive glycosyltransferases that synthesize beta-linked glycan polymers, such as those of some cell wall polysaccharides (Richmond and Somerville, 2000; 2001), and are included in glycosyltransferase family 2 (Saxena, 1995; Campbell et al., 1997; Delmer, 1999; Coutinho and Henrissat, 1999; Holland et al., 2000). Known products range from cellulose to hemicellulose backbones, and may include additional beta-linked glycan chains (Arioli et al., 1998; Dhugga et al., 2004; Liepman et al., 2005; Burton et al., 2006; Cocuron et al., 2007; Doblin et al., 2009). Despite evidence that the CSLDs are of ancient origin, extending to the earliest non-vascular land plants and possibly before (Roberts and Bushoven, 2007), their contributions to cell wall biosynthesis are yet to be defined.

Of the cellulose synthase-like protein families, CSLDs are the most closely related to the cellulose synthases (CESAs), leading to the suggestion that CSLDs may themselves function as cellulose synthases (Doblin et al., 2001). The CSLDs share the

greatest amino acid sequence similarity with CESAs (40-50% identity) and are of similar, though slightly larger size (Richmond and Somerville, 2001). The CSLDs are also the only members of the cellulose synthase superfamily to have the amino-terminal, RING-type Zn-finger-like domains typical of the CESAs (Richmond and Somerville, 2000). These Zn-finger domains are thought to function in protein-protein interactions, possibly mediating complex formation or protein turnover (Gamsjaeger et al., 2007).

The locations and sizes of introns in *CsID* genes led to the suggestion that this subfamily may be ancestral to the entire Cellulose Synthase superfamily (Richmond and Somerville, 2000; 2001; Yin et al., 2009). Also, *CsID* genes are present in all plant genomes examined thus far, including non-vascular mosses (Richmond and Somerville, 2000; 2001; Roberts and Bushoven, 2007; Yin et al., 2009). In contrast, many of the other *CsI* subfamilies appear in only specific taxa (Farrokhi et al., 2006; Keegstra and Walton, 2006; Vogel, 2008; Penning et al., 2009; Fincher, 2009). Of the five *CsI* subfamilies yet to be assigned a specific polysaccharide synthase role, only *CsID* and *CsIE* subfamilies are found in both dicot and monocot genomes (unlike *CsIB*, *CsIG*, and *CsIJ*). This broad taxonomic distribution of the *CsID* genes indicates a conserved function throughout the plant kingdom.

Clues to the biological roles of the CSLDs have been sought by defining their biochemical activity, but this has proven challenging. Heterologous expression studies, while successful in determining the functions of CSLA (Liepman et al., 2005), CSLF (Burton et al., 2006), CSLC (Cocuron et al., 2007), and CSLH (Doblin et al., 2009) proteins, have thus far been unsuccessful for CSLDs. However, based on the

identification of biochemical actions for CSLA, CSLC, CSLF, and CSLH enzymes, the *Cs/D* genes have been hypothesized to encode hemicellulose synthases (Sandhu et al., 2009). Other important lines of evidence have led to alternate interpretations. Analysis of cell-wall polysaccharides, for example, from key cell types, cell-culture treatments, or genetic perturbations have been consistent with roles for CSLDs in production of either cellulose (Manfield et al., 2004; Li et al., 2009) or hemicellulose backbones (Bernal et al., 2007; Li et al., 2009). A complicating factor is that alterations in cell wall composition are often broadly pleiotropic, making primary effects difficult to distinguish from secondary or other closely-related changes (Orfila et al., 2005; Persson et al., 2007; Bernal et al., 2007; Li et al., 2009).

Another valuable source of information has come from subcellular localizations of CSLD proteins. Although the majority of studies thus far have favored a Golgi apparatus localization, supporting a role in hemicellulose backbone synthesis (Favery et al., 2001; Bernal et al., 2007; 2008; Zeng and Keegstra, 2008; Li et al., 2009), these findings are also consistent with the possible transit of CSLD proteins through these compartments enroute to the plasma membrane, as is the case for CESAs (Kimura et al., 1999; Crowell et al., 2009; Gutierrez et al., 2009). Indeed, recent studies have indicated a plasma membrane locale for CSLD proteins in rice suspension culture cells (Natera et al., 2008) and Arabidopsis root hair cells (Neilson and coworkers, unpublished data, cited with permission). More work is needed to conclusively demonstrate the subcellular localizations for active, endogenous CSLDs.

Until recently, phenotypes from *cs/d* mutants in multiple species favored roles for these proteins in tip growth (Bernal et al., 2008). The moss, *Physcomitrella patens*,

where tip growth is the predominating form of cell growth, *CsID* genes comprise 46% of all expressed sequence tags from the Cellulose Synthase superfamily (*CesAs* and all *CsIs*) (Roberts and Bushoven, 2007). In higher plants, root hairs and pollen tubes provide classic models for cellular tip growth (Hepler et al., 2001; Cole and Fowler, 2006), but xylem fibers also elongate by intrusive tip growth (Mellerowicz et al., 2001; Samuga and Joshi, 2004). Expression of *CsID2* in developing xylem of *Populus* is thus consistent with its proposed influence on xylem fiber length and its role in tip-growing cells (Samuga and Joshi, 2004). Prior to the work reported here for maize *csld1* mutants, genetic studies of *CsID* genes were consistently interpreted in the context of CSLD contributions to the process of tip growth (Bernal et al., 2008). However, recent genetic studies indicate an alternate and/or additional role for CSLD proteins (Chapter 4; Bernal et al., 2007; Li et al., 2009).

Although *CsI* genes are found in fairly large gene families, and some of these genes may function in overlapping or redundant fashions, many act in a non-redundant, organ-specific, or developmentally-controlled manner. Large gene families for cell-wall biosynthetic enzymes may be related to the complexity and diversity of the many cell wall polysaccharides (Reiter, 2002; Coutinho et al., 2003). By characterizing individual *CsI* gene knockouts in key species, clues to their functions may be revealed, and our understanding of cell wall biosynthesis improved.

Results

Bioinformatic Analyses of the *CsID* Genes from Maize, Rice, and Arabidopsis

The availability of fully-sequenced genomes for maize (Schnable et al., 2009; Van Erp and Walton, 2009), rice (Yu et al., 2002; Goff et al., 2002; Hazen et al., 2002), and Arabidopsis (Arabidopsis Genome Initiative, 2000; Richmond and Somerville, 2000)

allowed identification of *Cellulose Synthase-Like D (CsID)* gene families in these species (Fig. 3-1). These families were relatively small, with five to six members. Among the cellulose synthase superfamily, the *CsID* subgroup stands out as having the longest coding sequences, as well as particularly small introns (70 to 110 bp) and large exons (Fig. 3-1). The *CsID* genes typically have well-conserved intron-exon boundaries, delineating two to four exons. Exceptions included maize *CsID2*, which has the largest intron (546 bp) of the *CsIDs* examined. Only three other *CsID* genes had introns longer than 200 bp (*Os-CsID2*, *Os-CsID4*, and *At-CsID3*) (Fig. 3-1). Also, *At-CsID1* had five introns, two more than any other *CsID* gene, and no introns were evident in *Os-CsID5* (Fig. 3-1). Both *Zm-CsID3* and *At-CsID6* had apparent five-prime deletions, with the coding sequence of these genes starting at a point well within what would be the first exon of the other *CsID* genes (Fig. 3-1).

Translation of each full-length *CsID* coding sequence was predicted to produce a protein product from 1000-1250 amino acids (with the exception of the five-prime truncated *Zm-CsID3* and *At-CsID6*) (Fig. 3-2). A high degree of conservation was indicated for numbers and locations of transmembrane domains within the CSLD proteins (predicted using TMHMM [cbs.dtu.dk/services/TMHMM]). These domains are thought to be important for protein conformation and/or localization, and thus function (Somerville, 2006). While the degree of confidence for individual transmembrane domains varied considerably, each CSLD protein sequence was predicted to contain six carboxy-terminal, and two amino-terminal, transmembrane domains (with the exception of *At-CSLD5*, which was predicted to contain a single amino-terminal domain) (Fig. 3-2). Of the six carboxy-terminal domains, the fourth from that terminus showed the greatest

range in probability scores among the CSLD proteins. Amino-terminal domains showed the lowest probability scores in Zm-CSLD1, At-CSLD5, and Os-CSLD4 (Fig. 3-2).

A key feature of CSLD proteins are the RING-type Zn-finger-like domains they are thought to share with the CESAs (Richmond and Somerville, 2000). To test for the presence/absence of these domains, as well as their similarity to those of CESAs, protein sequences for each of the CSLDs of Arabidopsis, maize, and rice, as well as two CESAs, were examined using SMART (smart.embl-heidelberg.de), a domain prediction web tool (Schultz et al., 1998; Letunic et al., 2009). While this program recognized RING-type Zn-finger domains in both CESA proteins with high confidence, only six of sixteen CSLD proteins contained sequences recognized by this program as having Zn-finger similarity, and those at low probabilities (scored below the threshold for significance) (Fig. 3-2). Direct examination of protein sequence alignments, however, revealed a highly-conserved motif with strong similarity to CESA RING-type Zn-finger motifs in all but four of the CSLD proteins. Exceptions were predicted to carry five-prime truncations (see Fig. 3-3). Eight highly-conserved cysteine residues matching those of the RING domain of the CESA proteins, and oriented in a way compatible with Zn-finger organization (Fig. 3-3), indicate that these CSLD proteins may indeed contain functional domains, despite their not being recognized by SMART.

Active sites for glycosyltransferase family-2 processive glycosyl transferases typically include the D,D,QxxRW conserved residues (Richmond and Somerville, 2000). This motif was readily identified in all of the CSLD proteins examined from maize, Arabidopsis, and rice (Figs. 3-2,3-3). Examination of 35 amino acid residues

surrounding this motif revealed very strong sequence conservation in each of the 16 CSLD proteins and both CESA proteins examined (Fig. 3-3).

Alignment of the CSLD proteins from maize, Arabidopsis, and rice, along with two Arabidopsis cellulose synthases (At-CESA1 and At-CESA7) revealed the extent of conservation among the CSLDs and between the CESAs and the CSLDs (Fig. 3-3). Near-perfect alignment was observed between large portions of these proteins, including transmembrane domains (evident by conserved regions of densely-packed hydrophobic residues), as well as substrate-binding and catalytic sites (Fig. 3-3). More significant changes between CSLD proteins were observed in predicted RING-type Zn-finger motifs, although near-perfect alignment was observed in the cysteine residues noted above (Fig. 3-3).

Phylogenetic analyses revealed three clades in the CSLD subfamily that correspond to three phenotypic classes among *csld* mutants described here and elsewhere (Fig. 3-4). In Arabidopsis, *CsID1* and *CsID4* are implicated in pollen tube growth (Bernal et al., 2008), whereas *CsID2* and *CsID3* act in root hair formation (Favery et al., 2001; Wang et al., 2001; Bernal et al., 2008), and *CsID5* disruption reduces overall plant growth (Bernal et al., 2007). Thus far, mutants of the most closely related *CsID* genes in rice and maize yield phenotypes that appear analogous to those of Arabidopsis. Rice *CsID1* (Kim et al., 2007), and its maize homolog, *CsID5* (Penning et al., 2009), result in root hair-deficient phenotypes. Disruption of rice *CsID4* (closest homolog of Zm-*CsID1* and At-*CsID5*), confer a *narrow-leaf and dwarf1 (nd1)* phenotype (Li et al., 2009). Similar functional roles are indicated by the reduced-growth phenotypes common to all three of these mutants (Chapter 4, Bernal et al., 2007; Li et

al., 2009). Collectively, data indicate conservation of specific developmental roles for individual CSLD proteins between Arabidopsis, rice, and maize.

Expression Profiles of the Maize *CsID* Genes

To evaluate the likely sites of action for each of the maize *CsID* genes, mRNA levels were determined by quantitative RT-PCR for selected maize tissues and developmental stages (Fig. 3-5). Each gene showed a distinctive pattern of expression, with the exception of *CsID3* and *CsID4*, whose patterns differed only in magnitude from one another (Fig. 3-5). Expression of most *CsID* genes was consistently low, compared to that of other genes in these tissues (data not shown). By far the greatest level of expression was that measured for *CsID4* (with *CsID3* close behind) in anthers 2 days before anthesis. The broadest expression profile was observed for *CsID2*, which was expressed in most tissues examined, including above- and below-ground structures, as well as in both vegetative and reproductive organs. In contrast, *CsID1* expression was more specific, having most abundant transcript levels in developing leaf blades and coleoptiles with enveloped young leaves. While *CsID5* mRNA was detectable in diverse tissues, levels were greatest in root hair cells (Fig. 3-5).

By tissue, the *CsID* gene with maximal expression in coleoptiles, shoot apical meristems, and developing leaves was *CsID1* (Fig. 3-5). Young and mature leaf blades were highest in *CsID5* mRNA, whereas midribs showed relatively high levels of *CsID2*, *CsID3*, *CsID4*, and *CsID5* expression. No *CsID* gene was detected at high levels in either mature stems or primary roots. The most highly-expressed gene in both silks and ligules was *CsID2*, whereas root hairs had elevated levels of *CsID5*, and ovaries showed significant expression of *CsID2*, *CsID3*, and *CsID4*. Finally, anthers had very high expression of both *CsID3* and *CsID4* (Fig. 3-5).

Reverse Genetic Screens for *csld* Mutants

Single-gene knockout mutations were sought for individual members of the maize *CsID* gene family by reverse genetic screening of around 15,000 lines from the UniformMu maize population (Yong et al., 2005; Penning et al., 2009). Mu transposon insertions were identified in *CsID1* (see Chapter 4) and *CsID5* (see below). No heritable insertions were recovered in *CsID2*, *CsID3* or *CsID4*.

Screening identified a Mu transposon in exon 2 of *CsID5* in UniformMu Grid 1 (coordinates X-13 and Y-37), indicating presence of a putative knockout mutant in UniformMu family 02S-1039-15. Seeds from this family were planted, grown, and tested for the presence of a Mu insertion. Results showed a heritable insert in *CsID5* with normal Mendelian segregation patterns in over 200 PCR-genotyped individuals (data not shown). Plants carrying the Mu insertion were back-crossed to W22 inbred progenitors for an additional three generations to establish the *csld5-1* line. Above-ground characteristics of plants homozygous for this mutation showed no visible abnormalities in plant height, growth rate, flowering time, or accumulated biomass (data not shown). However, examination of *csld5* mutant seedlings grown on germination paper revealed a near-complete lack of root hairs (Fig. 3-6).

Linkage between the root hair-deficient phenotype and the *Mu* insert in *CsID5* was confirmed by testing for the phenotype in an *Ac*-insertional allele with a transposon inserted upstream of the *csld5-1* allele in exon 1 (accession [AC027037] was obtained from the *Ac/Ds* collection at Cornell University, courtesy of Tom Brutnell [Kolkman et al., 2005]). Mutants from this line (established as *csld5-2*) were phenotypically identical to those of the *csld5-1* line (data not shown). Offspring of reciprocal crosses between

csld5-1 and *csld5-2* parents consistently showed the root hair-deficiency, conclusively linking disruption of *Cs/D5* with the phenotype.

Analysis of *csld5* Mutants

In-depth examination of primary roots from seedling-stage, *csld5* mutant and wildtype plants revealed that in the mutants, root hairs initiated but usually failed to elongate (Fig. 3-6). Although typical wildtype root hairs grew to around 600 μm , those of *csld5* mutants seldom elongated much after initiation, and in the rare instances of substantial growth, reached only around 300 μm (Fig. 3-6). From SEM analyses, it is estimated that as few as one in fifty root hairs grew to longer than 100 μm in *csld5* mutants. The majority of *csld5* mutant root hair initials appeared swollen and bulging, often wider at the base than typical wildtype root hairs (Fig. 3-6). Only root hairs appeared to be affected, since other root cells, including epidermal and internal cells, appeared to be normal in *csld5* mutants (Fig. 3-6). Under all growing conditions tested (from field to greenhouse and germination trays) plus a range of stresses, *csld5* mutant plants behaved no differently from wildtype plants as far as growth rates and flowering times. Above ground phenotype and biomass accumulation did not differ (data not shown).

Root-hair Transcriptome Profiling

Specificity of the root-hair phenotype in *csld5* mutants raised broader questions about distinctive features of gene expression and cell wall biosynthesis in this cell type. To obtain more global data on transcripts in these cells, we profiled mRNAs of root hairs from seedlings of W22 and B73 inbreds, and from their F1 hybrid progeny. We used three-prime anchored, 454 transcript sequencing, which allowed quantitative measurements of relative transcript levels without alignment to a reference genome

(each sequence read could be immediately assigned identity due to its 3'-anchor) (Eveland et al., 2008). A single titration run (1/16 plate) on a 454, GS-20 sequencer (Roche Biosciences, Indianapolis, IN) yielded 79,448 sequences corresponding to 10,618 unique transcripts, 6,273 present as 2 or more reads. Annotation of the 100 most highly-expressed genes based on similarity to previously-described genes, indicated that many of the most-abundant mRNAs were involved in amino acid metabolism, cell wall modification, and redox regulation (Fig. 3-7). Maize *CsID5* was not among the genes identified in this screen, presumably because of low expression.

Discussion

The *CSLD* Genes are Highly-conserved Among Diverse Species

The cross-species conservation of *CsID* gene copy number, intron-exon boundaries, gene size, and protein domains (Figs. 3-1, 3-2) are indicative of long-conserved function and strong selection against mutations. Compared to *CesA7* and other *CesAs*, *CsIDs* have remarkably few introns for such large genes (Fig. 3-1). Intron number and position can be important to gene regulation in a number of instances (Clancy and Hannah, 2002; Jeong et al., 2007; Rose et al., 2008), but whether differences between *CsIDs* and *CesAs* reflect functionally-significant aspects remains unclear. Either way, the similarities between *CsID* genes and *CesA* genes are consistent with a close relationship between these two gene subfamilies and have been used to support suggestions of a similar catalytic function (Doblin et al., 2001; Richmond and Somerville, 2001). Truncations to the five-prime regions of *Zm-CsID3* and *At-CsID6* result in loss of the RING-type Zn-finger-like domain thought to function in protein-protein interactions, supporting the possibility of these genes being non-functional pseudogenes.

The conservation of transmembrane domain position and number in the CSLD proteins indicates their importance for function (Fig. 3-2). In CESA proteins, these domains are thought to function together in forming a channel through the plasma membrane, through which the elongating glucan chain is excreted into extracellular space (Somerville, 2006; Zhang et al., 2009). Interestingly, the three proteins with amino-terminal transmembrane domains having the lowest probability of maintaining membrane-spanning capability (based on TMHMM predictions) are the same that result in the reduced-growth phenotypes when disrupted (Zm-CSLD1 [Chapter 4], At-CSLD5 [Bernal et al., 2007], and Os-CSLD4 [Li et al., 2009]). Although mutant phenotypes indicate that these three proteins have an *in vivo* function, they have either lost one or more transmembrane domains, or the domains have remained functional while diverging enough to not be recognized by TMHMM.

The active site of the sixteen CSD proteins analyzed here is extremely well conserved. Within the 35 amino acids surrounding the active site, there are only three amino acid differences likely to alter properties at that site (Fig. 3-3). In contrast, the Zn-finger-like domain and the transmembrane domains both showed considerably more variation between CSLD proteins (Fig. 3-3 and 3-2, respectively).

Conservation of Developmental Roles are Indicated by Phenotypic Similarities Across Taxa

Comparative phylogenetic analysis, combined with mutant phenotypes described here and elsewhere, indicate ancient functional divergence and highly-conserved developmental roles for sub-groups within the *CsID* gene family (Fig. 3-4). When mutant phenotypes from maize, rice, and Arabidopsis were overlaid on a neighbor-joining tree,

CSLD clades corresponded to distinct classes of phenotypes. These were: (i) root-hair-defective, (ii) male-transmission-defective, or (iii) reduced-growth (Fig. 3-4).

Several additional aspects of this association included, first, that all of the *csld* mutants identified thus far have visible phenotypes (Favery et al., 2001; Wang et al., 2001; Bernal et al., 2008, 2009; Kim et al., 2007; Li et al., 2009; Penning et al., 2009). Second, the associations shown in Figure 3-4 persist despite fundamental structural differences between the primary cell walls of Arabidopsis (Type I walls) and those of rice and maize (Type II walls) (Harris and Hartley, 1980; Carpita and Gibeaut, 1993; Carpita, 1996; Carpita et al., 2001). Roles of *CsID* genes thus apparently transcend major differences in non-cellulosic cell wall constituents between diverse plant species, and individual *CsID* genes appear to have maintained their primary developmental roles. Third, previous results suggested specific functions for CSLD proteins in tip-growing cells (Bernal et al., 2008), but data here and elsewhere indicate broader developmental roles as well.

Specificity of Expression Argues for Strictly-defined Roles for *CsID* Genes

Quantitative RT-PCR of individual maize *CsID* genes revealed distinct expression patterns (except for *CsID3*, a predicted pseudogene with a large deletion in its amino terminus) (Figs. 3-1, 3-2). These expression patterns contrast with those of *CesA* genes, which show apparently coordinated expression among defined subsets of the gene family (Burton et al., 2004; Nairn and Haselkorn; 2005). Coordinate expression of *CesA* subgroups is considered consistent with the hypothesis that the CESA proteins act together in functional rosettes. No obvious pattern of co-expression was observed between any of the *CsID* genes, indicating either a capacity to function alone, or at least independently of strictly-defined partners. The possibility remains that different

combinations of CSLD and/or CESA proteins may function together in an as-yet-undefined manner. Nonetheless, the well-defined expression pattern for each of the *CsID* genes is consistent with proposed specificity of function (Fig. 3-5). Also, although genetic studies of *csld* mutants have consistently indicated a role for CSLD proteins in tip-growing cells, the expression profiles of the *CsID* genes suggest potentially broader roles. No obvious tip-growth occurs in cell comprising many of the tissues in which relatively strong expression of one or more *CsID* gene was observed (Fig. 3-5). Developing leaves, silks, and ovaries, for example, have relatively abundant *CsID* gene expression, but few cells in these organs appear to use tip-growth-like mechanics.

The root hair-defective phenotype of *csld5* mutants (Fig. 3-6), is consistent with patterns of expression for the *CsID5* gene. Greatest levels of *CsID5* mRNA were observed in isolated root hairs (Fig. 3-5). In contrast, growing primary roots show little expression of *CsID5*, despite containing growing root hairs. The difference between expression in root hairs alone and whole root tips indicates the specificity of expression for this gene, which seems to be essentially limited to a single cell type in growing primary roots.

Functional *CsID5* is Required for Maize Root-hair Elongation

The lack of elongated root hairs on *csld5* mutants indicates a role for this gene product in the formation of new cell wall at the growing tip of these classic tip-growing cells (Fig. 3-6). Interestingly, *CsID5* is not required for initiation of root hairs, only their elongation (Fig. 3-6). The process through which a trichoblast cell initiates root hair formation has been extensively studied, and involves intense, coordinated cell wall modification and biosynthesis (Szymanski and Cosgrove, 2009; Anderson et al., 2010). Wall-loosening enzymes are focused at the site of root hair formation, and new cell wall

biosynthesis is targeted to the site via actin-mediated re-organization of the endomembrane system (František et al., 2000). That *csld5* mutants initiate root hairs indicates that CSLD5 is not essential to this process. One or more other CSLD enzymes may contribute to the first steps of root hair formation, or perhaps there is partial redundancy, with *Cs/D5* essential only during the most rapid phase of root hair growth.

In Arabidopsis *csld3* mutants (homologous to maize *Cs/D5*), root hairs have been reported to burst at the tip, release cytoplasm, and cease growth (Wang et al., 2001). Similar bursting does not appear to occur in root hairs of maize *csld5* mutants. Indeed, SEM analyses of *csld5* root hairs show them to be short, but intact (Fig. 3-6). The mutant root hairs are swollen and uneven compared to wildtype, but they do not appear ruptured (Fig. 3-6). Why some mutant root hairs undergo partial elongation (up to 250 μm), while the majority terminate growth much earlier remains unclear. One possibility is that another CSLD protein is able to partially compensate for loss of CSLD5, or rare instances of root hair growth could occur without the specific polysaccharide contribution of CSLD5. In Arabidopsis, mutations in either *Cs/D2* or *Cs/D3* result in aberrant root hairs, indicating either cooperation of those two gene products or limited redundancy (Favery et al., 2001; Wang et al., 2001; Bernal et al., 2008). From both the phylogenetic analysis (Zm-CSLD2 is closest to At-CSLD2 [Fig. 3-4]) and transcription profiles (Fig. 3-5), the most likely candidate for compensating for CSLD5 loss is CSLD2.

Transcript profiles from maize root hairs reveal the complexity of genetic activity in this single cell type (Fig. 3-7). The failure to detect *Cs/D5* transcript in this analysis is consistent with a relative scarcity of this mRNA compared to the more abundant

transcripts. If an arbitrary “abundance” score is set at detection of 10 mRNAs, at least 1,210 other genes are expressed at a higher level than *Cs/D5* in this cell type.

Presence of a mutant phenotype indicates that expression of this gene at some level is important to normal root hair elongation, but apparently a very small amount of this mRNA is sufficient. In either case, mRNA levels do not necessarily reflect CSLD5 protein levels, which could well be higher if the protein is long-lived.

The most highly expressed genes included many with high homology to genes of known function, and others that were not similar to any previously-characterized genes (thus were annotated as hypothetical or unknown). Genes for cell-wall modification, redox regulation, and amino acid metabolism were predominant. The 50 most highly expressed mRNAs included genes for a beta expansin, an arabinogalactan protein, and two xyloglucan endotransglycosylases (Fig. 3-7). Also in the top 50 genes were those encoding two adenosylmethionine synthases, two methionine adenosyltransferases, multiple transporter proteins, ubiquitin-related proteins, and redox-related proteins (Fig. 3-7).

Also evident in the root-hair transcript profiles were differences in the most abundant mRNAs between the three maize lines tested (B73, W22, and their hybrid). Most genes were expressed at similar levels in all lines (based on read numbers, normalized for total per library). However, there were also multiple cases showing very different expression of certain genes in W22 and B73. For instance, the most highly expressed gene in B73 (described in Figure 3-7 as a hypothetical protein) was expressed at very low levels in W22 (802 transcripts sequenced for B73, compared to 3 for W22). For the hybrid, transcript levels for most genes indicated additive effects,

being detected at levels between that of B73 and W22 (Fig. 3-7). In other instances, non-additive effects were observed, with apparent expression of a given gene in the B73-W22 hybrid much higher or lower, respectively, than in both inbreds (Fig. 3-7). The most highly expressed gene in the hybrid (again a hypothetical protein) ranked much lower in the expression profiles of both inbreds. The reverse was also observed in multiple instances, where a gene not detectable in the hybrid was expressed at relatively high levels in both inbreds.

Methods

Bioinformatic Analyses of *CsID* Genes from Maize, Rice, and Arabidopsis

Full-length coding sequences from each of the CSLD genes in maize, rice, and Arabidopsis were compared to genomic sequence to identify exon-intron boundaries. Coding sequences were used to predict amino acid sequences, using a web tool at changbioscience.com/res/rest. Each of these predicted amino acid sequences, as well as that of Arabidopsis Cellulose Synthase A 7 (At-CESA7), was independently analyzed with the protein domain-prediction software SMART (smart.embl-heidelberg.de) to test for presence of RING-type Zinc-finger-like domains. Proteins for which SMART failed to detect RING domains were manually examined after alignment with ClustalW for similar amino acid sequences. Putative trans-membrane domains were identified by TMHMM for each predicted protein (cbs.dtu.dk/services/TMHMM).

Phylogenetic Analyses

The neighbor-joining tree was created using Mega 4.0 (Tamura et al., 2007; megasoftware.net), with ClustalW-generated alignments of protein sequences predicted from full length cDNAs for each of the CSLD genes from rice, maize, and Arabidopsis. The resulting tree represents 2,000 bootstrap repetitions using the pairwise deletion

option. Nomenclature for proteins encoded by the *Cs/D* gene family in maize was assigned as per Van Erp and Walton (2009).

Real-Time RT-PCR

For each sample, RNA was extracted from approximately 200 mg of tissue, initially frozen in liquid nitrogen, then homogenized in 1.0 mL Trizol (Invitrogen Cat # 15596-018) using a Q-BIOgene FastPrep 120 with Lysing Matrix D (MP Biomedicals Cat # 116913). Samples were incubated for 5 min at 25°C, with frequent vortexing. Chloroform (200 µL) was added and samples were vortexed 15 sec before and after a 1-min incubation at 25°C. Phases were separated by centrifuging 10 min at 15,000 x g, followed by transfer of 200 µL of the aqueous layers to 700 µL of Qiagen RLT buffer (from RNeasy Plant Mini kit, Qiagen Cat # 74904). Ethanol was added (500 µL, 100% EtOH) and samples were vortexed. Half of the resulting volume was used to clean and elute total RNA as per the RNeasy Plant Mini kit (Qiagen Cat # 74904). Resulting RNA was treated with DNase-1 (Ambion Cat # AM1906), and quantified using a BioRad SmartSpec 3000. The cDNA was synthesized using a SuperScript One-Step kit and protocol (Invitrogen Cat # 10928-042).

Levels of mRNA were quantified from selected maize tissues at a range of developmental stages using quantitative Real-time RT-PCR (Step One Plus Real-Time PCR System [Applied Biosystems]). At least three biological replicates were analyzed for each tissue or time point, and for each of these replicates, reactions were performed in duplicate. A given reaction included 10 µL Fast SYBR Green Master Mix (ABI Lot # 1003024), 5.0 µL of cDNA sample (diluted 10x from cDNA reaction), and 100 nM of each gene-specific primer (Table 3-2) in a final volume of 20 µL. The relative abundance of transcripts was normalized with 18S rRNA controls (Taqman Ribosomal

RNA Control Reagents, ABI Lot # 0804133) as in Eveland et al., 2008. Primer pairs for all genes were designed using Primer Express 3.0 (ABI).

Reverse Genetic Screening

The UniformMu population was screened using PCR-based assays to identify Mu transposon insertions in each of the maize *Cs/D* genes as per Penning et al., (2009). Close to 15,000 UniformMu lines were screened using a series of pooled DNA samples. These lines were forerunners of the sequence-indexed materials currently available at MaizeGDB (maizegdb.org; UniformMu.UF-genome.org). For PCR screening, gene-specific primers were used along with TIR6, a Mu-specific primer (Table 3-2). Resulting products were separated on 1% agarose gels, blotted onto nylon membranes, and probed with gene-specific PCR products. Where positive results were obtained in both x- and y-axes (as for *Cs/D1* and *Cs/D5*), seeds from the identified UniformMu family were planted, leaf tissue was harvested, and DNA was tested by PCR for segregation of homozygous mutants.

Growth Conditions for *cs/d5* Mutant Analyses

Maize seeds were sterilized by soaking in 15% bleach while stirring for 10 min, then rinsed thoroughly with water. Kernels were allowed to imbibe water overnight and pericarps were manually removed. Seeds were arranged on wet germination paper in glass trays with embryos facing up, sprayed with Captan solution (1% Captan), and covered in plastic wrap. Air was pumped through these trays to prevent CO₂ and ethylene build-up, and seeds were allowed to germinate.

Fixation and Sectioning

One-cm-long pieces of primary root from 10-day-old seedlings were collected and fixed in FAA (10% formaldehyde [Fisher Lot # 992720], 5% acetic acid, 50% EtOH).

Samples were vacuum infiltrated overnight at 4°C, then shaken at 4°C during a dehydration series using ethanol in PBS (60 min each, progressing from 1X PBS with 30% EtOH to 40%, 50%, 60%, 70%, 85%, and finally 95% EtOH). Samples were stained overnight with eosin in 95% EtOH, followed by four, 1-hr incubations in 100% EtOH and eosin at 25°C. Wax imbedding was initiated by introducing CitriSolv (Fisher Cat # 22-143975) into samples using a series of 1-hr incubations (while shaking) in ethanol with increasing CitriSolv/EtOH content (25/75, 50/50, 75/25, 100/0). Paraplast wax chips (Fisher Cat # 23-021-399) (1 g wax/mL CitriSolv) were added to the 100% CitriSolv and incubated overnight at 25°C. Additional wax was added, followed by a 2-hr incubation at 42°C. Samples were transferred to 60°C for 1 hr. Wax was poured-off and replaced eight times before samples were allowed to harden in molds. Sections (10 µm, cut with a Leitz 1512 microtome) were de-waxed with three, 5-min incubations in xylene (Fisher Lot # 083423), then washed twice in 100% EtOH (5 min each), and once in 95% EtOH (3 min). Slides were dried and examined under an Olympus BH2 light microscope.

Scanning Electron Microscopy

Primary roots, approximately 5-cm long from *csld5* mutant and non-mutant seedlings, were fixed in FAA (10% formaldehyde [Fisher Lot # 992720], 5% acetic acid, 50% EtOH), dehydrated in an ethanol series 75%, 95%, 100%, and critical point dried (Bal-Tec CPD030, Leica Microsystems, Bannockburn, IL). Dried samples were mounted with carbon adhesive tabs on aluminum specimen mounts, Au/Pd sputter coated (DeskII, Denton Vacuum, Moorestown, NJ), and examined with a field-emission scanning electron microscope (S-4000, Hitachi High Technologies America, Inc. Schaumburg, IL). Digital micrographs were acquired with PCI Quartz software.

Isolation of Root Hair mRNA

Maize seedlings were grown as above. When primary roots averaged 5 cm in length (10 days after germination), individual seedlings were suspended in liquid nitrogen until completely frozen. Root hairs were then harvested using a metal spatula to shatter them from the root body and into a small weigh boat of liquid nitrogen. Root hairs from around 150 individual seedlings were pooled to get approximately 100 mg, which were stored at -80°C until further use. A modified RNA extraction protocol was used to recover adequate amounts of RNA from root hairs. Total root hair samples were added to 200 µL of extraction buffer (50 mM TRIS [pH 8.0], 150 mM LiCl, 5 mM EDTA [pH 8.0], 1% SDS), and ground in liquid nitrogen. Samples were allowed to thaw and immediately transferred to tubes containing 200 µL of 1:1 Phenol-Chloroform, shaken, and placed on ice for 5 min, with periodic mixing. Samples were transferred to 2-mL Phase Lock Gel tubes (Eppendorf, cat # 2302830), and centrifuged (10 min, 10,000 x g, 4°C). After centrifugation, 200 µL of 1:1 Phenol-Chloroform was added, samples were well-shaken, then centrifuged (10 min, 10,000 x g, 4°C). Next, 200 µL of Chloroform was added, samples were shaken then placed on ice for 5 min, with occasional mixing for centrifuging (10 min, 10,000 x g, 4°C). The aqueous layer was poured into a new PHASE LOCK tube (Eppendorf) and 1 mL of TRIZOL (Sigma, Lot # MKBD6639V) was added. Tubes were shaken well for 15 sec and incubated at room temperature for 5 min. After incubation, 200 µL Chloroform was added, tubes were shaken, and incubated at room temperature for 3 min before centrifuging (10 min, 10,000 x g, 4°C). The aqueous layer was transferred to new microfuge tubes and 500 µL of Isopropanol was added. Samples were mixed and placed on ice for 10 min before centrifuging (10 min, 10,000 x g, 4°C) to precipitate RNA. Supernatant was removed by

pipetting, 1 mL 70% EtOH was added, and samples were centrifuged (5 min, 10,000 x g, 4°C). Supernatant was carefully removed by pipetting, pellets were allowed to air dry, and RNA was re-suspended in 30 µL water.

Three-prime Anchored 454 Sequencing

Libraries for 454-based sequencing were prepared as per Eveland et al. (2008). Total RNA (5 µg) from root hairs of B73, W22, and the B73 x W22 hybrid was used for cDNA synthesis (MessageAmp II, Ambion, Cat # AM1793) by priming with 6 pmol of biotinylated (T12) B-adaptor oligo (modified from Margulies et al., 2005) (Table 3-2). Purified cDNA (DNA clear, Ambion) was bound to M-270 Strepavidin Dynabeads (Invitrogen, Cat # 653.05), immobilized on a magnetic tube stand (Applied Biosystems, Lot # 0804015), and digested with *Msp1* (Promega) to create 2-base CG overhangs for adaptor ligation. A-adaptor oligos (modified from Margulies et al., 2005) included 3-base multiplex keys (Table 3-2). Adaptor pairs (top-strand and bottom-strand for each sample [Table 3-2]) were combined and concentrated to 1 pmol/µL in (10 mM Tris, 1 mM EDTA, 50 mM NaCl [pH 8.0]) and annealed by gradual 1°C/min decreases (95°C-4°C, holding at 72°C for 30 min). Adaptors (5 pmol) with the correct multiplex keys were ligated to digested samples. Unligated adaptors were removed by washing beads twice with 1X B&W (2.5 mM Tris-HCL [pH 7.5], 0.25 mM EDTA, 0.5 M NaCl) followed by two washes with water. The template strands were eluted with 100 mM NaOH, neutralized, and concentrated on a Qiagen column (from RNeasy Plant Mini kit, Qiagen Cat # 74904). Sequencing was conducted as per Margulies et al., (2005) on a 454 GS-20 instrument (Roche Biosciences, Indianapolis, IN).

Analysis of 454-generated Sequence Data

Trimmed 454 reads were filtered for valid key-code sequences and ligation junction sites (CGG) at 5`-ends. Poly-A tails were trimmed to 6-A's at the 3`-end using custom, java-based programs (courtesy of Don McCarty). Trimmed sequences were assembled using CAP3 (genome.cs.mtu.edu/sas). The nonredundant set of consensus cDNA sequences were annotated by BLASTN searches of cDNA databases for maize. These included publicly available cDNAs on maizegdb.org and IUC, a collection of cDNAs provided by an industry consortium via a user's agreement (maizeseq.org).

Accession Numbers

Accession numbers for each of the gene sequences are *At-CsID1*:AT2G33100.1, *At-CsID2*:AT5G16910.1, *At-CsID3*:AT3G03050.1, *At-CsID4*:AT4G38190.1, *At-CsID5*:AT1G02730, *At-CsID6*:AT1G32180.1, *Os-CsID1*:AC027037.6, *Os-CsID2*:Os06g0111800, *Os-CsID3*:AC091687.1, *Os-CsID4*:AK242601.1, *Os-CsID5*:Os06g0336500, *Zm-CsID1*:GRMZM2G015886, *Zm-CsID2*:GRMZM2G052149, *Zm-CsID3*:GRMZM2G061764, *Zm-CsID4*:GRMZM2G044269, *Zm-CsID5*:GRMZM2G436299, *At-CesA7*: AT5G17420.

Table 3-1. Three prime-anchored 454-sequencing transcript profiles.

	B73	B73xW22	W22	Combined
Total reads	27,675	36,816	14,957	79,448
Unique transcripts	5,634	6,815	3,972	10,618

Total reads from a single 454 titration run. Each library was key-coded prior to combining for sequencing. Total reads are the number of individual sequences recovered. Unique transcripts are the number of different genes represented based on alignment to cDNA collections.

Table 3-2. PCR primers utilized in Chapter 3.

For Real-Time RT-PCR		
Gene	Forward primer	Reverse primer
<i>CsID1</i>	GCCGCTCACGTCAATGG	CTGGGCATCTTCATGGAGTGT
<i>CsID2</i>	ACGTCTCCAACCTCCTTTCAC	CGGCTTCAACAGTGTC
<i>CsID3</i>	TCCATCGTGTGCGAGTTCTG	CAGCTTTGGCATCTGATCCA
<i>CsID4</i>	ATGAAGGCCGAGGAGCAGTA	CGCGTGACGCTGTTGAAC
<i>CsID5</i>	GGGCGCTTCATCAGCTACTC	GGACGTGGTAGTCCTGGAAGTC
For reverse genetic grid screening		
Gene	Forward primer	Reverse primer
<i>CsID1</i>	AGTTCGTGCACTACACCGTGACATCC	TGCTACCTGTAAGGACTGAGGATGGCCTG
<i>CsID2</i>	TCTCACTGTCCCCCGTGACCTTCTGGATG	ACTCTCCCAGGCTGATCCCCGACCACTTG
<i>CsID3</i>	GTCAAGATGGAGGACCTCGTTGACAAGCC	CTCCGCCATTGCTTCGAAGGTTAGCAGC
<i>CsID4</i>	CCAACAACAACACCGTCTTCTTCGACGGC	GTCTGCACGATGAAGAAGCCCCGAGAAGAG
<i>CsID5</i>	TTGTTCTCCATCCATCCAGGCTCCTC	TAGCACGCAAGCTTCTCGACGGGGTAGTC
TIR6	AGAGAAGCCAACGCCAWCGCCTCYATTTTCGTC	
For Three-prime-anchored 454 transcript profiling		
B-adaptor	Biotin- CCTATCCCCTGTGTGCCTTGCCTATCCCTGTTGCGTGTCTCAGTTTTTTTTTTTT T[AGC]	
B73 top	CCATCTCATCCCTGCGTGTCCCATCTGTTCCCTCCCTGTCTCAG <u>AGC</u>	
B73 bot.	CGG <u>TT</u> CTGAGACAGGGAGGGAACAGATGGGACACGCAGGGATGA	
W22 top	CCATCTCATCCCTGCGTGTCCCATCTGTTCCCTCCCTGTCTCAG <u>ACA</u>	
W22 bot.	CG <u>ATT</u> CTGAGACAGGGAGGGAACAGATGGGACACGCAGGGATGA	
BxW top	CCATCTCATCCCTGCGTGTCCCATCTGTTCCCTCCCTGTCTCAG <u>ATG</u>	
BxW bot.	CG <u>CTT</u> CTGAGACAGGGAGGGAACAGATGGGACACGCAGGGATGA	

For sublibrary oligos, 3-bp keys are underlined. BxW: B73xW22 hybrid. bot = bottom.

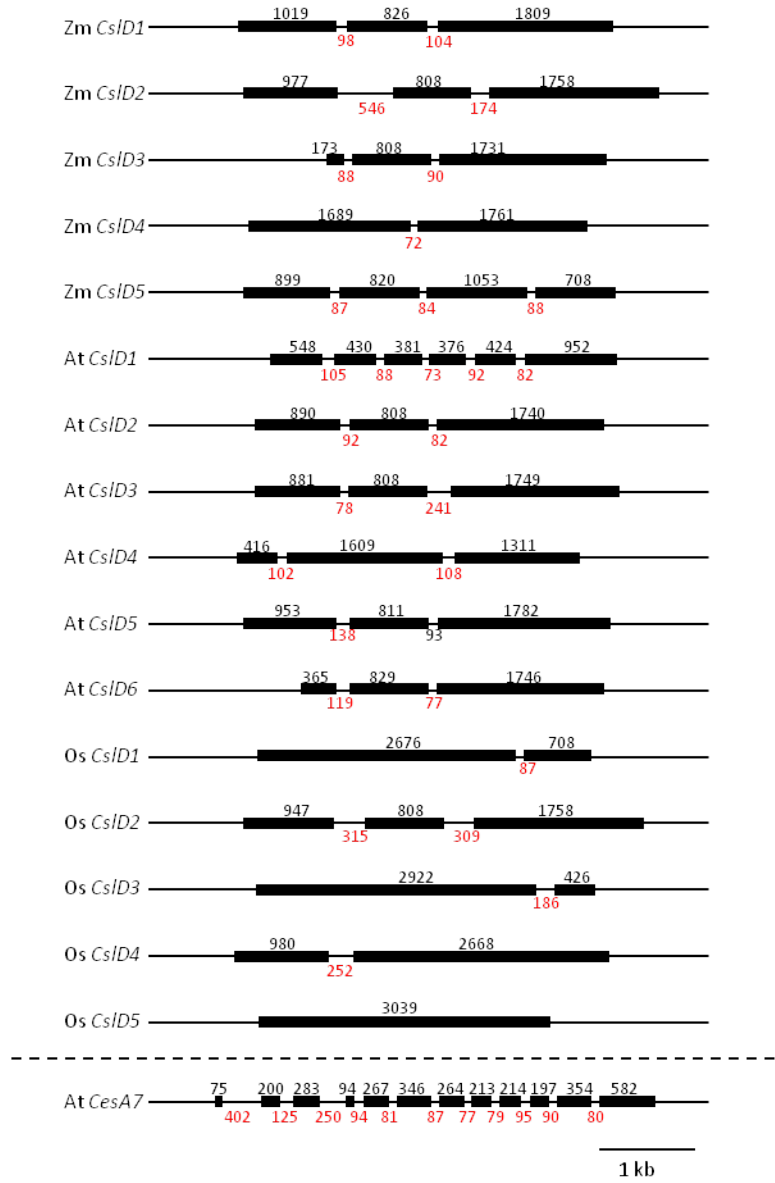


Figure 3-1. *Cellulose synthase-like D (CsID)* genes from Arabidopsis, maize, and rice. Each of the *CsID* gene coding sequences from maize (5), Arabidopsis (6), and rice (5), as well as Arabidopsis *CesA7*, are diagrammed with exon/intron locations and sizes drawn proportionally. Untranslated regions are not included. Exons are represented by black bars and their length is indicated above each. Intron lengths are indicated in red.

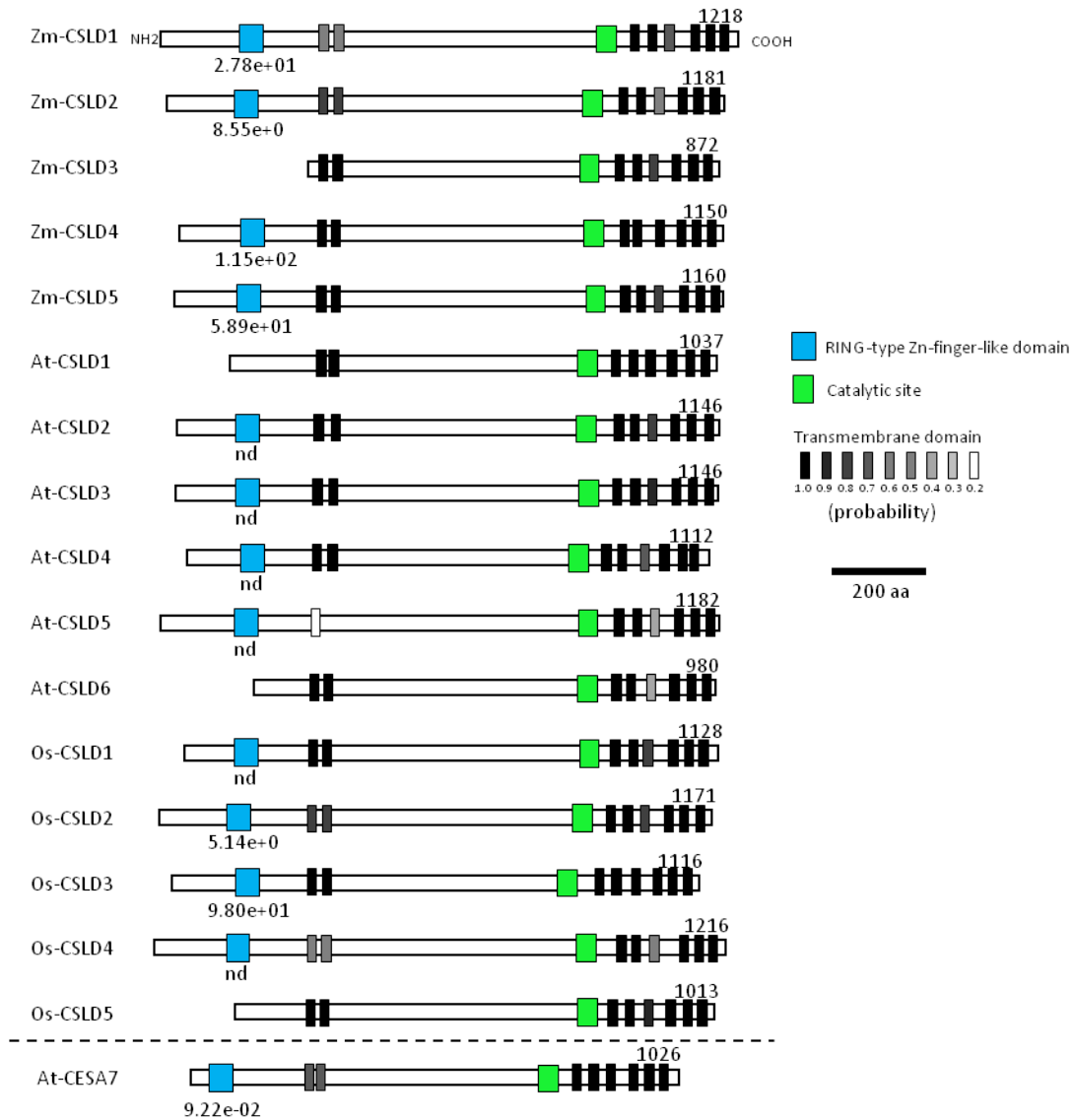


Figure 3-2. Cellulose synthase-like D proteins from Arabidopsis, maize, and rice. All of the CSLD proteins are diagrammed as predicted from translation of *CSLD* genes of maize (5), Arabidopsis (6), and rice (5). Protein length is indicated above each diagram. Transmembrane domain predictions were generated using TMHMM (cbs.dtu.dk/services/TMHMM). Color scale shows the probability of a transmembrane domain, based on TMHMM output. The Zn finger-like domains were predicted using SMART (smart.embl-heidelberg.de). E-values (from SMART output) for Zn-finger-like domains are indicated below each diagram, nd = not detected by SMART, but apparent in direct sequence visualization (see Figure 3-3).

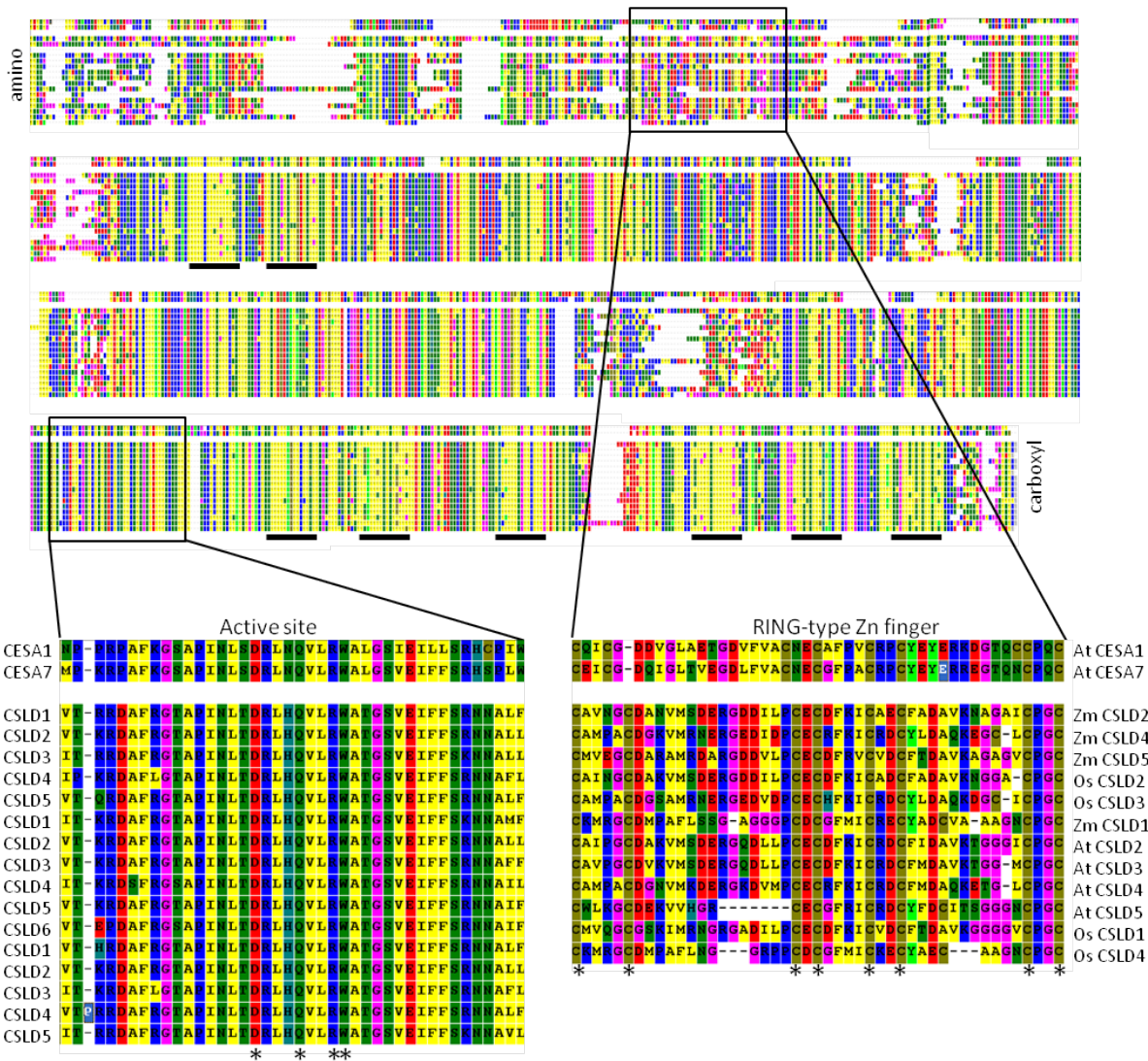


Figure 3-3. Protein sequence alignment and analysis of conserved motifs. All of the CSLD amino acid sequences from maize, Arabidopsis, and rice, as well as two Cellulose Synthases (At-CEA1 and At-CEA7) were aligned using MEGA 4.0 (www.megasoftware.net/). Predicted transmembrane domains are underlined. Domains of interest were expanded for detailed visualization. Near-complete conservation was observed at the predicted active site of all the CSLD proteins. Amino acids that characterize the GT family 2 processive glycosyltransferase (D, QxxRW) are starred. The alignment showing the RING-type Zn finger motifs was ordered by conservation of the domain, and does not include putative CSLD proteins that lacked this domain. Cysteine residues (expected Zn-binding sites) are starred. The only consistent difference between proteins for which SMART recognized a Zn-finger-like motif, and those it did not, was at position 17 of the RING-type domain (arrow).

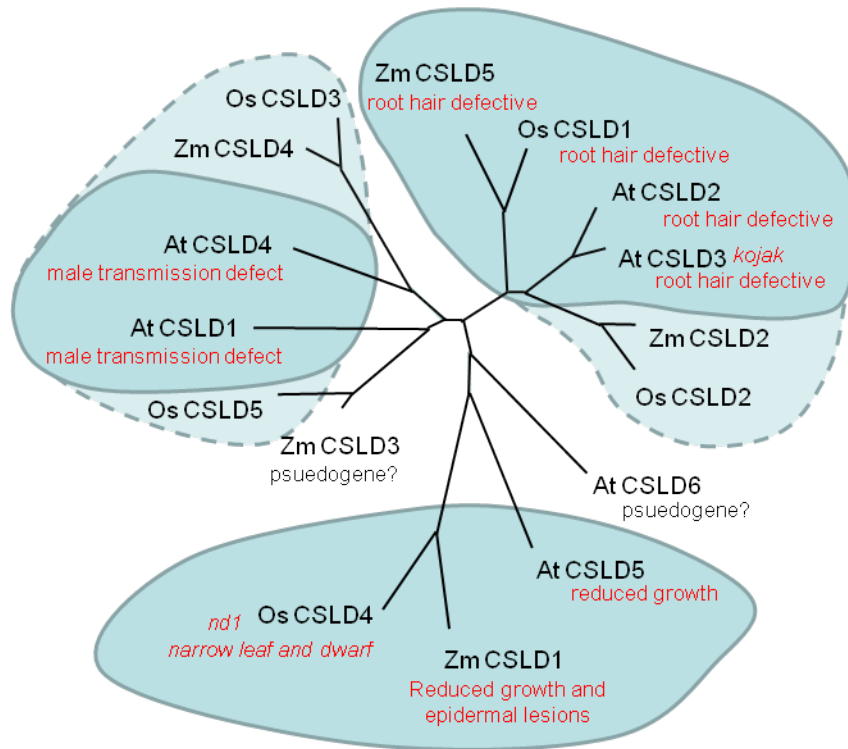


Figure 3-4. Comparison of mutant phenotypes to CSLD protein phylogeny. Neighbor-joining tree of predicted protein sequences encoded by *CsID* genes in maize, rice, and *Arabidopsis*. Reported phenotypes for null alleles are shown in red (Zm-CSLD5 [Penning et al., 2009], Os-CSLD1 [Kim et al., 2007], At-CSLD2 [Bernal et al., 2008], At-CSLD3 [Favery et al., 2001; Wang et al., 2001], At-CSLD5 [Bernal et al., 2007], Os-CSLD4 [Li et al., 2009], At-CSLD1 and At-CSLD4 [Bernal et al., 2008]). At-*CsID6* and Zm-*csld3* are predicted to be psuedogenes. The tree was created using Mega 4.0 (megasoftware.net/mega.html; Tamura et al., 2007), with 2,000 bootstrap repetitions and a pairwise deletion option. Units are in amino acid substitutions per site.

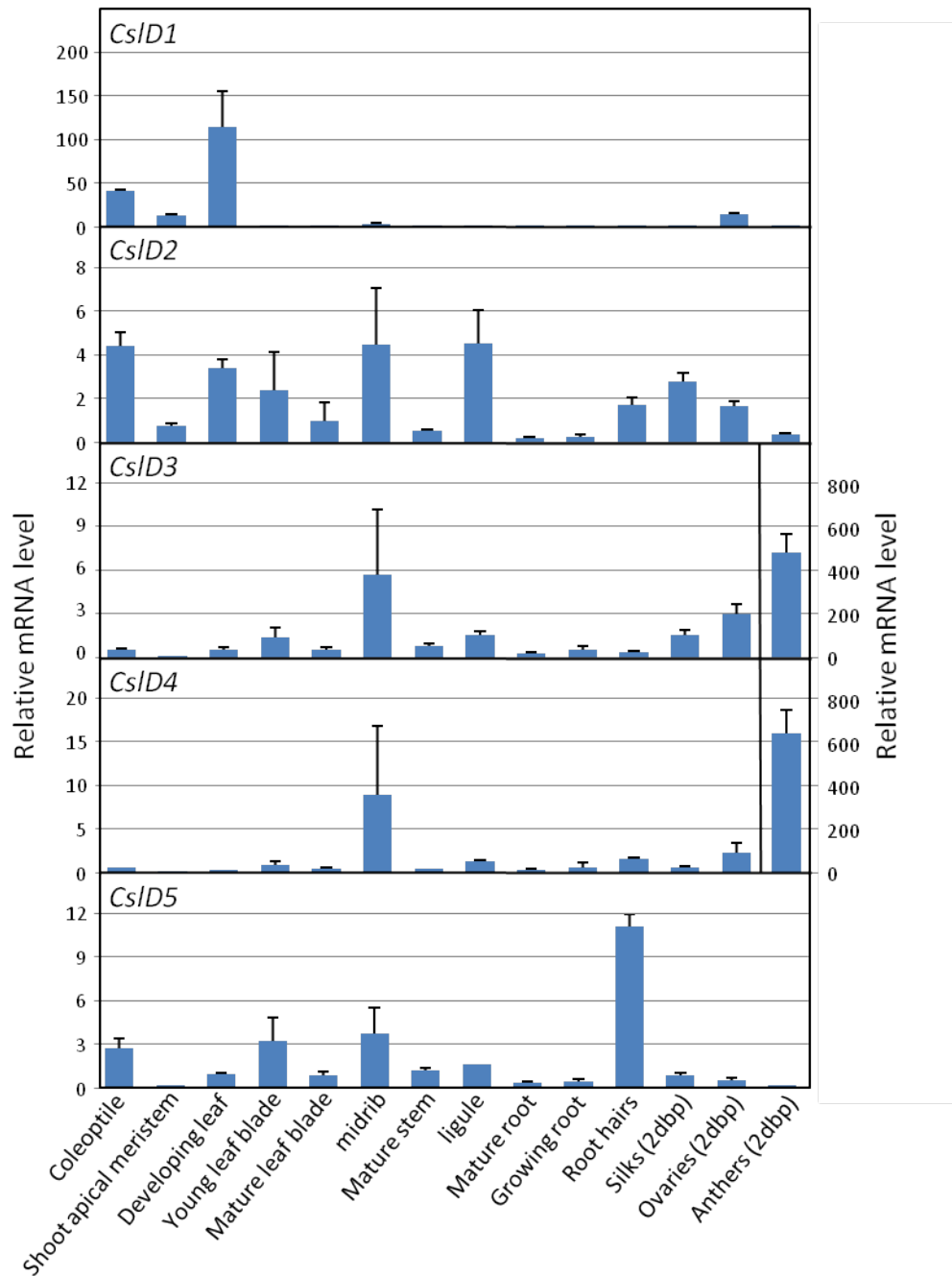


Figure 3-5. Quantitative RT-PCR showing mRNA levels of the maize *CsID* genes in selected tissues and stages of development. Error bars represent standard errors from three biological replicates. Note that the scale bar is different for each gene, and for *CsID3* and *CsID4* expression in anthers (2dbp). dbp = 2 days before pollination.

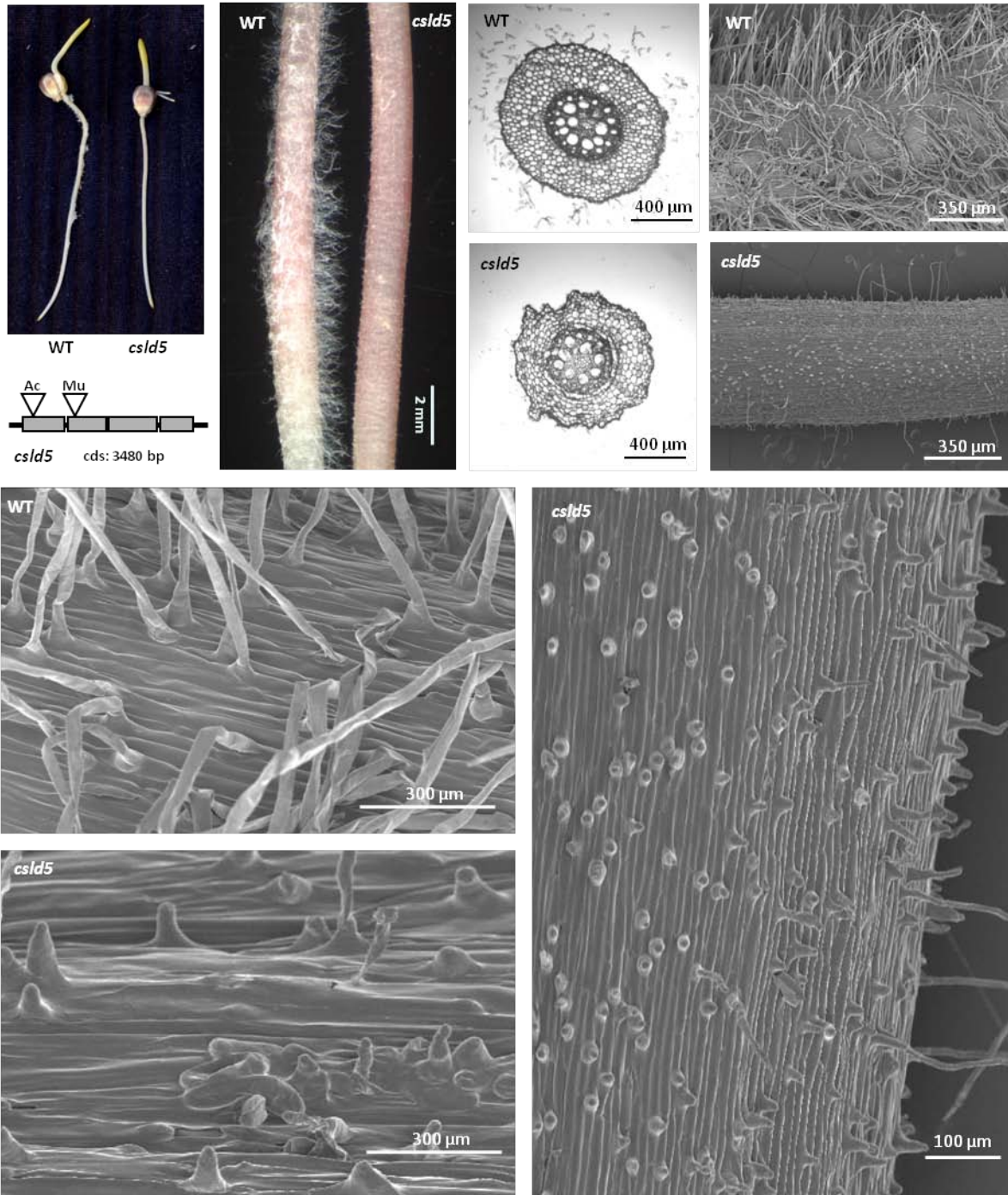


Figure 3-6. The root hair phenotype caused by mutation of *Cs/D5*. Note that although the *csld5* roots appear hairless, they retain a capacity to initiate-, but not necessarily elongate hairs (see hair initials).

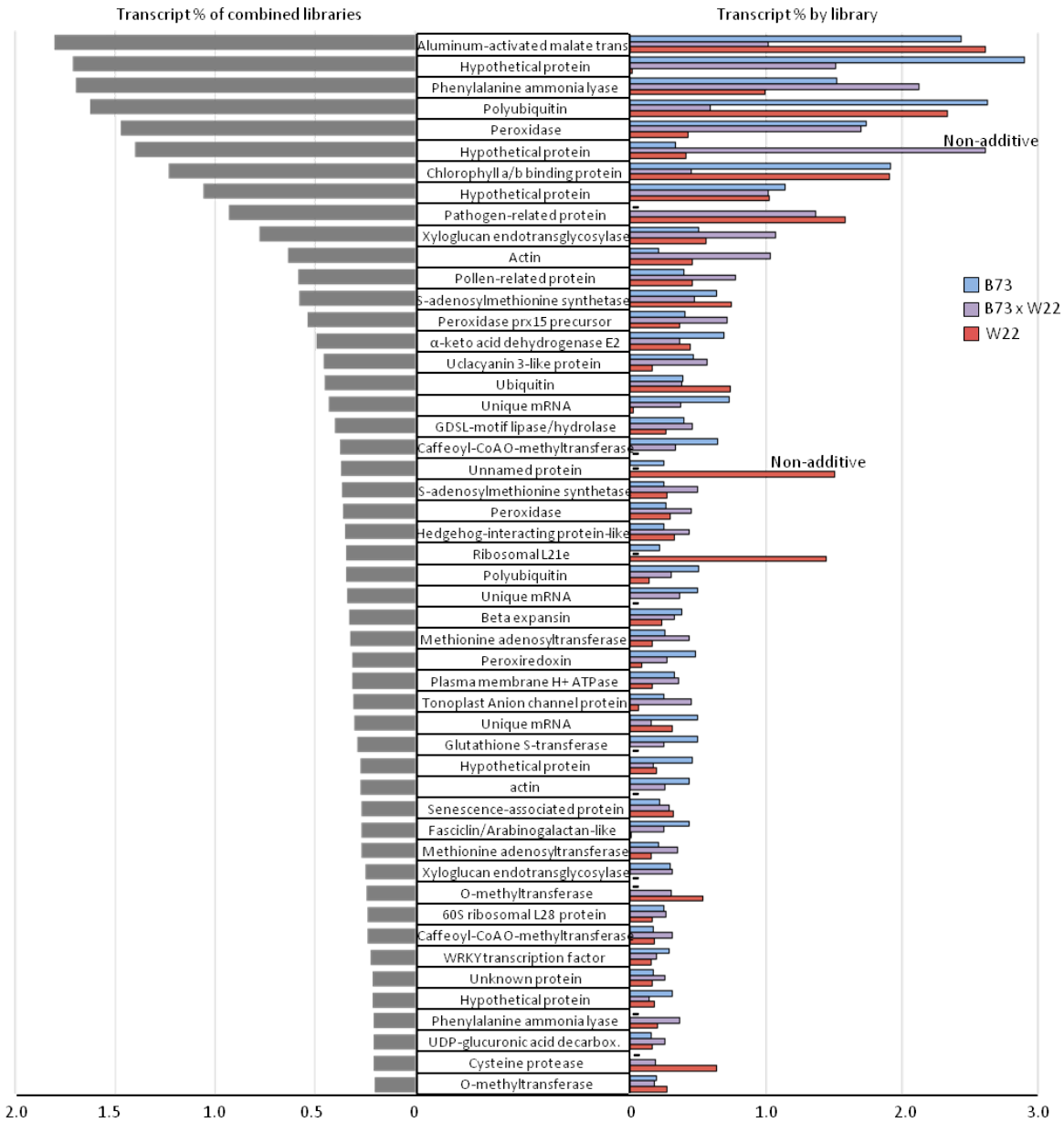


Figure 3-7. Transcript profiles of maize root hairs. Analysis of the 50 most highly-abundant transcripts as quantified by 3'-anchored 454 sequencing revealed genes related to cell wall modification, redox regulation, and amino acid metabolism, among others. Separate libraries were generated using cDNA from root hairs of B73, W22, and their F1 hybrid. Percentage of total reads represented by each gene when the three libraries were combined is charted on the left. Abundance in individual libraries for each gene is charted on the right, and shown as message level in proportion to each library separately.

CHAPTER 4
MUTATIONS OF *CELLULOSE SYNTHASE-LIKE D1* DISRUPT CELL DIVISION AND
LEAD TO A *NARROW-LEAF WARTY* PHENOTYPE IN MAIZE

Introduction

Plant form depends on coordination of cell division and selective cell expansion (Sylvester, 2000; Szymanski, 2009). Cell wall deposition is centrally important to both of these processes, forming cross walls *de novo* during cell division, and excreting new cell wall material and cell wall modifying enzymes during cell expansion (Cosgrove, 2005). Despite its central importance to plant biology, very little is currently understood about cell wall formation during cell division.

Investigations of maize mutants that show aberrant cell divisions, but maintain overall leaf shape, have led to the suggestion that an as-yet-undefined mechanism may maintain of leaf shape (Smith, 1996; Reynolds et al., 1998; Walker and Smith, 2002). For such a mechanism to accommodate aberrantly-shaped cells, some cells must develop in ways that compensate for malformed ones (Walker and Smith, 2002). The basis for such a mechanism remains uncertain.

The rigid walls of plant cells mean cytokinesis by constriction is impossible, and plants have, instead, evolved elaborate mechanisms of cell division. These involve cytoskeletal-based organization of cellular bodies and targeting of cell wall material to a defined division plane. In this process, Golgi- and endocytosis-derived vesicles containing cell wall polysaccharides, structural proteins, and enzymes, are targeted to the division plane, where they merge to form the cell plate (Samuels et al., 1995; Staehelin and Helpler, 1996; Smith 2001; Dhonukshe et al., 2006). As vesicles fuse with the cell plate, this structure expands radially, spreading from the inner cell to the parental walls at the cell boundaries. The position of a new wall, determined by actin-

myosin-dependent alignment of the cell plate, is defined by markers associated with the preprophase band (Gallagher and Smith, 1999; Chaffey and Barlow, 2002; Molchan et al., 2002). Others have highlighted the similarities between cell division and the targeted cell wall deposition seen in tip-growing cells such as root hairs (Bednarek and Flabel, 2002). Callose is thought to be among the first polysaccharides deposited at a new cell wall (Samuels et al., 1995; Hong et al., 2001). However, current unknowns include how cellulose, hemicelluloses, pectins, and structural proteins are delivered, synthesized, and meshed to form a functional wall.

Work presented here provides evidence for an unexpected, but integral role for CSLDs (see Chapter 3) in plant cell division. In *csld1* mutants of maize, defects in cell division are revealed as the probable cause for pleiotropic phenotypes that include reduction in plant growth, altered leaf morphology, distinctive epidermal warts, and changes in cell wall properties of stems. Analysis of leaf-blade epidermis shows that cells in *csld1* mutants are consistently wider and fewer in number compared to wildtype. This result, along with the close association between *csld1* expression and zones of cell division in basal regions of developing maize leaves, suggests a role for CSLD1 in cell division. Other evidence for cell division-related defects includes aberrantly-shaped epidermal cells, disruption of cell files, an abundance of mega-nucleate cells, and misplaced and partially-formed cell walls. These data provide new insights into the function of CSLD proteins during plant growth, expanding the understanding of their roles from that of tip-growth alone, to include cell division and consequent pleiotropic effects on development.

Results

An Allelic Series of *csld1* Mutants in Maize Enabled Functional Analysis

Seven independent loss-of-function mutants for the maize *Cs/D1* gene were identified in reverse genetic screens, including two from the UniformMu maize population (University of Florida) and five from the Trait Utilities System in Corn (TUSC) lines (Pioneer Hi-Bred International) (Fig. 4-1). The two UniformMu alleles, *csld1-1* and *csld1-2*, were examined in the greatest depth because of their uniform genetic background (McCarty et al., 2005). Phenotypes of *csld1-1* and *csld1-2* homozygous mutants, as well as offspring from their reciprocal F1 hybrids, were indistinguishable, thus demonstrating a causal role for the dysfunctional Zm-*Cs/D1* gene. These plants showed overall reduced growth, narrow leaves, and had a rough leaf texture due to warty protrusions from the mature leaf epidermis. Genotypic analysis of over 200 individuals from segregating families showed a 100% correspondence between this phenotype and homozygosity for the *csld1-1* mutation, as well as Mendelian segregation ratios typical of a recessive mutation (data not shown). Finally, the five other transposon insertions in *Cs/D1* (courtesy of Pioneer Hi-Bred Int.) also showed reduced vegetative growth, narrow leaves, and epidermal warts, regardless of the phenotypic variation and heterologous genetic backgrounds.

Plant Dry Weight and Organ Width are Reduced in *csld1* Mutants

Overall growth and organ size were reduced in homozygous *csld1* mutants (Figs. 4-2 and 4-3). However, general plant shape, leaf number, and flowering time, were similar for *csld1* mutant and wildtype progeny under field and greenhouse conditions (data not shown). Mean height of mutant plants (to auricle of the uppermost leaf) was only 11% ($p < 0.001$) less at maturity (Fig. 4-2), but more pronounced differences were

evident in both above- and below-ground dry weight (reduced 44% [$p < 0.0025$], and 49% [$p < 0.002$], respectively) (Fig. 4-2). Proportional reductions were evident for all organs examined, including ears, tassels, stalks, roots, and leaves. Length and width of mature leaf blades were also decreased, but disproportionately more so for width (35% [$p < 0.0003$]) than length (10% [$p < 0.0003$]) (Fig. 4-3), giving a narrow-leaf phenotype. The reduction was proportional in all leaves examined, indicating a consistent defect in lateral expansion rather than an ontological effect at specific leaf positions (Fig. 4-3).

Leaf-blade curling (adaxial rolling) was also a consistent feature of *csld1* mutants (Fig. 4-4), and affected all leaves, regardless of position. Blade rolling was most apparent as leaves matured, and occurred regardless of watering regime or growing conditions (field or greenhouse). The amount of leaf-blade rolling was greatest where size and extent of epidermal warts (see below) on the leaf was also maximal. Although leaf rolling in non-mutant maize plants is a common response to water stress, this aspect of the phenotype persisted in well-watered plants. Most likely, it is the leaf epidermis itself which promotes the curling effect, as the abaxial surface of mutant leaf blades accumulate relatively more warty cell clusters, thus extending the abaxial surface and causing the leaf to curl in the opposite (adaxial) direction (see below).

Epidermal Cells Balloon into Warts on *csld1* Mutants

The rough texture of *csld1* mutant leaves was due to irregular swelling of epidermal cells and groups of cells (Fig. 4-5). This phenotype was observed along the entire length of mature leaf blades and midribs (Fig. 4-5A), but not on leaf sheaths or stalks (data not shown). Some epidermal cells in warts expanded to many times their normal size (about 75-fold greater volume), and were generally arranged in linear profiles along the longitudinal axis of the leaf blade (Fig. 4-5B). Swollen cells remained

fluid-filled until the onset of leaf senescence (Fig. 4-5C). Warts were present on both surfaces of mutant leaf blades, but were larger and more abundant on the abaxial face (Fig. 4-5D). As noted above, this was likely the cause of the rolled-leaf phenotype (Fig. 4-4). These malformed cells consistently lacked chloroplasts (Fig. 4-5C, E), indicating an epidermal origin. Also, serial sectioning of the leaf revealed that the cells in the warts originated from the epidermal layer (Fig. 4-5F, G). Ballooned epidermal cells in *csld1* mutants often had diameters over 100 μm , at least five times greater than epidermal pavement cells in leaves of wildtype plants (Fig. 4-5G).

Topographical data from SEM analyses and epidermal impressions allowed more specific definition of the surface dimensions and distribution of lesions, as well as analysis of their maximal growth and advanced development. Groups of warty cells were randomly interspersed with normal-appearing regions of leaf epidermis (Fig. 4-6A). Clusters of swollen cells tended to be evenly distributed over large areas, along the entire length of the leaf blade (Fig. 4-6A). Both SEM and optical microscopy of fresh, intact leaves showed that lesions continued to grow until leaves reached full expansion, and that the largest clusters often included swollen cells that had collapsed (Fig. 4-6B, center panel). In other instances cells remained intact, even in lesions greater than 300 μm wide (Fig. 4-6B, right panel). Individual cells in these cluster were identified at least 5-fold wider and 3-fold longer than more standard epidermal cells (Fig. 4-6B, right panel).

Cells of *csld1* Mutant Leaves are Larger, but Fewer in Number

We initially hypothesized that epidermal pavement cells in the narrow-leaf mutants might also be narrow (where not ballooning), but the opposite was observed (Fig. 4-7). Examination of epidermal impressions from non-warty areas of mutant and

non-mutant leaves revealed that although there was no significant difference in cell length, there was a consistent increase in width of mature *csld1* mutant epidermal pavement cells ($p < 0.0003$). This 17% greater cell width, together with 35% narrower leaves, indicated that mutant plants had fewer total epidermal cells across their width. This decrease in cell number translated to an estimated 40-45% reduction in epidermal cell divisions compared to wildtype.

Further analyses showed that *csld1* mutant leaf blades were also visibly thicker, with less distance between vascular bundles (Fig. 4-8, top three panels). Fully-expanded *csld1* mutant leaf blades were on average 40% ($p < 0.004$) thicker than non-mutant leaf blades (Fig. 4-8, lower left). To determine whether this increase in thickness was due to larger epidermal cells alone or non-epidermal cells as well, inter-epidermal distance was measured. Sub-epidermal contributions to total leaf thickness were proportional to epidermal contributions, being 43% ($p < 0.002$) greater for *csld1* mutant leaf blades (Fig. 4-8, lower left). The *csld1* phenotype is therefore not limited to the epidermis alone. Additionally, mutant leaves showed a 12% ($p < 0.03$) increase in vascular-bundle density (Fig. 4-8, lower right), an effect also evident from visual appraisal. These data, along with average leaf width (excluding the midrib) of 80.2 mm for non-mutant and 51.1 mm for mutant leaves (Fig. 4-2), were used to estimate the number of vascular bundles across the widest portion of fully-expanded leaves. Resulting values were 601 and 429 vascular bundles per leaf, for non-mutants and *csld1* mutants, respectively (Fig. 4-8, lower right).

Stalks of *csld1* Mutants Contain Altered Vascular Bundle Number and Cell Wall Properties

Analysis of mutant stalks confirmed that organ width and vascular bundle number were also affected elsewhere in *csld1* mutant plants (Fig. 4-9). Cross-sectional area of *csld1* mutant stalks was reduced by 24% ($p < 0.025$) on average compared to non-mutant stalks (Fig. 4-9). As with leaf blades, total number of vascular bundles was also decreased. At the third internode from the ground, mutant plant stalks had an average of 11% ($p < 0.025$) fewer vascular bundles than non-mutant stalks (Fig. 4-9). Again as observed for mutant leaves, *csld1* mutant stalks had more vascular bundles per unit area than non-mutants, with an average of 2.0 (SE, 0.1) bundle per mm^2 compared to 1.7 (SE, 0.1) bundle per mm^2 for non-mutants across the entire stalk (Fig. 4-9). This increase was partly due to the relative increase in rind-to-pith ratio in *csld1* mutants, but even in the central pith, greater vascular bundle density was evident.

To further characterize differences between mutant and non-mutant stalks, high-resolution X-ray micro computed tomography (micro CT) was employed on hand-cut stalk sections (Fig. 4-10). Three-dimensional reconstruction of these data revealed a shift in the distribution of cell wall thickness between mutant and non-mutant stalks, with mutant walls in this tissue generally thinner (Fig. 4-10). Additionally, this approach allowed comparison of the density of cell wall material, which was greater for cell walls of *csld1* mutant stalks (as measured by X-ray beam attenuation) compared to non-mutant stalks (Fig. 4-10).

Cell Wall Sugar Components were not Detectably Altered by Loss of *CsID1* Function

With the goal of determining whether the changes in wall material properties from stem sections observed via micro CT were reflected in global changes in cell wall

polysaccharide composition, we examined cell wall composition from mature leaf blades as well as isolated leaf epidermis of both mutant and wildtype plants. No significant differences in alcohol-insoluble cell wall composition were found between wildtype and *csld1* mutants for either cellulose or sugar subunits of non-cellulosic constituents (Table 4-1). Cell walls from epidermal cells of both genotypes revealed distinctive composition relative to samples from whole-leaf blades. Specifically, epidermal cell walls had less glucose, rhamnose, galactose, and galacturonic acid, but relatively more xylose, compared to whole-leaf blades (Table 4-1).

Levels of Maize *CsID1* mRNA are Greatest in Regions of Active Cell Division

In order to view the phenotypes of *csld1* mutants in context of where the wildtype gene is expressed, quantitative RT-PCR was used to determine levels of *CsID1* mRNA across diverse tissues and stages of development (Fig. 4-11). Highest levels of *CsID1* transcript were evident in young, pre-emergent leaves (inside the whorl), with lesser expression in young primary roots and bases of more mature leaves (Fig. 4-11A). To more clearly define the pattern of transcript accumulation during leaf development, staged samples of very young to mature leaves were analyzed. The *CsID1* mRNA was most abundant in tissues containing actively dividing cells, highest in shoots 6 days after germination (Fig. 4-11B). Samples of more mature, single leaves showed that basal portions of blades from expanding leaves 15-25 cm long had the greatest levels of *CsID1* mRNA accumulation. By the time of cessation of cell division in fully-expanded leaves, *CsID1* mRNA dropped to undetectable levels and remained nearly undetectable in the fully-differentiated portions of leaves (Fig. 4-11B).

Multiple Cell Division Defects are Evident in *csld1* mutant Epidermis.

Dark-field images of single-cell-layer epidermal peels from mature leaf blades showed that the normally highly-ordered epidermal cells of maize leaves were disrupted in epidermis of *csld1* mutants (Fig. 4-12). Also striking was the extent of apparent cell division anomalies in the mutant epidermis (Fig. 4-12). Cell wall stubs were commonly observed in samples from mutant plants, where cells apparently failed to complete cell division (Fig. 4-12). These incomplete cell walls were observed exclusively in the longitudinal plane (Fig. 4-12). Other frequent occurrences of altered cell shape and misaligned cell walls also implicated cell-division defects as the cause (Fig. 4-12).

To determine when these cell abnormalities could first be detected, fresh, 5-10 cm, immature leaves of *csld1* mutant and wildtype plants were stained with propidium iodide. Confocal microscopy imaging of abaxial epidermal cells from the pre- and post-differentiation zones (determined by the absence/presence of stomata), revealed disrupted cell files and misshapen cells (Fig. 4-13A, B), similar to what was observed in epidermal peels of mature leaves (Fig. 4-12). Cell wall stubs were frequently observed in both pre- and post-differentiation epidermis (Fig. 4-13). Again, they were typically oriented in the longitudinal direction (Fig. 4-13). While many epidermal cells at these stages were approximately twice the normal width (as if they failed to undergo a single division), nearly all cells of *csld1* mutants were visibly larger than wildtype (Fig. 4-13 A, B), supporting the findings that even non-warty, otherwise normal-looking cells, were wider in the mutant (Fig. 4-7). In multiple instances, a series of large epidermal cells were located at positions normally inhabited by two distinct cell files, indicating either failure of consecutive neighboring cells to divide or, more likely, a clonal file derived from a single cell that failed to complete division, as indicated by oppositely-facing cell

wall stubs at either extreme of such cell files (Fig. 4-13C). Three dimensional imaging with confocal microscopy identified a large number of gaps in cell walls that initially appeared complete (Fig. 4-13D), suggesting the many more walls than at first apparent were incomplete.

Because cells with large or multiple nuclei are commonly observed in cell division defective mutants (Smith et al., 1996; Lukowitz et al., 1996; Spitzer et al., 2006), propidium-iodide stained nuclei were examined in immature *csld1* mutant leaves (Fig. 4-14A). Compared to wildtype epidermis of the same stage (pre-differentiation zone of 5-10 cm leaves), *csld1* mutant cells generally had larger-appearing nuclei (Fig. 4-14A). While significant variation in nuclear size was observed even in wildtype tissue, the range in *csld1* mutants was much greater, with cells containing nuclei ranging from normal to approximately four times larger in size (Fig. 4-14A). Large nuclear size was generally correlated with large cell size (Fig. 4-14A). Flow cytometry of nuclei from basal regions of immature leaves showed a small, but significant ($p < 0.05$), increase in ploidy level in *csld1* mutants compared to wildtype (Fig. 4-14B). Relatively more tetraploid nuclei were identified in *csld1* mutants than in wildtype, while no significant differences were observed at any other ploidy level (Fig. 4-14B).

Discussion

The CSLD1 Enzyme Appears to Affect a Mechanism Other than Tip-growth

Previous results suggested specific functions for CSLD proteins in tip-growing cells (Bernal et al., 2008), but data here and elsewhere indicate broader developmental roles as well. Disruptions in *At-CsID5*, *Os-CsID4*, and *Zm-CsID1*, in particular (Bernal et al., 2007; Li et al., 2009), lead to reduced overall plant growth without visibly altering classic tip-growing cells (root hairs and pollen tubes). Among the

reduced-growth phenotypes, maize *csld1* is unique in production of visible epidermal warts. This difference might lie in the greater growth and expansion of maize leaves. In other respects, however, commonalities between the reduced-growth phenotypes suggest a shared function for this sub-group of CSLDs.

The Maize *CsID1* Gene is Essential for Normal Plant Dry Weight and Organ Width

An underlying basis for the pleiotropic *csld1* phenotype is indicated by the proportional reduction in dry mass (~45%) and size affecting all organs including leaves, shoots, roots, tassels and ears (Figs. 4-2, 4-3, and data not shown). A reduction in cell number was partially compensated by an increase in average cell size, and in epidermis of narrow leaves, expansion was increased only in the lateral direction. These results are broadly consistent with work on other, non-allelic warty mutants in maize that suggest a compensatory mechanism in young leaves which might regulate the balance between cell division and expansion, especially in response to defects that could alter organ shape (such as the disrupted cell divisions and epidermal lesions shown here) (Reynolds et al., 1998). While this is compatible with a primary defect in division rate or total number of cell divisions, indirect effects at the whole-plant level could also reduce dry matter accumulation. The narrow leaves of *csld1* mutants, for example, are likely to result in decreased photosynthetic capacity and the smaller root system may further reduce growth (Figs. 4-3, 4-4). Finally, the epidermis may have a prominent physical role in organ expansion and meristem geometry (Green, 1980; Moulia, 2000) providing additional potential for secondary or tertiary effects of the *csld1* mutations.

Warty Cells Represent Distinctive and Informative Features of Maize *csld1* Mutants

Warts created by excessive swelling of epidermal cells on *csld1* mutant leaves (Figs. 4-5, 4-6) result from apparent cell division flaws early in leaf development. The epidermal lesions were broadly distributed across leaf blades, with essentially any epidermal cell having potential to swell (including, albeit rarely, stomata or trichomes). This lack of a discernable pattern or position dependence of wart formation is consistent with a random process for determining which epidermal cells have division defects during development (Fig. 4-5).

Whether cell division defects alone are responsible for the entirety of epidermal wart formation remains unclear. Another possibility is that altered cell walls (missing a CSLD1 product) are weakened and less able to withstand normal turgor pressure. Swelling of weakened epidermal cells in the mutant would lead to further weakening (stretching/thinning) of the cell wall, and a still-greater tendency to expand. This abnormal expansion would in turn enhance physical stress on cell walls of neighboring cells, which could account for the lateral spreading that is observed in warty lesions. The suggestion of more-easily-stretched cell walls would be consistent with the larger size of even the non-ballooned epidermal cells as well as the later development of swollen cell clusters.

Possibly-analogous wart-like epidermal swellings were described by Burton et al., (2000) in a VIGS gene silencing experiment in tobacco. Although a *CESA* gene was targeted, conceivably the highly-similar *CSLD* genes may also have also been silenced. In any case, the transgenic tobacco had a reduced stature, chlorotic regions, and “a relatively crisp or crunchy texture... [with]... numerous surface lumps” predominately on

the abaxial side of leaves (Burton et al., 2000). This *csld1*-like phenotype would be consistent with some degree of repression of the *Zm-CsID1* ortholog in the tobacco experiment. Alternatively, if observed lesions did result from down-regulation of CESA genes alone, then this would be consistent with a role for CSLD proteins in cellulose biosynthesis (Doblin et al., 2001).

Larger, Non-warty Epidermal Cells Suggest a Limitation in Cell Division

The combination of narrower leaves and wider pavement cells resulted in an estimated 45% fewer epidermal cells across a mutant leaf blade (Fig. 4-7), supporting an early role for CSLD1 in leaf development. The majority of mutant leaf epidermal cells, while wider than normal, do not form warts and have a standard pavement-cell appearance, with typical neighbor-cell boundaries, suggesting a link between CSLD1 and the number of cell divisions in developing leaf epidermis. Similar effects were evident in internal leaf structures, where non-epidermal cells contributed to thicker leaf blades for *csld1* mutants (Fig. 4-8). While examination of cross-sections suggested that leaf vascular bundle number and density was altered in mutant leaves, the size and shape of vascular bundles were generally unchanged (Fig. 4-8). Instead, the greater thickness of *csld1* leaf blades was due to increased mesophyll cell size, indicating a broader role for CSLD1 than epidermal development alone. Alternatively, a less-expanded epidermis might constrain internal structures (mesophyll and bundle sheath cells) into a more limited space, resulting in leaf swelling.

Cell Walls of the *csld1* Mutant are Thinner and More Dense, but of Normal Composition

While the overall quantity of cell wall material is reduced in the *csld1* mutant plants by 45%, cell wall composition is largely unaffected (Table 4-1). There are several

alternative possibilities that may account for a lack of detectable differences in cell wall composition between mutant and wildtype leaves, or in epidermal peels alone. First it is possible that the CSLD1 polysaccharide product may normally be present in only very small amounts and thus be masked by more abundant polymers. Alternatively, the CSLD1 product may be synthesized early in development, but not be abundant in mature leaves, such as those analyzed here. Levels of *CsID1* mRNA were maximal in very young leaves and basal portions of fast-growing leaves, the zone most active in cell division (Sylvester et al., 1990; Freeling, 1992), as well as in primary root tips (Fig. 4-11). Another interpretation could be that the CSLD1 enzyme might synthesize a limiting constituent of specialized cell walls, such that when production is limited, other cell-wall polymer synthesis is similarly reduced. In this way, *csld1* mutants may produce less total cell wall, but remain unchanged in relative proportions of individual cell-wall constituents. In this respect, the implication that CSLD1 has an essential role in formation of new cell walls during cell division is intriguing.

High-resolution X-ray micro CT technologies allow for detailed structural analyses of internal regions of intact tissue, including the relative density of cell wall material, based on x-ray beam attenuation (Steppe et al., 2004; Dhondt et al., 2010). Examination of *csld1* mutant and non-mutant stem sections revealed increased wall density and a shift in the distribution of cell wall thickness (Fig. 4-10). These findings suggest an altered architecture for these cell walls that could be independent of a change in composition, and led to the hypothesis that these changes may reflect a relative increase in cellulose crystallinity, with decreased amounts of amorphous cellulose being present in the cell walls of *csld1* mutants.

Maize *CsID1* has a Role in Plant Cell Division

The primary evidence supporting a role for CSLD1 during cell division lies in the degree to which *csld1* mutations disrupt the otherwise highly-ordered epidermal cell files (Fig. 4-12). The appearance of incomplete cross walls between what would normally have been two cells, indicate a failure of cells to complete division. This observation may be interpreted in several ways. First, it is possible that the polysaccharide product of the CSLD1 enzyme functions in cell plate formation. If this constituent is limiting, cell plates may be less likely to form correctly or completely. Alternatively, because epidermal cells in *csld1* mutants are abnormally large prior to initiation of cell division (Fig. 4-13), cell plates may be unable to readily span the entire length of a cell, leading to incomplete cell wall formation. Both could also be true. The observation that cell wall stubs were almost universally oriented in the longitudinal direction (Fig. 4-12, 4-13) suggested a bias towards effecting longitudinal cell division defects, rather than lateral divisions. Whether this indicates separate mechanisms for these two types of cell division remains unclear.

Cell-level abnormalities were evident even at the earliest stages of leaf-blade development examined (Fig. 4-13A). Uneven and disrupted cell files, large and misshapen cells, and incomplete cell walls within a cell are all indicative of defects in cell division (Fig. 4-13A, B). Even undifferentiated regions of epidermis contained some cells which occupied a two-dimensional area over 30-fold greater than a standard epidermal pavement cell. The presence of long files of cells being uniformly large (Fig. 4-13C) suggests either the congruent failure of a string of cells to complete cell division, or clonal inheritance, where one mis-divided cell gives rise to abnormally-large daughter cells. Without the support of the highly-ordered, brick-like pattern of wildtype epidermal

cells, the large, misshapen and unorganized epidermal cells in the *csld1* mutants seem prone to excessive expansion during turgor-driven growth. The defects in cell division at the earliest stages of leaf development might account for the entirety of the warty phenotype of the *csld1* mutants. In this way, the polysaccharide product of CSLD1 might have its direct role limited to cell division, and its presence may be essentially transitory.

An interesting aspect of maize leaf epidermis shown here is the differential effect of *csld1* mutations on lateral and longitudinal cell divisions. Only longitudinal divisions seem to be affected by mutations of *CsLD1*, possibly indicating a highly-specific role for CSLD1 activity. Supporting evidence includes reduced leaf width (but not length) (Fig. 4-3), reduced cell width (but not length) (Fig. 4-7), and the exclusivity of cell wall stubs being oriented only along the longitudinal axis (Figs. 4-12, 4-13). Additionally, the long files of uniformly un-divided cells demonstrate that in *csld1* mutant epidermis, lateral divisions have the capacity to reach completion across cells two-times their normal width (Fig. 4-13). The same was not evident for divisions parallel to the leaf axis however, and consequences are consistent with the linear, clonal propagation of a single mis-divided cell into a file of subsequently ballooning cells observed here.

Large-nucleate cells have been reported in studies of cell division-defective mutants (Lukowitz et al., 1996). In pre-differentiation zones of *csld1* immature leaves, abnormally large cells were consistently observed to contain larger nuclei than normal (Fig. 4-14A). Compared to confocal imaging, where a large number of cells (estimated at 40-50%) contained excessively large nuclei, flow cytometry showed only a modest increase in endoreduplication (Fig. 4-14B). This result fits with the interpretation that

the large nuclei phenotype predominately affects the epidermis. Even with 50% of epidermal cells undergoing endoreduplication, the relative scarcity of these cells compared to other leaf cells would result in partial masking of the effect when analyzing nuclei from whole-leaf tissues. Whether the increase in endoreduplication and larger nuclei size reflects a response to larger cell size or the arrest of the cell cycle after DNA replication but before nuclear division remains unclear. The arrest of cells at the G2 phase would implicate a cell wall biosynthetic enzyme in feedback to the cell cycle, and seems unlikely. More likely, when a mis-divided cell (with two nuclei) undergoes later divisions, the nuclei would replicate and segregate as tetraploid nuclei, and be passed on as such in future divisions.

Broader Perspectives

The unique features of the *csld1* phenotype observed in maize provide insights into the function of the *CsID* subfamily in all plants. Data demonstrate a link between this putative cell-wall polysaccharide synthase and cell division during early maize leaf development, as well as connections between early cell divisions and subsequent organ development. The disproportionate reduction in plant dry weight compared to plant height can be accounted for by the larger but fewer cells, as observed in leaf epidermis (Fig. 4-7), along with thinner cell walls, as indicated by micro CT analysis of mature stems (Fig. 4-10). Together, along with narrow leaves (Fig. 4-3) and smaller stems (Fig. 4-9), these effects could account for the decrease of dry weight by 45% in mutant plants reduced in stature by only 11% (Fig. 4-3). In contrast to previous analyses of *CsID* family members, our results show that maize *CsID1* mutations have a dramatic effect at the whole-plant level and on leaf epidermis in particular. These studies contribute a new dimension to the understanding of CSLD protein function in plants.

Some aspects of the *csld1* phenotype reported here have also been observed in other mutants. Among these are the similar (but less severe) clusters of swollen, epidermal cells reported in the *warty-1* maize mutant (Reynolds et al., 1998). However, the *csld1* mutants described here show distinctive changes in stature, leaf width, and morphology not observed elsewhere. Also, maize *tangled-1* mutants show irregular cell divisions in leaves, but maintain their overall shape and plant architecture (Smith et al., 1996). Initially, the leaf epidermal surface of these mutants may seem similar to that of *csld1*, but in leaves of the *tangled-1* mutants, aberrantly dividing cells are evident in all cell layers, as opposed to the prominent epidermal locale in *csld1* (Smith et al., 1996; Cleary and Smith, 1998). The *Tangled-1* gene encodes a microtubule binding protein (Smith et al., 2001).

While at first glance it might seem surprising that a CSLD protein would be involved in the development of non-tip-growing cells like maize epidermal pavement cells, upon consideration, cell division involves a strikingly similar process to that of tip-growth. Cell plate formation during cell division has many parallels with the process of tip-growth, including the delivery of cell wall material being focused to a very specific subcellular position via cytoskeletal-mediated organization of the exocytic pathway machinery (reviewed in Bednarek and Falbel, 2002). Other examples of individual proteins from common families functioning in either tip-growing cells or cytokinesis include the formins (Ingouff et al., 2005; Backues et al., 2007) and ROP GTPases (Molendijk et al., 2001; Xu and Scheres, 2005).

Methods

Identification of *csld1* Mutants

The UniformMu population was screened using PCR-based assays to identify Mu transposon inserts in *Zm-CsID1* as per Penning et al., (2009). Close to 15,000 UniformMu lines were screened using a series of pooled DNA samples, which were forerunners of the sequence-indexed materials currently available at MaizeGDB (maizegdb.org; UniformMu.UF-genome.org). For PCR screening, *CsID1*-specific primers (AGTTCGTGCACTACACCGTGACATCC and TGCTACCTGTAAGGACTGAGGATGGCCTG) were used along with the Mu-specific primer TIR6 (AGAGAAGCCAACGCCAWCGCCTCYATTTCGTC). Resulting products were separated on 1% agarose gels, blotted onto nylon membranes, and probed with a *CsID1*-specific PCR product (Fig. 4-1). Positive probe-binding samples were identified at X45:Y4 of the UniformMu Reverse Genetics Grid 6 (of 8 total) (Fig. 4-1). Seeds from this UniformMu family corresponding to these coordinates (04S-1130-27) were grown, and PCR-genotyped to identify individuals homozygous for an insertion in *csld1*. The *csld1-1* allele was identified from this family, and a *csld1-1* line established after three generations of successive backcrosses to the W22 inbred.

A second mutant allele, *csld1-2*, was identified during a visual screen of field-grown UniformMu lines. Its phenotype was indistinguishable from that of *csld1-1*. PCR primers (ACCAGATCCTCTTCCTCCTCGGTTTGC, ACCTTGTTCTGAGGAAGTCCCTCTTC, GTGGTGATCACGCTGGCATCATTAG, AGGAGGGCTGATGTAGACCCACAG,) were designed to cover nearly the entire length of the *CsID1* gene and identified a Mu insertion in the third exon. Homozygous recessive mutants of this allele were obtained from segregating progeny from this

family, and used to generate *csld1-2* line after two successive backcrosses into the W22 inbred.

Additional Mu-insert alleles of *csld1* were identified from the The Trait Utilities System in Corn (TUSC) population of Pioneer Hi-bred as per McCarty and Meeley, (2009). Primers used were: ACCAGATCCTCTTCCTCCTCGGTTTGC, ACCTTGTTCCCTGAGGAAGTCCCTCTTC, GTGGTGATCACGCTGGCATCATTGAG, AGGAGGGCTGATGTAGACCCACAG, which identified five additional mutant alleles designated *csld1-3* through *csld1-7* (Fig. 4-1).

Overall Phenotypic Analyses and Size Measurements

Plant height was measured from soil level to auricle at the base of upper-most leaf blades for 55 field-grown, mature plants (25 mutant, 30 non-mutant). These same 55 plants were used to measure width (at the widest point) and length of leaves at positions three, four, and five (relative to the apex). For dry weight measurements, whole-plant samples (including released root mass) were collected three days after ear harvest and did not include mature ears. Samples were weighed after drying for 4 weeks at 38°C. Below-and above-ground dry weights were determined by separating root masses from the aerial portions of these plants.

Leaf thickness was measured on images from *csld1* mutant and non-mutant sectioned leaf blade pieces (4 each). Non-epidermal contributions were determined by measuring the inter-epidermal space of each of these pieces. Total thickness and inter-epidermal space were reported as averages of 10 independent measurements. Vascular bundles per leaf were estimated by multiplying the average vascular bundle density by the average leaf width (excluding midrib).

For analysis of leaf-blade conformation (adaxial curling), leaf blades were harvested from position three during the anthesis-silking interval of mutant and non-mutant greenhouse-grown plants. Samples included 1-cm sections from the base, middle, and tip of each blade (Fig. 4-4). Excised leaf strips were allowed to assume their natural conformations, and imaged immediately.

Cell Volume Estimates

Extent of maximal expansion was estimated for ballooning epidermal cells of the *csld1* mutant by comparing their volume to standard epidermal pavement cells of wildtype plants. Cells were considered to be roughly cylindrical ($V=\pi r^2 \cdot m$), with wildtype pavement cell dimensions approximately 40 μm (diameter) x 200 μm (length) (Figs 4-5, 4-6). Ballooned epidermal cells of blades from *csld1* mutant plants were often as large as 200 μm (diameter) x 600 μm (length) (Figs. 4-5, 4-6).

Epidermal Impressions and Non-warty Cell Size Determination

Fresh samples from mature leaves of greenhouse-grown plants were cut into 2-cm² pieces and firmly pressed into Superglue on glass slides. Glue was allowed to dry completely before leaf tissue was removed, leaving detailed epidermal impressions. These were imaged under a light microscope (Olympus BH2) with an RT SPOT camera (Diagnostic Instruments). Average cell length and width were determined by quantifying the total number of cells in a given distance (1.88 x 1.40 mm). Longitudinal and lateral transects were used that did not include warty protrusions.

Tissue Fixation and Sectioning

One-cm squares were excised from leaves of greenhouse-grown plants and fixed in FAA (10% formaldehyde [Fisher Lot # 992720], 5% acetic acid, 50% EtOH). Samples were vacuum infiltrated overnight at 4°C, then shaken at 4°C during a

dehydration series using ethanol in PBS (60 min each, progressing from 1x PBS with 30% EtOH to 40%, 50%, 60%, 70%, 85%, and finally 95% EtOH). Samples were stained overnight with eosin in 95% EtOH, followed by four, 1-hr incubations in 100% EtOH and eosin at 25°C. Wax imbedding was initiated by introducing CitriSolv (Fisher Cat # 22-143975) into samples using a series of 1-hr incubations (while shaking) in ethanol with increasing CitriSolv/EtOH content (25/75, 50/50, 75/25, 100/0). Paraplast wax chips (Fisher Cat # 23-021-399) (1-g wax/mL CitriSolv) were added to the 100% CitriSolv and incubated overnight at 25°C. Additional wax was added, followed by a 2-hr incubation at 42°C. Samples were transferred to 60°C for 1 hr. Wax was poured off and replaced eight times before samples were allowed to harden in molds. Sections (10 µm, cut with a Leitz 1512 microtome) were de-waxed with three, 5-min incubations in xylene (Fisher Lot # 083423), then washed twice in 100% EtOH (5 min each), and once in 95% EtOH (3 min). Slides were dried and examined under a Olympus BH2 light microscope.

Scanning Electron Microscopy

Mature leaf pieces (1-cm²) from *cs/d1* mutant and non-mutant plants were fixed in FAA (10% formaldehyde [Fisher Lot # 992720], 5% acetic acid, 50% EtOH), dehydrated in an ethanol series 75%, 95%, 100%, and critical point dried (Bal-Tec CPD030, Leica Microsystems, Bannockburn, IL). Dried samples were mounted with carbon adhesive tabs on aluminum specimen mounts, Au/Pd sputter coated (DeskII, Denton Vacuum, Moorestown, NJ), and examined with a field-emission scanning electron microscope (S-4000, Hitachi High Technologies America, Schaumburg, IL). Digital micrographs were acquired with PCI Quartz software.

Phloroglucinol Staining and Stalk Measurements

Cross-sections of stalks from field-grown plants were examined using hand-cut sections (about 5 mm) from mid-way up the second internode (from ground level). Tissue was stained by incubating 45 sec in Phloroglucinol (1% in 95% EtOH), then adding excess 25% HCl. Images were acquired using a RT SPOT camera (Diagnostic Instruments) attached to a Leica MZ 12-5 dissection microscope. Cross-sectional area for these sections was determined using ImageJ software (rsbweb.nih.gov/ij/index.html). Vascular bundle density was determined by dividing the number of vascular bundles per section by the cross-sectional area.

High-resolution X-ray Micro Computed Tomography Analysis

Field-grown plants were collected three days after harvesting ears and dried at 38°C for three weeks. Sections (~0.5 cm) from mid-way up the second internode of the conditioned stems (~9% moisture content) were cut using a small band saw and scanned using a Scanco Medical Ag uCT35 instrument (Brüttisellen, Switzerland). Initial measurements were conducted on whole-stem sections at 10-micron resolution. Regions including pith and rind (3 x 4 mm) were hand-cut from the edge of these sections and scanned at 3.5- μ M resolution over a 0.88 mm high region for quantitative measurements of cell wall and air space sizes. The 232 slices from each scan were reconstructed into three dimensional images and contoured over whole stems for volumetric analyses. Scans at 3.5 micron and 10.0 micron resolutions were conducted with integration times of 600 microseconds and averaging two times. Both a fixed, common threshold and an adaptive threshold were used to segment cell wall from airspace and volumetric analyses were calculated with an algorithm developed for trabecular bone (Hildebrand and Rueggsegger, 1997). For rind-only analyses, hand-

drawn contours were used to isolate the vascular bundle-rich region along the edge of the stem prior to 3D reconstruction.

Epidermal Isolation

Epidermal peels were manually removed from the abaxial surfaces of fully-expanded leaf blades from greenhouse-grown plants. Each of the peels were harvested as in Figure 4-15. For dark-field imaging, peels were placed on droplets of water on glass slides and allowed to dry. For cell-wall composition analysis, 100 mg of peels were collected, frozen in liquid nitrogen, and stored at -80°C until cell wall extraction.

Cell Wall Composition Analysis

Samples from leaves and epidermal peels were ground in liquid nitrogen along with 200 μ L of extraction buffer (50mM Tris-Cl with 1% SDS at pH 7.2). Homogenate was transferred to 14-mL polypropylene, round-bottom tubes (Falcon product # 352059) along with 9 mL of extraction buffer, incubated for 15 minutes at 80°C, and centrifuged at 3,500 rpm for 5 min (~2,000 x g) in a swinging-bucket rotor centrifuge (ThermoForma 1LGP). Supernatant was removed with an aspirator, and pellets (water-insoluble cell-wall fraction) were washed, resuspended, and re-pelleted three times in about 10 mL 80°C water. The same process was repeated three times with 50% EtOH at 80°C, followed by three washes with 80°C water. Samples were transferred to 1.5-mL Eppendorf tubes, alcohol-insoluble cell wall fractions were pelleted and dried, and composition was analyzed by the Complex Carbohydrate Research Center (University of Georgia; Athens, GA).

For cellulose content, the alcohol-insoluble cell wall fractions from whole-leaf samples were isolated in the same way, dried for 16 h at 60°C, transferred to 14-mL

polypropylene, round-bottom tubes, and weighed. For each sample, approximately 50 mg of cell wall isolate was used, to which 3 mL 80% aqueous acetic acid and 300 μ L 70% nitric acid were added. Tubes were incubated in an oil bath at 110°C and 120°C for 20 min each, to hydrolyze hemicellulose and lignin (from Sun et al., 2004). Samples were allowed to cool, 1.8 mL distilled water was added, tubes were centrifuged for 5 min (~2,000 x g), and supernatant was removed with an aspirator. Cellulose was rinsed thoroughly with water (3 times) and 95% EtOH (3 times), and dried for 16 h at 60°C. Samples were weighed and compared for cellulose content as a fraction of alcohol-insoluble cell wall isolate.

Real Time Quantitative RT-PCR

For each sample, RNA was extracted from approximately 200 mg of tissue, initially frozen in liquid nitrogen, then homogenized in 1.0 mL Trizol (Invitrogen Cat # 15596-018) using a Q-BIOgene FastPrep 120 with Lysing Matrix D (MP Biomedicals Cat # 116913). Samples were incubated 5 min at 25°C, with frequent vortexing. Chloroform (200 μ L) was added and samples were vortexed 15 sec before and after a 1-min incubation at 25°C. Phases were separated by centrifuging 10 min at 15,000 x g, and 200 μ L of the aqueous layers were transferred to 700 μ L of Qiagen RLT buffer (from RNeasy Plant Mini kit, Qiagen Cat # 74904). Ethanol was added (500 μ L, 100% EtOH) and samples were vortexed. Half of this volume was used to clean and elute total RNA as per RNeasy Plant Mini kit (Qiagen Cat # 74904). Resulting RNA was treated with DNase-1 (Ambion Cat # AM1906), and quantified using a BioRad SmartSpec 3000. The cDNA was synthesized using SuperScript One-Step kit and protocol (Invitrogen Cat # 10928-042).

Levels of *CsID1* mRNA were quantified in diverse maize tissues and in leaf blades at a range of developmental stages via Real-time RT-PCR using a Step One Plus Real-Time PCR System (ABI, Carlsbad, CA). At least three biological replicates were analyzed for each tissue or time point, and for each of these replicates, reactions were performed in duplicate. A given reaction included 10 μ L Fast SYBR Green Master Mix (ABI Lot # 1003024), 5.0 μ L of cDNA sample (diluted 10x from cDNA reaction), and 100 nM of each gene-specific primer (Fwd: GCCGCTCACGTCAATGG, Rev: CTGGGCATCTTCATGGAGTGT) in a final volume of 20 μ L. The relative abundance of transcripts was normalized with 18S rRNA controls (Taqman Ribosomal RNA Control Reagents, ABI Lot # 0804133) as in Eveland et al., 2008. Primer pairs for *CsID1* were designed using Primer Express 3.0 (ABI).

Propidium Iodide Staining

Immature leaves (10-15 cm) were dissected from whorls of *csld1* mutant and non-mutant plants. The basal portions (2 cm) of these leaves were immediately submerged in a solution of 0.1 mg/mL propidium iodide, and allowed to absorb the dye for 5 min at 25°C. Samples were then rinsed thoroughly in water to remove excess stain and flattened on a glass slide. The abaxial epidermis was imaged using a Zeiss confocal microscope. For visualization of nuclei, the same process was followed, but leaf samples were first fixed in FAA (10% formaldehyde [Fisher Lot # 992720], 5% acetic acid, 50% EtOH), before staining with propidium iodide.

Flow Cytometry

The basal 1 cm of immature leaves (2-3 cm) were dissected and finely sliced (~0.5 mm) with a razor blade in ice-cold chopping buffer (4% MOPS [0.5 M, pH 7.2], 9% MgCl₂ [0.5 M], 6% Na₃Citrate [0.5 M], 0.1 % Triton X-100 [Sigma, Lot # MKBD6639V], 1

mg RNase [Thermo Scientific, Cat # AB-0549], in water). Homogenate was filtered through 50 micron nylon mesh followed by 20 micron nylon mesh, then transferred to a 1.5-mL microcentrifuge tube. Nuclei were pelleted at 1,000 rpm for 3 min and supernatant was discarded. Pellets were resuspended in staining buffer (chopping buffer plus 1% propidium iodide [5 mg/mL]), and incubated at room temperature for 5 min. Nuclei were re-pelleted at 1,000 rpm for 3 min and supernatant was discarded. Pellets were resuspended in 300 μ l of staining buffer and analyzed on a LSR-II cytometer (BD Biosciences, San Jose, CA). Nuclei were excited using a solid state laser emitting 100 milliwatts at 488 nm. Forward light scatter and orange fluorescence (575 +/- 13 nm) were collected on up to 5,000 particles per sample. Small particles of debris were gated out using a fluorescence vs forward light scatter dot plot. Peaks were identified on a fluorescence histogram plotted on logarithmic scale and the geometric and median fluorescence values for each peak were calculated. Software used was Diva 6.1.2 (BD Biosciences).

Table 4-1. Cell wall composition of whole-leaf blades and epidermal peels from *csld1* mutant and non-mutant plants.

	Sample	Ara	Rha	Fuc	Xyl	Man	GalA	Gal	Glc	GlcA	Cellulose
Whole leaf	WT	11.43 (0.33)	0.53 (0.02)	nd	81.40 (0.01)	nd	1.36 (0.07)	0.85 (0.69)	4.43 (0.41)	nd	26.6 (1.8)
	<i>csld1</i>	11.84 (0.18)	0.57 (0.05)	nd	81.18 (1.31)	nd	1.59 (.016)	0.80 (0.04)	4.03 (1.41)	nd	22.9 (3.1)
Epidermal peels	WT	10.66 (0.54)	0.31 (0.02)	nd	85.04 (0.69)	nd	0.95 (0.29)	0.65 (0.08)	2.39 (0.34)	nd	nt
	<i>csld1</i>	11.93 (0.63)	0.34 (0.03)	nd	84.37 (0.96)	nd	0.71 (0.05)	0.69 (0.08)	1.97 (0.22)	nd	nt

Alcohol-insoluble residues were prepared from both whole-leaf-blade sections and isolated epidermal strips of greenhouse-grown plants identified as mutant or wildtype by PCR of a segregating family. Analysis of non-cellulosic cell wall sugars was done at the CCRC at the University of Georgia using combined gas chromatography/mass spectrometry (GC/MS) of the Tetramethylsilane (TMS) derivatives of the monosaccharide methyl glycosides produced by acidic methanolysis. Values for non-cellulosic sugars are given as mole percent, with standard error in parentheses. Cellulose content was estimated based on remaining weight after hydrolysis of hemicelluloses and lignin. Cellulose content is given as weight percentage of alcohol-insoluble cell wall fraction, with standard error in parentheses. None of the differences between *csld1* mutant and wildtype samples were statistically significant at $p < 0.05$ ($N = 4$, for each sample). nd = not determined, nt = not tested.

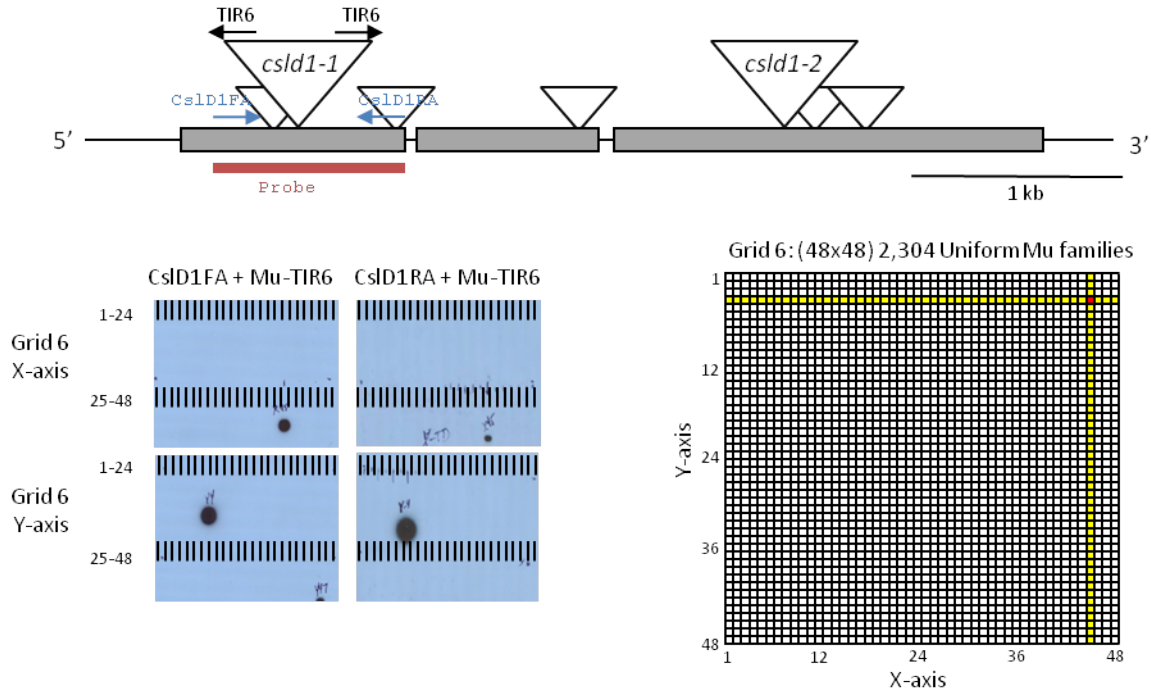


Figure 4-1. Gene diagram of *Zm-CsID1* and location of each of the Mu insertions identified. Large triangles represent the two UniformMu alleles (*csld1-1* and *csld1-2*) and small triangles show locations of TUSC alleles (*csld1-3* through *csld1-7*). Southern Blots are from the original hit in UniformMu Grid 6, with positive probe-binding lanes being identified in X45 and Y4 for both forward and reverse primers along with TIR6 primers (as diagramed above). Right panel shows the intersect in Grid 6 corresponding to UniformMu family 04S-1130-27.

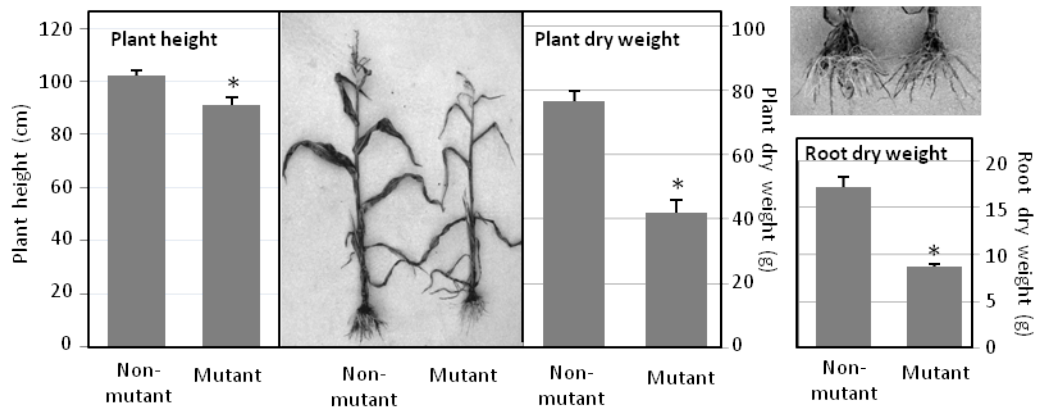


Figure 4-2. Morphology and dry weight of the *csld1-1* mutant. Plant height and dry weight (above- and below-ground) were quantified for field-grown *csld1* mutant and non-mutant plants. Non-mutant plants included both wildtype and heterozygous individuals from segregating progeny after 3 back-crosses into the W22 inbred. Height was measured from the soil line to the flag leaf of each plant. Below-ground dry weight was based on recovery of major roots as shown in the image above (root systems were compact in the irrigated sandy field conditions). Mutant plant height was reduced (av. 9%), and total plant dry weight decreased (av. 45%). Above- and below-ground dry weights were reduced by similar amounts (av. 44% and 49%, respectively). For dry weight measurements, whole plants were sampled three days after ear maturity (40 days post pollination), and did not include mature ears. Significant difference ($p < 0.05$) from WT indicated by *.

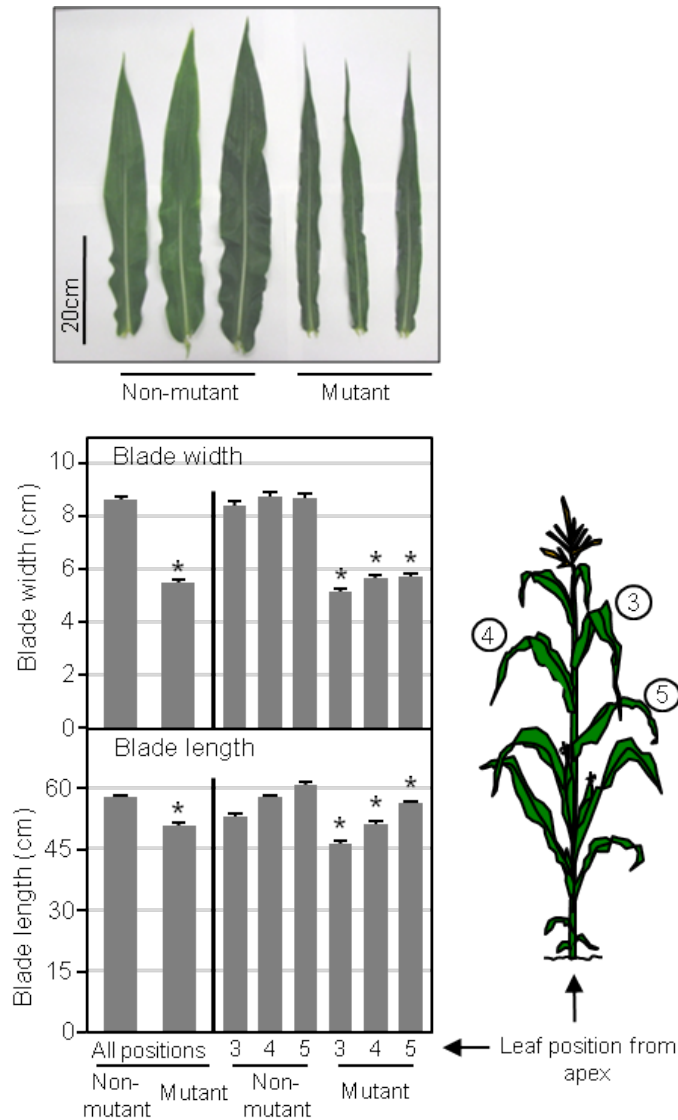


Figure 4-3. The narrow-leaf phenotype of *csld1-1* mutant plants. Leaf blade length and width (at widest point) were quantified for leaf positions 3 through 5 (as diagramed) for field-grown mutant and non-mutant plants. Non-mutant plants included both wildtype and heterozygous individuals from segregating progeny after 3 back-crosses into the W22 inbred. Imaged blades were from leaves in position #3 from the apex. The left-most portion of each graph shows combined data from all leaf positions measured. The leaf blade width-to-length ratio was 27% less for mutant plants. Blade width and length are reduced 35% and 10% respectively, relative to those of non-mutant plants. Data are similar for *csld1-2* (not shown), and visual appraisals of the five other *csld1* mutants. Note: Leaf photo is from greenhouse-grown plants, whereas quantifications are from field-grown plants. Significant difference ($p < 0.05$) from WT indicated by *.

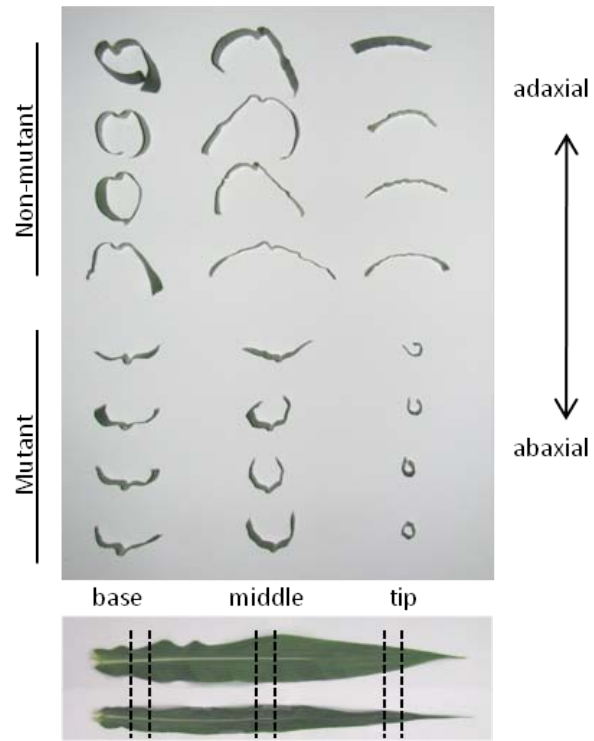


Figure 4-4. Leaf blade curling in *csld1* mutants. Leaf blades of *csld1* mutant leaves curl adaxially compared to non-mutant leaves, which typically flex downward (abaxially). Here, 1-cm sections of mutant and non-mutant leaf blades from well-watered plants were excised and imaged after adopting their natural conformations.

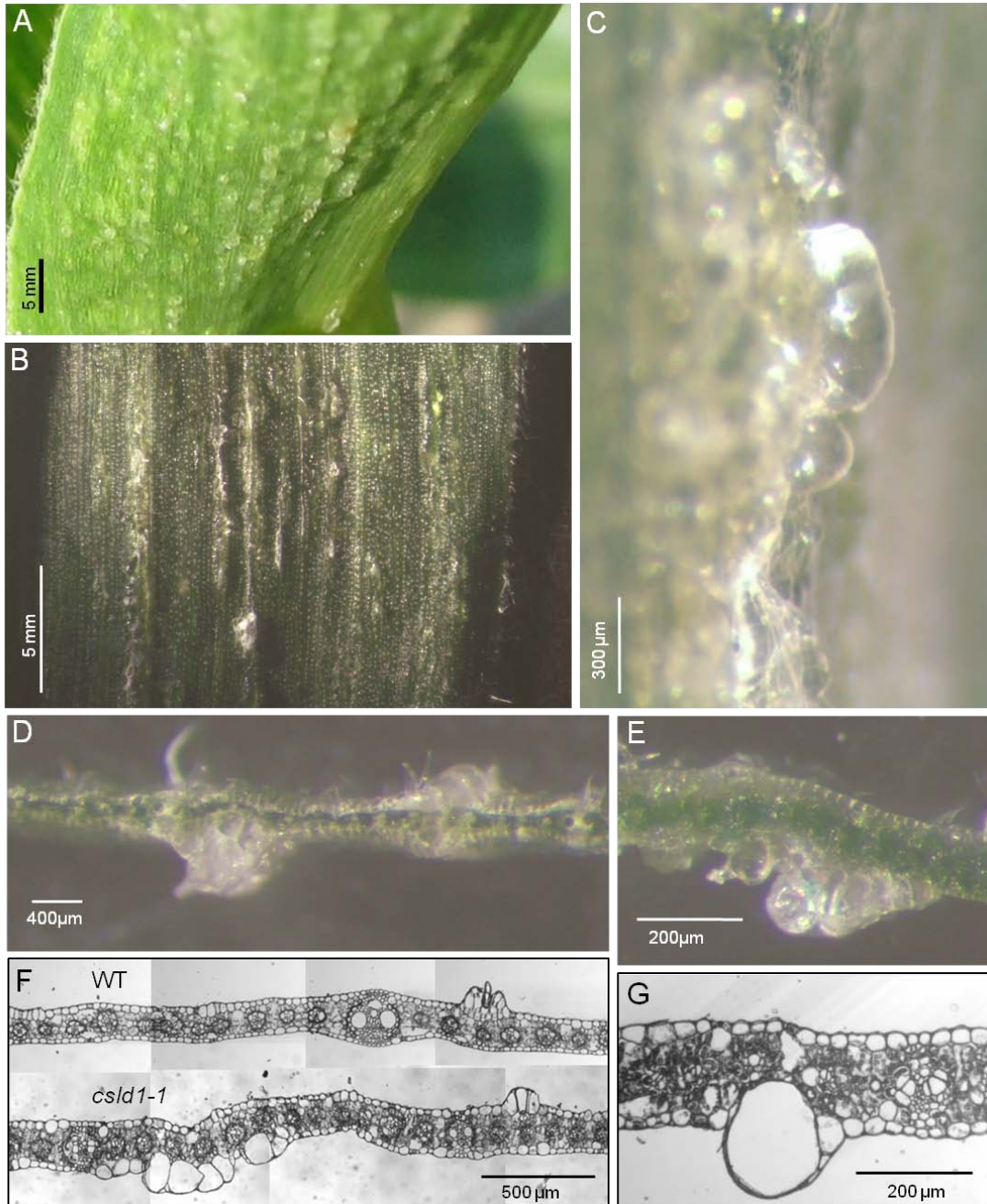


Figure 4-5. The warty phenotype of *csld1* mutant leaf blades. (A-C) Fresh, intact leaves. Epidermal warts were distributed in a non-uniform, apparently random manner across the entire blade and midrib of a mature fully-expanded leaf. (D, E) Fresh-sectioned leaf blades. Swollen lesions were most abundant on the abaxial leaf blade surface. (F, G) Fixed, imbedded cross-sections. Leaf blade interior is less visibly affected than epidermal cells in *csld1* mutants. Some epidermal cells have two-dimensional, cross-sectional areas up to 25-fold greater than normal ($r = 100 \mu\text{m}$ for swollen cell in G). Image in F is composed of overlapping composite images.

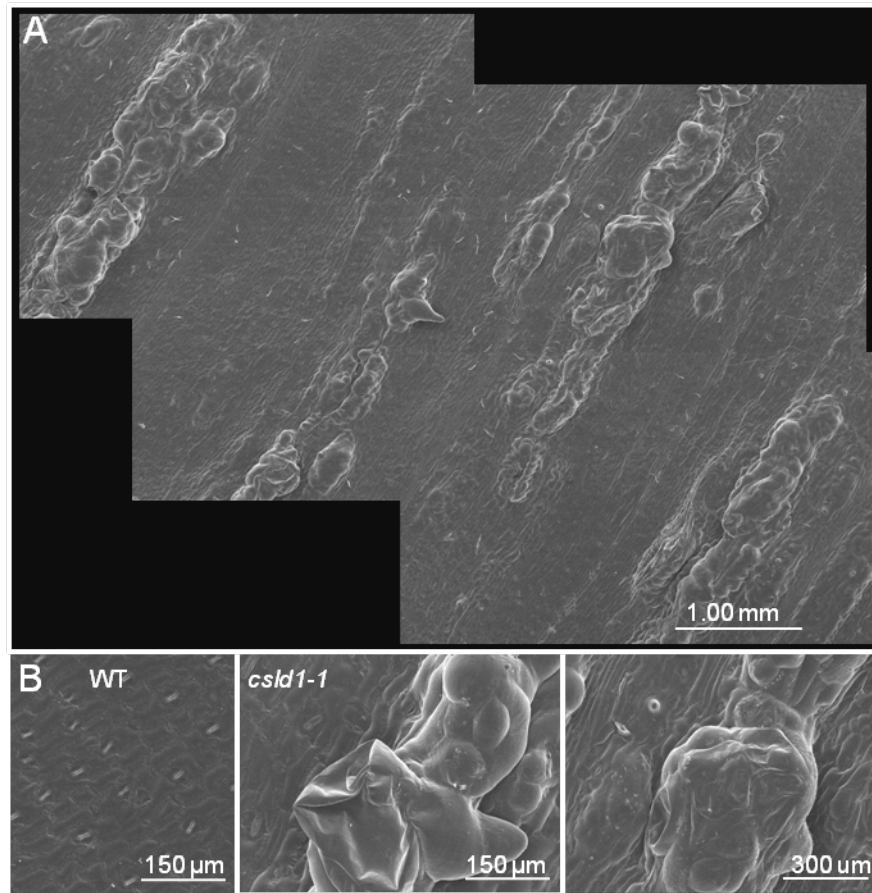


Figure 4-6. SEM of *csld1* mutant and wildtype leaves showing advanced development of epidermal lesions that continue growing after leaves reach full expansion. (A) Composite of overlapping images from of a mature, *csld1* mutant leaf revealing the complexity, dimensions, and distribution of the continually-expanding epidermal lesions. Clusters of swollen cells alternate with less-disturbed areas of epidermis. (B). Contrast between surfaces of wildtype (left panel) and *csld1* mutant leaves showing advanced development of large globular clusters, some having lost integrity and collapsed (center panel), others remaining intact and continuing to expand (right panel, expanded from composite image).

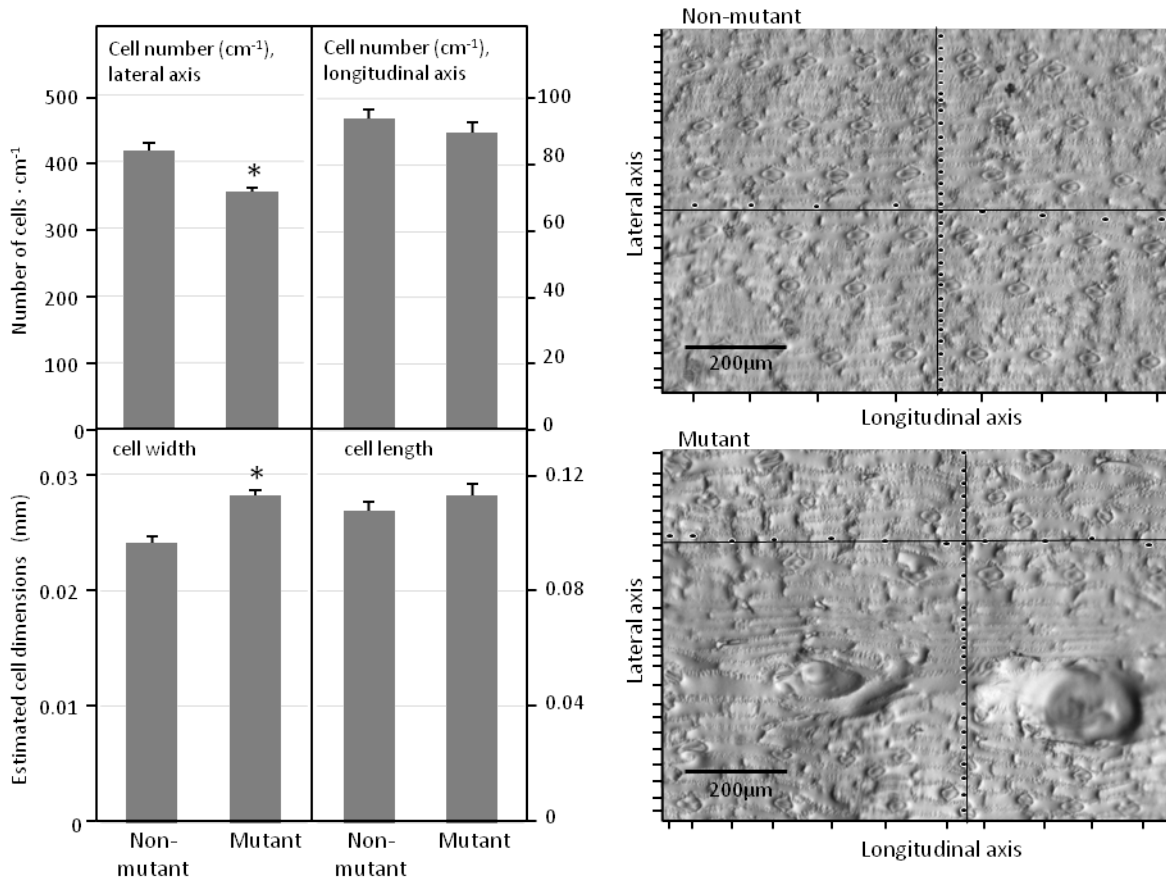


Figure 4-7. Size estimates for epidermal cells of inter-lesion regions on *csld1* mutant and non-mutant leaf blades. Epidermal impressions were taken from abaxial surfaces of fully-expanded leaf blades on mature, greenhouse-grown plants. Non-mutant plants included both wildtype and heterozygous individuals from segregating progeny after 3 back-crosses into the W22 inbred. Cell numbers were quantified along longitudinal and lateral axes of defined length. Mean cellular dimensions were determined by dividing number of cells along an axis by the length of that axis. (mutant N=14; non-mutant N=10; longitudinal axis 1.88 mm; lateral axis 1.40 mm). Axes used for analyses of epidermal cell size on mutant leaves did not include cells in the ballooning protrusions. Significant difference ($p < 0.05$) from non-mutant indicated by *.

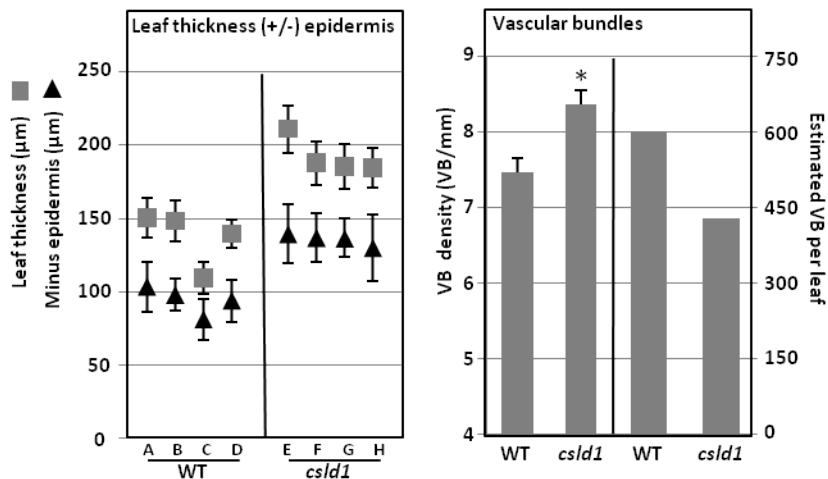
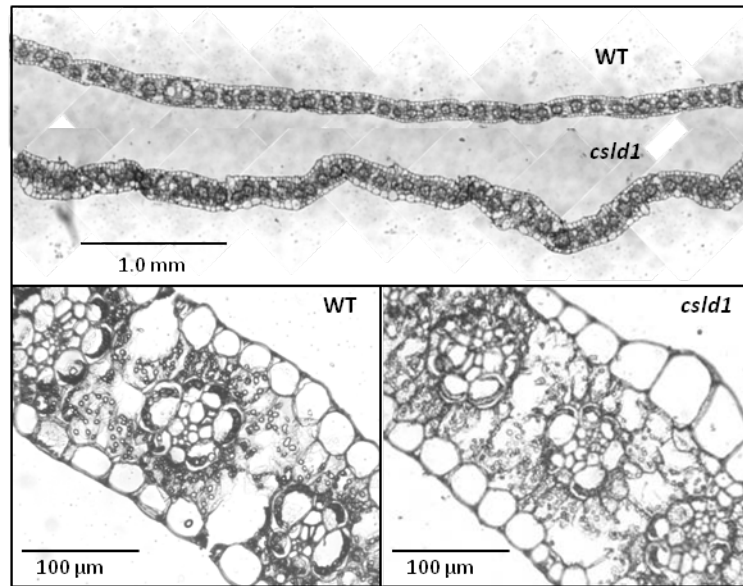


Figure 4-8. Internal structure of *csld1* mutant and non-mutant leaf blades. Sections of fully-expanded leaves from greenhouse-grown *csld1* mutant and wildtype plants showing visible differences in leaf thickness, vascular-bundle density, and mesophyll structure (upper three panels, top panel is a composite of overlapping images). Leaf thickness was quantified with- and without epidermal layers (lower left panel) for eight sections of fully-expanded leaves labeled A-H. Error bars show SEM for 10 measurements across each leaf. Mutant leaves were a mean of 40% thicker than those of wildtype, and proportional increases were observed for internal tissues alone. Vascular bundle density was also quantified (lower right panel), and used to estimate vascular bundle number per leaf (with mean leaf-width values [excluding midribs] being 80.2 mm and 51.1 mm for wildtype and *csld1*-mutant blades, respectively). Resulting estimates of vascular bundle number per leaf width were 29% less for *csld1* mutants. Error bars indicate standard error. Significant difference between *csld1* and wildtype ($p < 0.05$) is indicated by *.

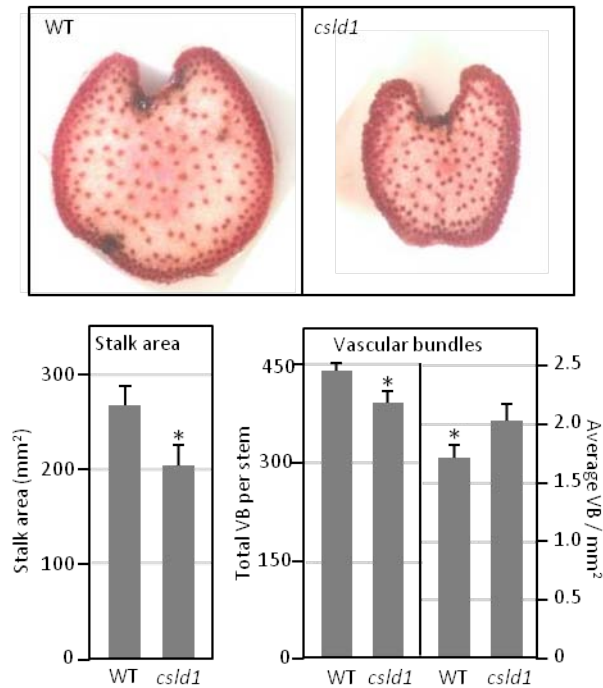
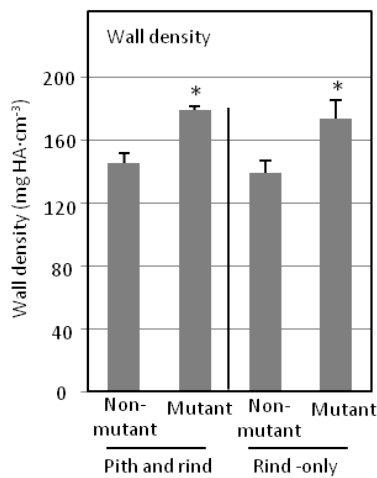
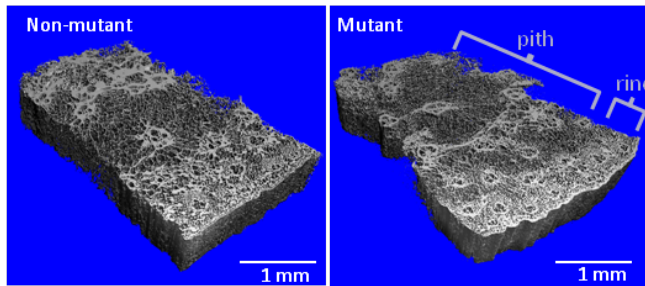


Figure 4-9. Internal structure of *csld1* mutant and non-mutant stems. Stem sections from the third internode of greenhouse-grown *csld1* mutant and wildtype plants (PCR-genotyped). Material was stained with phloroglucinol, imaged, and cross-sectional area was calculated using Image-J. Measurements were collected for 11 WT and 8 mutant stalks. Mutant stalks were on average 24% smaller than those of wildtype. Mutant sections had a mean of 12% fewer vascular bundles, while bundle density was increased by 14%. Error bars indicate standard error. Significant differences between mutant and wildtype ($p < 0.05$) are indicated by *.

Three-dimensional reconstructions of stem sections from *csld1* mutant and non-mutant plants



Percentage of walls in thickness classes

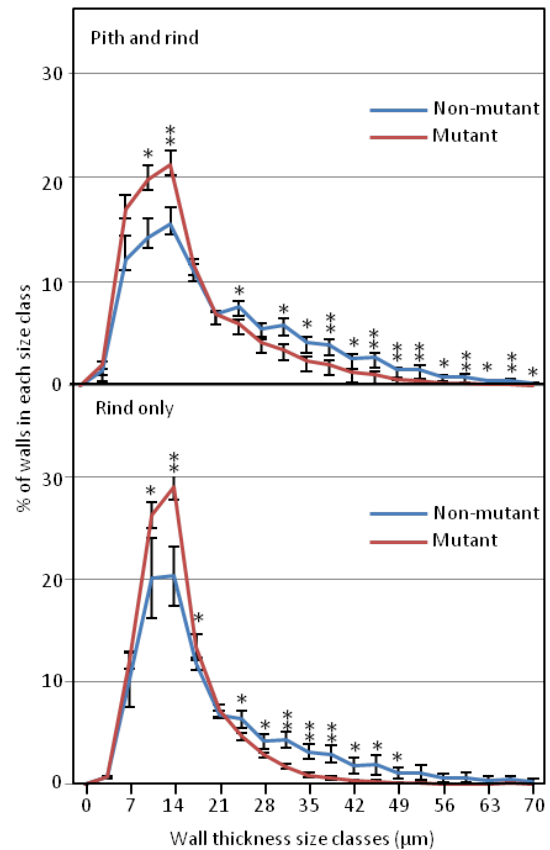


Figure 4-10. High-resolution X-ray micro computed tomography analysis of *csld1* and wildtype stalks. Analysis of stem sections from the third internode of greenhouse-grown *csld1* mutant and wildtype plants using high-resolution X-ray micro-CT. Hand-cut sections approximately 3 x 2 x 10 mm from the edge of mutant and wildtype stems (four each) were scanned at 3.5 µm resolution. Three-dimensional analyses revealed significant differences in density of wall material (lower left) and distribution of wall thickness (right). Mutant stems had more dense, but generally thinner, walls, even when analyses were limited to the rind only. Volumetric analyses were calculated with an algorithm developed for trabecular bone (Hildebrand and Regsegger, 1997). Error bars represent standard error. Significant differences from WT are indicated, ($p < 0.05$)** and ($p < 0.1$)*.

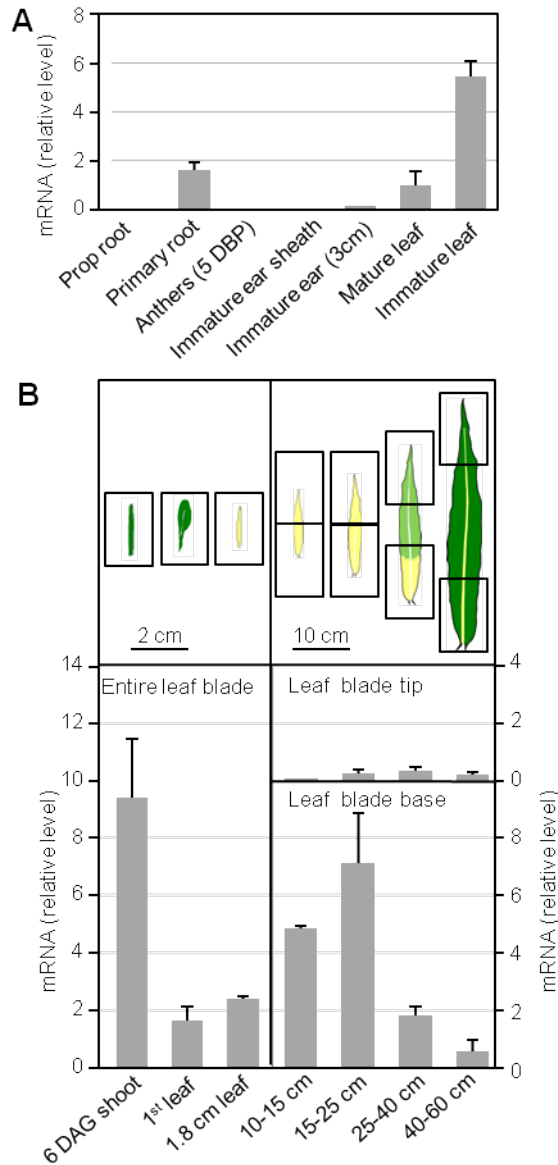


Figure 4-11. Levels of *Zm-CsID1* mRNA in diverse tissues from wildtype plants of the W22 inbred. (A) Expression of *Zm-CsID1* in diverse organs. (B) *Zm-CsID1* mRNA levels in leaf blades and blade-regions at different stages of development. Levels of mRNA was quantified by CyberGreen quantitative Real Time RT-PCR. Three biological replications were analyzed for or each tissue. Note abundance of *CsID1* transcripts in pre-emergent immature leaves. Maximal expression was observed in very young shoots (including coleoptile and enfolded leaves), followed by the basal portion of intermediate-staged developing leaves.

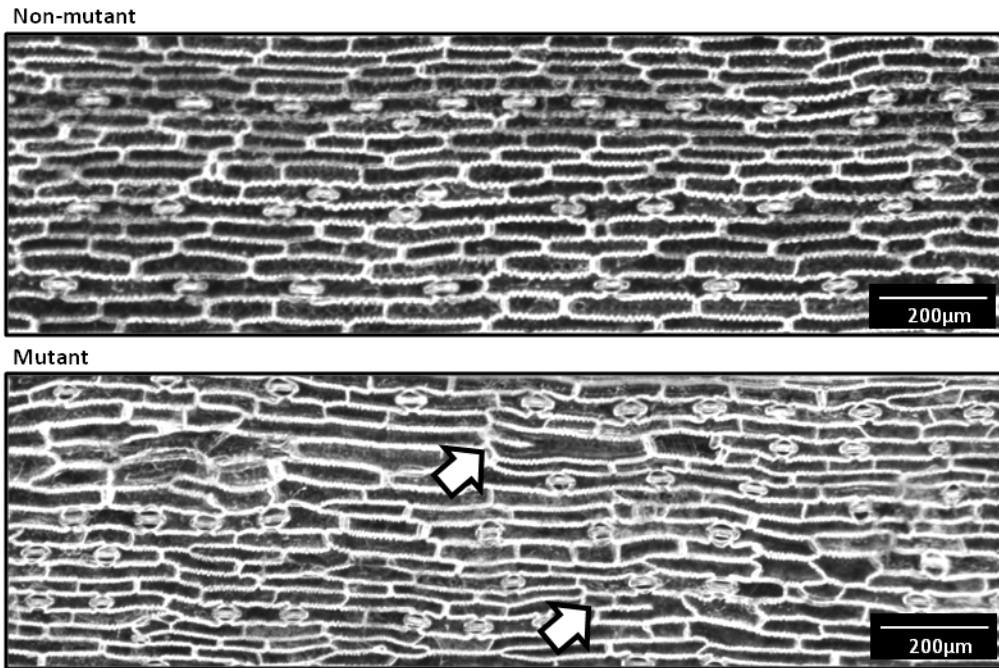


Figure 4-12. Mature *csld1* mutant and non-mutant epidermis revealed apparent defects in cell division. Comparison of isolated epidermis from non-warty areas of mature *csld1* mutant and non-mutant leaves using dark-field microscopy revealed a number of striking defects. Mutant epidermis appeared disrupted and unorganized compared to non-mutant epidermis. There were also numerous cases of misshapen cells and cell wall stubs (arrows), indicating a failure of cells to complete cell division.

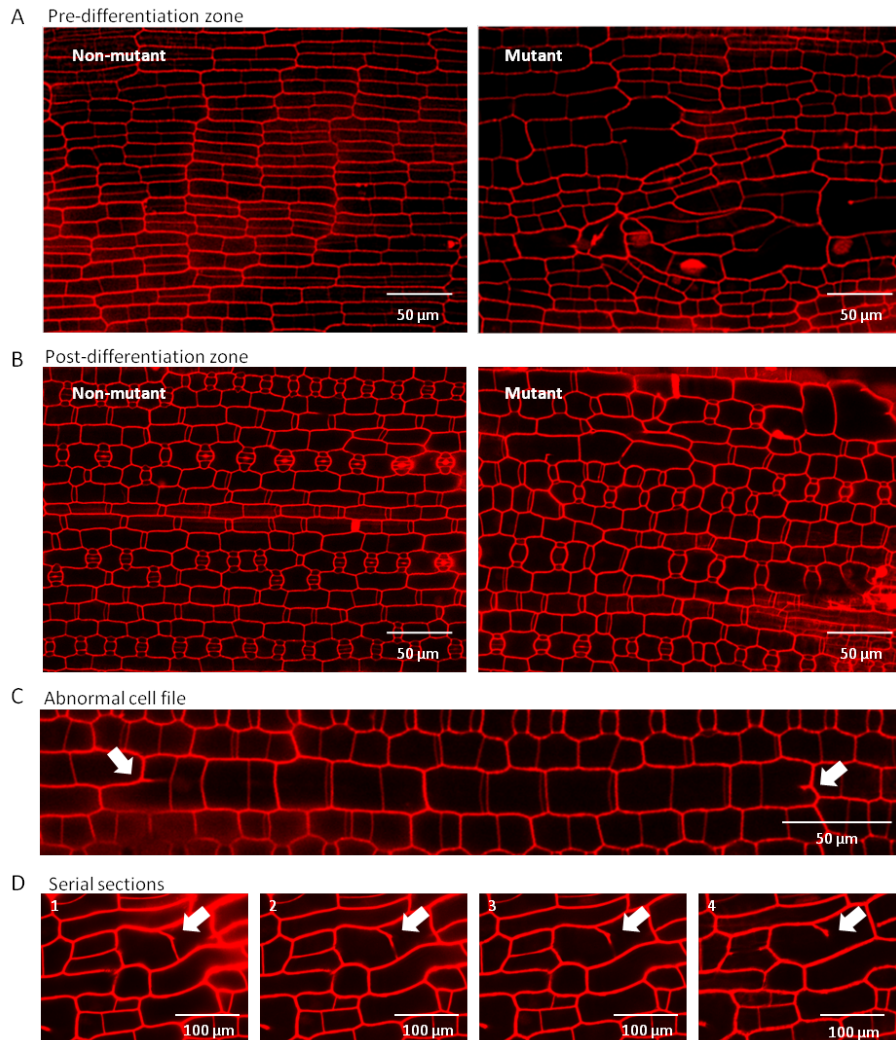


Figure 4-13. Confocal images showing defects early in development of *csld1* mutant leaf epidermis. Propidium iodide-stained cell walls from fresh, immature *csld1* mutant and wildtype leaves. (A) Pre-differentiation zones of basal portions of wildtype leaves contrasting with the abnormal *csld1-1* cell size, shape, and organization. Leaf blades were approximately 10-cm long. (B) Post-differentiation zones showing persistent effects of altered cell division in large, misshapen, unordered cells of the *csld1-1* leaf epidermis. Again, leaf blades were approximately 10-cm long. (C) A typical file of large, irregular cells bounded by individuals with incomplete cell walls protruding from their outer edges, consistent with clonal inheritance of large cell size. (D) Serial optical sections revealing irregular gaps in cell walls (arrow) that occur frequently in epidermal cells of the *csld1* mutant.

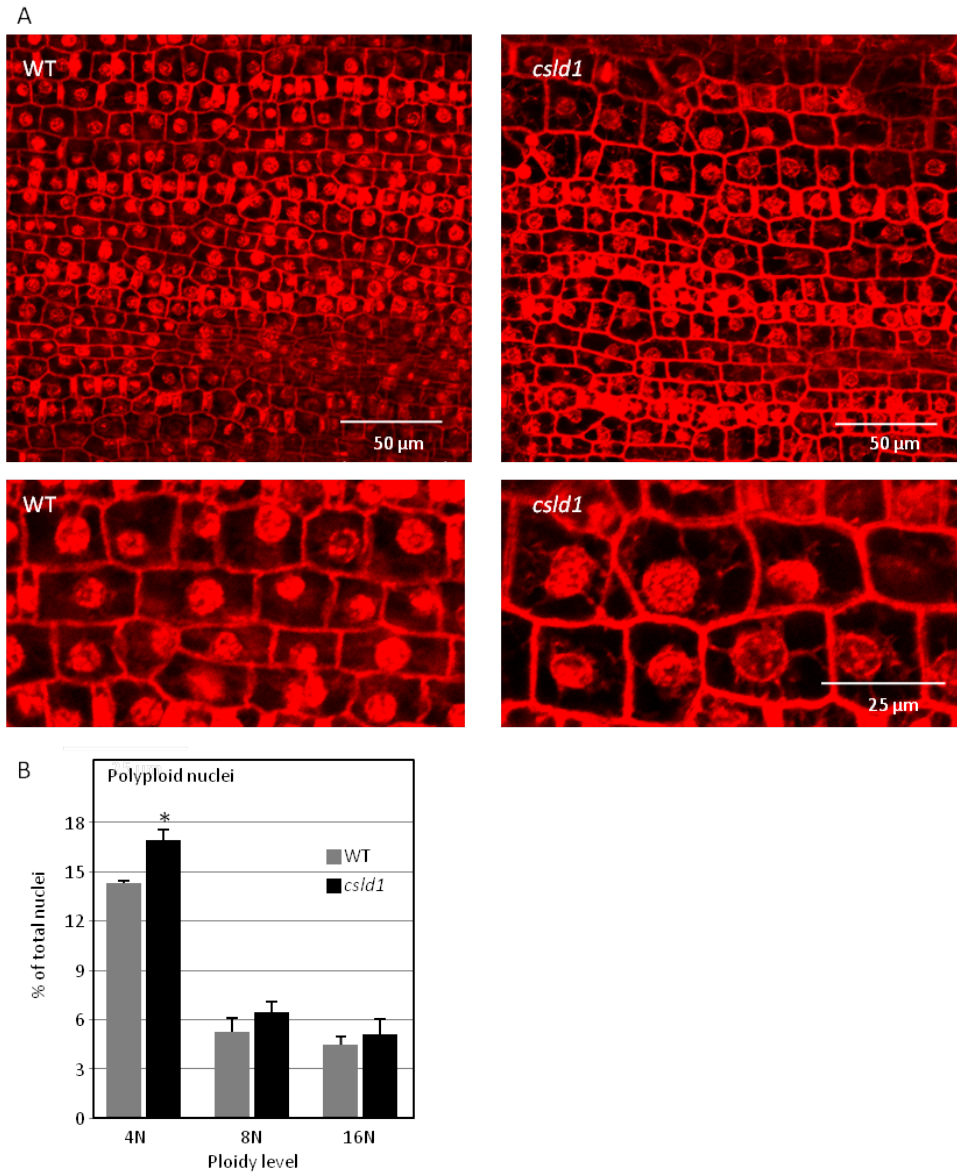


Figure 4-14. Nuclei of immature *cslD1* mutant and non-mutant epidermis. (A) Confocal imaging of fixed cells stained with propidium iodide revealed an abundance of large nuclei in *cslD1* mutant epidermis. Larger nuclei corresponded with the larger cell size of mutant epidermis. (B) Percent of total nuclei with 4N, 8N, and 16N. Nuclei from immature tissue from basal portions of *cslD1* mutant and wildtype leaves were examined using flow cytometry of isolated nuclei stained with propidium iodide. The majority of nuclei were 2N and are not displayed here. Significant difference between *cslD1* and wildtype ($p < 0.05$) are indicated by *, N = 5.

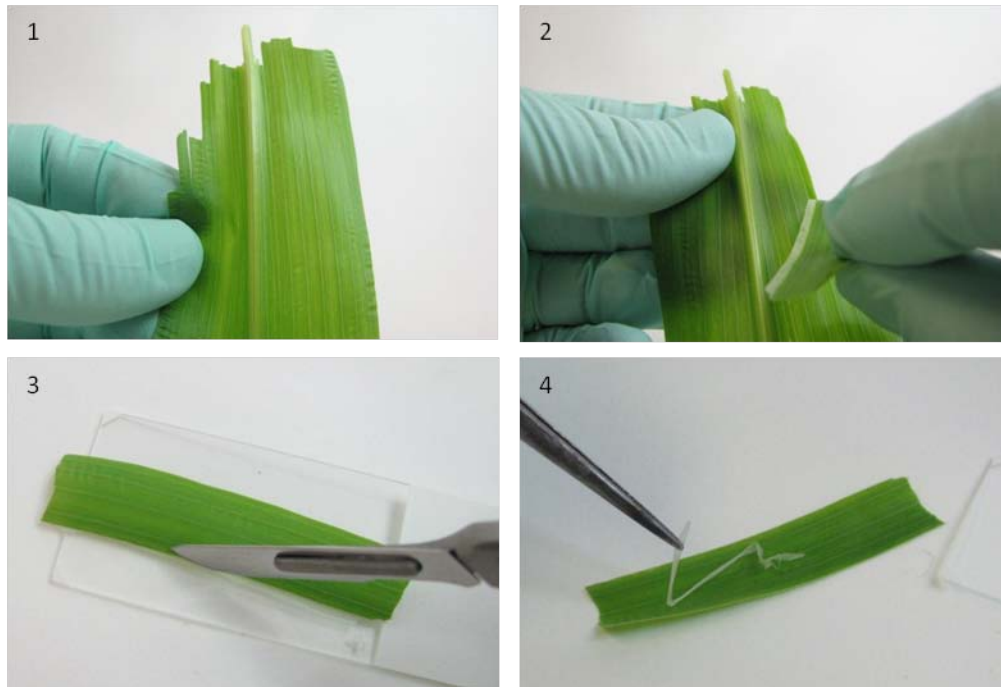


Figure 4-15. Isolation of maize leaf epidermis. 1) Hold a piece of fresh leaf tissue, with the epidermal surface to be isolated facing inward (abaxial surface in this case). 2) Pull back on part of the leaf so that it tears along the longitudinal leaf axis. As a strip of epidermis is revealed, angle the piece towards the main leaf body to maximize epidermal strip width. Typical epidermal strips are between 2-5 mm. 3) Completely remove the leaf piece containing the epidermal strip, hold against a hard surface (such as a glass slide), and slice off clean epidermis using a scalpel. Areas with non-epidermal contaminants should be visible against a white background. 4) Use forceps to transfer epidermal strip to collection tube, or leave strip on glass slide (with a small amount of water) for visualization under dark-field microscopy.

CHAPTER 5 CONCLUSIONS AND FUTURE DIRECTIONS

Work presented here revealed a surprisingly large number of Mu transposable elements, with extensive divergence, and widely-varying sites of insertion in maize and teosinte inbreds (Chapter 2). Results have been immediately incorporated into new attempts to harness the mutagenic power of these transposons in the UniformMu maize population (a globally-accessed community resource initiated at the University of Florida [McCarty et al., 2005]). Preliminary results from high-throughput sequencing of UniformMu DNA identified large numbers of apparently unique Mu12 elements that were not previously recognized in this population. The extent of activity by these Mu's was unexpected due to previous reports that detected little activity of Mu10s and Mu12s (Dietrich et al., 2002; Liu et al., 2009). However, previous studies did not utilize Mu12-specific primers for their Mu-flanking sequence generation. Regardless, results here show these to be an abundant, diverse, and active component of the Mu system. A re-appraisal of Mu10s and Mu12s in other mutagenic maize lines may yield results similar to those shown here. We will soon be able to test the degree to which the divergent and abundant Mu12 elements of the UniformMu population are active, and if so, a large number of insertional mutants will become available for the global community of maize geneticists and breeders. Even if the UniformMu population itself does not harbor particularly active Mu12 elements, our current sequencing protocols and materials should allow identification of lines that do have highly active Mu12s. These could be bred or engineered to create future mutagenic populations.

The presence of a previously unrecognized, possibly active transposase in the B73 maize genome is indicated by data shown here (Chapter 3, Figure 3-7). Additional

analyses will be needed to confirm function, but a clear homology and extensive conservation was shown between Mu10 elements in the B73 genome and the known MuDR transposase. Expression of the putative transposase genes in such Mu10 elements would indicate function, although their expression could be low, highly regulated, and/or limited to specific sites or times, thus not easily detectable. As of now, no Mu10-derived transcripts have been deposited in public maize EST collections (data not shown). Another line of future experimentation to test hypotheses for Mu10 activity would be to compare segregation of these (or similar elements) in wildtype and Mu-active populations such as UniformMu. If Mu-active lines could be identified that lacked classical MuDR elements, but which included these Mu10 elements, then this observation would support the hypothesis that some Mu10s encode functional transposases.

Evidence here revealed an unexpected role of a cell wall biosynthetic gene in plant cell division (Chapter 4), yet the specific biochemical mechanism is yet to be defined. Future work on sub-cellular localization of the maize CSLD1 protein may also provide valuable information about its specific biological role in the process of cell division. Transgenic maize lines with YFP-tagged CSLD1 protein driven by the CSLD1 native promoter are currently being generated by the Maize Cell Genomics group (Mohanty et al., 2009). We hypothesize that the CSLD1 enzyme is targeted to, and functional at, the newly-forming cell plate in epidermal cells of developing maize leaves. If so, then the tagged protein may localize to these regions near newly-forming cross walls. New evidence (from Erik Neilson, University of Michigan) also supports action by CSLD proteins in synthesis of cellulose, and a specialized form of cellulose could possibly be

required for cell wall formation at not only the tips of elongating cells such as root hairs and pollen tubes, but also at the cell plate of dividing plant cells.

The increased density and thinner cell walls of the *cs/d1* mutant stems, as revealed by high-resolution micro CT analyses, highlight another intriguing possibility regarding the function of CSLD proteins. Estimation of the cellulose crystallinity using X-ray diffraction and/or NMR spectroscopy (Park et al., 2010) could provide important evidence for the biochemical and/or biophysical basis for roles of the CSLD1 protein. If the *cs/d1* mutant walls contain more crystalline cellulose (as implied by results presented here), such data would provide still further resolution of whether CSLD enzymes produce contribute to formation of cellulose with a more amorphous nature.

APPENDIX A

All mapped Mu insertions in ten Zea inbreds, arranged by inbred, followed by Mu class and chromosome location. TSD: tandem-site duplication.

Inbred	Mu	chr	start	TSD
B73	Mu-9	chr1	215947275	GTCGGCTGG
B73	Mu-9	chr1	245365818	GTGTTAGGT
B73	Mu-9	chr1	245367837	GTGTTAGGT
B73	Mu-9	chr1	264263006	TTAGGTCCG
B73	Mu-9	chr1	264267812	TTAGGTCCG
B73	Mu-9	chr10	146901724	CTCGATTTG
B73	Mu-9	chr10	146912555	CTCGATTTG
B73	Mu-9	chr2	17647	CTCTCTTTC
B73	Mu-9	chr2	61514	GAAAGAGAG
B73	Mu-9	chr2	25300688	GAGGCTCTC
B73	Mu-9	chr2	25302603	GAGGCCCTC
B73	Mu-9	chr2	31723258	GGAGTGCGG
B73	Mu-9	chr2	135007660	GGCTGGCGG
B73	Mu-9	chr2	194078115	GCCGGGGGC
B73	Mu-9	chr2	194082980	GCCGGGGGC
B73	Mu-9	chr3	63759	CTGCATGGG
B73	Mu-9	chr3	63767	CTGCAGGGG
B73	Mu-9	chr3	170233622	GTCGCCAGC
B73	Mu-9	chr3	170235173	GTCGCCAGC
B73	Mu-9	chr3	192454287	AAATGGATG
B73	Mu-9	chr4	159505930	GCCGTGCGA
B73	Mu-9	chr4	165969433	GGGCTAGG
B73	Mu-9	chr5	17111268	CAAGGTGGG
B73	Mu-9	chr5	17197656	CAAGGTGGG
B73	Mu-9	chr5	116267118	TCACCCAAG
B73	Mu-9	chr5	116268617	TCACCCGAG
B73	Mu-9	chr6	107992293	CACAAAAAA
B73	Mu-9	chr6	161765840	CTGGTAGTG
B73	Mu-9	chr6	161770900	CTGGTAGTG
B73	Mu-9	chr7	48473780	GCGGGAGAG
B73	Mu-9	chr7	48474915	GCGGGAGGG
B73	Mu-9	chr7	72528765	CTATGCGAT
B73	Mu-9	chr7	72530965	CTATGCGAT
B73	Mu-9	chr7	134022998	CTCCTTAAG
B73	Mu-9	chr8	3812868	GTTGTGCTC
B73	Mu-9	chr8	3875319	GAGCACAAC
B73	Mu-9	chr8	138633675	GTTGTATTC

B73	Mu1-9	chr8	151461730	CTCTCTACC
B73	Mu1-9	chr8	153725735	GTTAGTTGT
B73	Mu1-9	chr8	153727357	GTTAGTTGT
B73	Mu1-9	chr9	40134754	GGCGCCCAG
B73	Mu1-9	chrUNKNOWN	13826404	TGCAGTACA
B73	Mu1-9	chrUNKNOWN	13829283	TGCAGTACA
B73	Mu10	chr2	63630170	GCACAAACT
B73	Mu10	chr2	76218121	TCGAGAGGG
B73	Mu10	chr2	76222892	TCGAGAGGG
B73	Mu10	chr3	32832334	CTCGCTGCC
B73	Mu10	chr4	40201165	TCGAGCGCG
B73	Mu10	chr4	170887654	GCGGGCGGA
B73	Mu10	chr5	70381872	GTTTTTCGG
B73	Mu10	chr5	70386843	GTTTTTCGG
B73	Mu10	chr5	73323804	GTCGAAATC
B73	Mu10	chr5	73327895	GTC ^A AAATC
B73	Mu10	chr5	145977953	TCCCCTCCA
B73	Mu10	chr6	160446766	TCCCACGAG
B73	Mu10	chr6	160464150	CTCCTGGGA
B73	Mu10	chr7	134021621	TTCTTTAAG
B73	Mu10	chr9	11643467	TGGGTTGGG
B73	Mu10	chr9	11653693	GGGCTGGGA
B73	Mu10	chrUNKNOWN	5300073	ATGGGAGTG
B73	Mu12	chr1	5853336	CCCGTCAGT
B73	Mu12	chr1	5855090	CCCGTCAGT
B73	Mu12	chr1	9045993	CTAGATTTG
B73	Mu12	chr1	10975143	CTCTCCTCG
B73	Mu12	chr1	19513553	CGAGAGCAG
B73	Mu12	chr1	37644606	ACCGAATGT
B73	Mu12	chr1	65294475	TAACATATC
B73	Mu12	chr1	65294573	CGACATATC
B73	Mu12	chr1	78845541	TGGACACTA
B73	Mu12	chr1	78847493	ATGGACACT
B73	Mu12	chr1	148130653	TGGCCCGTG
B73	Mu12	chr1	148231792	CACGGGCCA
B73	Mu12	chr1	164914751	CTGCTCTAC
B73	Mu12	chr1	255428941	GTTTCCCAA
B73	Mu12	chr1	255431229	TTTCCTTGG
B73	Mu12	chr1	259661577	CCATTTTTT
B73	Mu12	chr1	297180880	GAGAGATGA
B73	Mu12	chr1	297188349	GAGAGATGA
B73	Mu12	chr10	4001312	CCCTCTCCT
B73	Mu12	chr10	15300760	CTTGCAATG

B73	Mu12	chr10	15308429	CTTGCAATG
B73	Mu12	chr10	55963355	CCTCTAGAG
B73	Mu12	chr10	97224421	TGACGAAAC
B73	Mu12	chr10	97271042	TGACGAAAC
B73	Mu12	chr10	99885745	TGATGGTAT
B73	Mu12	chr10	116689007	GCAGGGCAG
B73	Mu12	chr10	135327980	GTCAGGGCT
B73	Mu12	chr10	135329008	GTCAGGGCT
B73	Mu12	chr10	138397252	TCCCAGGAT
B73	Mu12	chr10	141276026	GTGGCTGAC
B73	Mu12	chr10	141279103	GTGGCTGAC
B73	Mu12	chr10	141729910	CTCAGAAAG
B73	Mu12	chr2	9947891	CTTGACGA
B73	Mu12	chr2	24581453	TCGGTTGCG
B73	Mu12	chr2	24982189	GACCTCAA
B73	Mu12	chr2	25000049	TTTGAGGTC
B73	Mu12	chr2	25001836	CAAAGGGTC
B73	Mu12	chr2	37869180	GGGCACGAG
B73	Mu12	chr2	126547121	AGCTGCGGC
B73	Mu12	chr2	149547189	TCCATATGG
B73	Mu12	chr2	149548163	TCCATATGG
B73	Mu12	chr2	197215143	CGCGGGGGC
B73	Mu12	chr2	229531942	AGAGGGGGG
B73	Mu12	chr2	229540123	AGGAGGGGG
B73	Mu12	chr3	1603146	CATGAACCC
B73	Mu12	chr3	1703348	GGGTTTCATG
B73	Mu12	chr3	9282491	ATTTCCCGT
B73	Mu12	chr3	9286569	ATTTCCCGT
B73	Mu12	chr3	64925288	GATGCCGGC
B73	Mu12	chr3	64927462	GATGCCGGA
B73	Mu12	chr3	79376179	CCATTTTTT
B73	Mu12	chr3	89795711	CTTCAGAGA
B73	Mu12	chr3	121611818	GGCGTAACT
B73	Mu12	chr3	121613607	GGCGTAACT
B73	Mu12	chr3	121613610	GGTGTAAC
B73	Mu12	chr3	156342516	GTCCCCAGC
B73	Mu12	chr3	181510576	CTCCCGAAC
B73	Mu12	chr3	181511716	CTCCCGAAC
B73	Mu12	chr3	216632366	TACTGCAGT
B73	Mu12	chr3	223787656	CCTGTAGGA
B73	Mu12	chr4	25856208	TCGAGCTG
B73	Mu12	chr4	58603310	TGCGCGTGC
B73	Mu12	chr4	73211942	CAATGCCGC

B73	Mu12	chr4	96634756	GGGCTCAAT
B73	Mu12	chr4	117222508	ACCGCAGAC
B73	Mu12	chr4	117224174	ACCGCAGAC
B73	Mu12	chr4	166495091	GTACATATG
B73	Mu12	chr4	166547003	CATATGTAC
B73	Mu12	chr4	182833406	AGTTTCAGA
B73	Mu12	chr4	199244475	AGTTCGGAC
B73	Mu12	chr4	208777269	CCTGGTGGA
B73	Mu12	chr4	210943904	GAGAGAGAT
B73	Mu12	chr4	210945539	GAGATGTCA
B73	Mu12	chr4	211398529	GCGAGCGAG
B73	Mu12	chr4	211400767	GCGAGCGAG
B73	Mu12	chr4	231573451	GGTGTTTGA
B73	Mu12	chr4	244759229	GATGAGGAG
B73	Mu12	chr5	5197195	GCGTGGGCG
B73	Mu12	chr5	5199460	GCGTGGGCG
B73	Mu12	chr5	23237962	GACGTGCTC
B73	Mu12	chr5	26466383	AGCCTAGGA
B73	Mu12	chr5	26839718	CGCGGGCGG
B73	Mu12	chr5	33848208	CGTTAGGTC
B73	Mu12	chr5	33849953	CGTTAGGTC
B73	Mu12	chr5	42849194	AATATGATG
B73	Mu12	chr5	58608495	CCTCCTTAA
B73	Mu12	chr5	65382203	AGGGGGGGG
B73	Mu12	chr5	155255661	GCCTTGGGC
B73	Mu12	chr5	155260687	GCCTTGGGC
B73	Mu12	chr5	163935903	GATGTAGCC
B73	Mu12	chr5	180873325	GTTGCGTGC
B73	Mu12	chr5	180877223	CGTTGCGTG
B73	Mu12	chr5	185079405	GAATGTTTT
B73	Mu12	chr5	186969978	AGAGGGGGG
B73	Mu12	chr5	190223449	TAAACCACC
B73	Mu12	chr5	190225195	CTAAACCAC
B73	Mu12	chr5	203749481	TTCGTGCGAC
B73	Mu12	chr5	203763309	TTCGTGCGC
B73	Mu12	chr6	2917476	TCCATGATG
B73	Mu12	chr6	14213991	GTGTTTCATG
B73	Mu12	chr6	28306795	GCTGCAGGA
B73	Mu12	chr6	92047273	ATGCAGATG
B73	Mu12	chr6	92197928	CCTTGCAAG
B73	Mu12	chr6	129097781	GGAACGAAT
B73	Mu12	chr7	16535034	AATGGTCCA
B73	Mu12	chr7	20735964	CCAATTTCGG

B73	Mu12	chr7	50182115	GCCCGTGAG
B73	Mu12	chr7	121684992	CCAAAAATG
B73	Mu12	chr7	147322983	GGCGTGCTA
B73	Mu12	chr7	161229569	ATCTGTCAG
B73	Mu12	chr7	169729474	CCATTTCCA
B73	Mu12	chr8	5414131	GCGCGCGAG
B73	Mu12	chr8	5414433	CTCGCGCGC
B73	Mu12	chr8	42932444	GACCTCAAA
B73	Mu12	chr8	100614801	CATTGTAGG
B73	Mu12	chr8	106152637	TCATTGCAA
B73	Mu12	chr8	130925131	GGCTGCGGA
B73	Mu12	chr8	141273174	GTAGATTGG
B73	Mu12	chr8	141274171	CTGATTGGG
B73	Mu12	chr8	148886228	CCTGTTTGA
B73	Mu12	chr8	148887210	CCTGTTTGA
B73	Mu12	chr8	148887211	CTGTTTGAA
B73	Mu12	chr9	4231266	GCACGCAAC
B73	Mu12	chr9	4231339	CGCACGCAA
B73	Mu12	chr9	15061435	GCGAGCGTC
B73	Mu12	chr9	25697019	CCTAATTTT
B73	Mu12	chrUNKNOWN	12783521	AGTGGCCGG
MO17	Mu1-9	chr1	152954540	ACCAATTGG
MO17	Mu1-9	chr1	192534615	CCAATTGGT
MO17	Mu1-9	chr1	264263006	TTAGGTCGG
MO17	Mu1-9	chr1	264267812	TTAGGTCGG
MO17	Mu1-9	chr1	273709444	ATCTCTGAG
MO17	Mu1-9	chr10	88102930	CTTGTGAAG
MO17	Mu1-9	chr10	103741428	CTTGTGAAG
MO17	Mu1-9	chr10	129970873	CTGGTAATA
MO17	Mu1-9	chr10	146901724	CTCGATTTG
MO17	Mu1-9	chr10	146912555	CTCGATTTG
MO17	Mu1-9	chr2	25300688	GAGGCTCTC
MO17	Mu1-9	chr2	25302603	GAGGCTCTC
MO17	Mu1-9	chr2	31723258	GGAGTGCGG
MO17	Mu1-9	chr2	31723266	GAGTGCGGG
MO17	Mu1-9	chr2	135007660	GGCTGGCGG
MO17	Mu1-9	chr2	135009766	GGCTGGCGG
MO17	Mu1-9	chr2	142272069	CATCCAAAC
MO17	Mu1-9	chr2	142324924	CCATCCAAA
MO17	Mu1-9	chr2	158559629	CTCTCTTTC
MO17	Mu1-9	chr2	214951873	TTAGGTCGG
MO17	Mu1-9	chr2	214951881	TTAGATCGG
MO17	Mu1-9	chr2	220443225	CCAGCAGCC

MO17	Mul-9	chr3	219993784	CCCTTGATT
MO17	Mul-9	chr3	219993791	CCCTTGATT
MO17	Mul-9	chr3	230139824	CCCATGCAG
MO17	Mul-9	chr3	230143403	CCCCTGCAG
MO17	Mul-9	chr4	118954521	CCTTGTGAA
MO17	Mul-9	chr4	159505930	GCCGTGCGA
MO17	Mul-9	chr4	159506805	GCCGTGCGA
MO17	Mul-9	chr4	165969433	GGGCTTAGG
MO17	Mul-9	chr5	17111268	CAAGGTGGG
MO17	Mul-9	chr5	17197656	CAAGGTGGG
MO17	Mul-9	chr5	116267118	TCACCCAAG
MO17	Mul-9	chr5	116268617	TCACCCGAG
MO17	Mul-9	chr5	178759106	GTTTGGAGT
MO17	Mul-9	chr5	178759114	GTTTGCAGT
MO17	Mul-9	chr5	201460195	GTCGGTCTA
6_8	Mul-9	chr5	201460203	GTCGGTCTA
MO17	Mul-9	chr6	47652355	CCACAAATA
MO17	Mul-9	chr6	47652364	CACAAATAG
MO17	Mul-9	chr6	107992299	CACAAAAAA
MO17	Mul-9	chr6	167002619	CTTCACAAG
MO17	Mul-9	chr6	167003111	CTTCACAAG
MO17	Mul-9	chr6	167011925	CTTGTGAAG
MO17	Mul-9	chr8	85028236	CAAGGTGGG
MO17	Mul-9	chr8	139599679	ACAACAAAC
MO17	Mul-9	chr8	151461730	CTCTCTACC
MO17	Mul-9	chr8	151463296	CTCTCTACC
MO17	Mul-9	chr8	152812782	ATTGAAAGG
MO17	Mul-9	chr8	152814820	ATTGAAAAG
MO17	Mul-9	chr8	153725735	GTTAGTTGT
MO17	Mul-9	chr8	153727357	GTTAGTTGT
MO17	Mul-9	chr8	169907702	CTCACACAC
MO17	Mul-9	chr8	169907706	CTCACACAC
MO17	Mul-9	chr9	12106581	TCTCCCGAG
MO17	Mul-9	chr9	26352347	CTTGTGAAG
MO17	Mul-9	chr9	26352355	CTTGTGAAG
MO17	Mul-9	chr9	106850972	CACCGGGAG
MO17	Mul-9	chr9	106850980	CACCGGGAG
MO17	Mul-9	chr9	129919432	GGCGTGCGT
MO17	Mul-9	chr9	145681991	GAAAGAGAG
MO17	Mul-9	chrUNKNOWN	8109034	CACCAGAAA
MO17	Mul-9	chrUNKNOWN	13826404	TGCAGTACA
MO17	Mul-9	chrUNKNOWN	13829283	TGCAGTACA
MO17	Mul0	chr1	17669069	GTTTGTTCGC

MO17	Mu10	chr1	17669186	GTTTGCCGC
MO17	Mu10	chr1	127026395	GCCCCAGAT
MO17	Mu10	chr2	76218121	TCGAGAGGG
MO17	Mu10	chr2	76222892	TCGAGAGGG
MO17	Mu10	chr2	79137485	GGTGGCAAC
MO17	Mu10	chr2	187496817	CTCAGCGCC
MO17	Mu10	chr2	187496825	CTCAGCGCC
MO17	Mu10	chr2	220443225	CCAGCAGCC
MO17	Mu10	chr2	220448990	CCTAGCAGC
MO17	Mu10	chr3	32827320	CCCCTGCC
MO17	Mu10	chr3	32832334	CTCGCTGCC
MO17	Mu10	chr4	40176738	TCGAGCGCG
MO17	Mu10	chr4	40201165	TCGAGCGCG
MO17	Mu10	chr4	158906485	AGAAGAGGG
MO17	Mu10	chr4	165967845	GGGCCTAGG
MO17	Mu10	chr4	199095951	TTTTGAATA
MO17	Mu10	chr4	199095959	TTTTGAATA
MO17	Mu10	chr5	17197656	CAAGGTGGG
MO17	Mu10	chr5	73323804	GTCAAAATC
MO17	Mu10	chr5	73327895	GTCAAAATC
MO17	Mu10	chr6	82267957	GCACAGGGG
MO17	Mu10	chr8	162447325	CAAATAAAC
MO17	Mu10	chr9	907863	GTTTACTTG
MO17	Mu10	chr9	83025615	CGCGCTCGA
MO17	Mu12	chr1	5852728	CCCGTCAGT
MO17	Mu12	chr1	5855090	CCCGTCAGT
MO17	Mu12	chr1	10975143	CTCTCCTCG
MO17	Mu12	chr1	37644610	ACCAAATGG
MO17	Mu12	chr1	47209329	AAAAAAACG
MO17	Mu12	chr1	55607850	TGTGGTAAG
MO17	Mu12	chr1	55607855	TGTGGTAAG
MO17	Mu12	chr1	114596663	CCATTTCCA
MO17	Mu12	chr1	148517216	TAAAAAAC
MO17	Mu12	chr1	148517219	TAAAAAACG
MO17	Mu12	chr1	168938431	GGGCACAAG
MO17	Mu12	chr1	228684862	TGGAAGTGG
MO17	Mu12	chr1	259661577	CCATTTTTT
MO17	Mu12	chr1	297188349	GAGAGATGA
MO17	Mu12	chr10	2305173	GAGGTCGGC
MO17	Mu12	chr10	15300760	CTTGCAATG
MO17	Mu12	chr10	15308429	CTTGCAATG
MO17	Mu12	chr10	17855413	GGCCCCAC
MO17	Mu12	chr10	45432395	CATCATATT

MO17	Mu12	chr10	49804591	TGACATCTC
MO17	Mu12	chr10	55963355	CCTCTAGAG
MO17	Mu12	chr10	71415205	CCTGTTTGA
MO17	Mu12	chr10	74883501	TGGACAGGT
MO17	Mu12	chr10	89755300	TTCTTGTGG
MO17	Mu12	chr10	90179710	ACCTGTCAA
MO17	Mu12	chr10	90179749	ACCTGTCAA
MO17	Mu12	chr10	91858466	CCAGAACCC
MO17	Mu12	chr10	114389638	CTCTAGTTC
MO17	Mu12	chr10	132217391	CGTTTTTTTT
MO17	Mu12	chr10	135327980	GTCAGGGCT
MO17	Mu12	chr10	135329008	GTCAGGGCT
MO17	Mu12	chr10	135454667	CCGTCAGTG
MO17	Mu12	chr10	137135412	CATATGTAC
MO17	Mu12	chr10	137392165	TCAAACAGG
MO17	Mu12	chr10	144196261	GAGATGAGA
MO17	Mu12	chr2	1208535	CTTTGGATA
MO17	Mu12	chr2	2004537	GGTGATGAG
MO17	Mu12	chr2	6579102	ACTGACGGG
MO17	Mu12	chr2	24982189	GACCTCAAA
MO17	Mu12	chr2	25000049	TTTGAGGTC
MO17	Mu12	chr2	25001836	CAAAGGGTC
MO17	Mu12	chr2	32730341	CAGGGAAAC
MO17	Mu12	chr2	37869180	GGGCACGAG
MO17	Mu12	chr2	90728755	GGGTTCTGG
MO17	Mu12	chr2	155007653	GGGCGGTGG
MO17	Mu12	chr2	207958804	GTACAGAAC
MO17	Mu12	chr2	207958827	GTACAGAAC
MO17	Mu12	chr3	3839648	GCTTGCCAA
MO17	Mu12	chr3	3839656	GCTTGCCGA
MO17	Mu12	chr3	89795711	CTTCAGAGA
MO17	Mu12	chr3	121611818	GGCGTAACT
MO17	Mu12	chr3	121613607	GGCGTAACT
MO17	Mu12	chr3	156342516	GTCCCCAGC
MO17	Mu12	chr3	165906824	TTGACAGGT
MO17	Mu12	chr3	165906845	TTGACAGGT
MO17	Mu12	chr3	216037776	GTGTGTCGG
MO17	Mu12	chr3	216632366	TACTGCAGT
MO17	Mu12	chr3	223664317	TCCTACAGG
MO17	Mu12	chr3	223787656	CCTGTAGGA
MO17	Mu12	chr4	7227108	AAAATCAAG
MO17	Mu12	chr4	25856207	CTCGCAGCT
MO17	Mu12	chr4	68421868	CCCACCGCC

MO17	Mul2	chr4	68421874	CCCACCGCC
MO17	Mul2	chr4	90878858	ACCTGTCAA
MO17	Mul2	chr4	90878875	ACCTGTCAA
MO17	Mul2	chr4	96634756	GGGCTCAAT
MO17	Mul2	chr4	103973120	CGCCCACGC
MO17	Mul2	chr4	166495091	GTACATATG
MO17	Mul2	chr4	166547003	CATATGTAC
MO17	Mul2	chr4	182724999	GTTTTTCAGA
MO17	Mul2	chr4	182813239	AGTTTTTCAGA
MO17	Mul2	chr4	208777269	CCTGGTGGA
MO17	Mul2	chr4	210943904	GAGAGAGAT
MO17	Mul2	chr4	210945539	GAGATGTCA
MO17	Mul2	chr4	211398529	GCGAGCGAG
MO17	Mul2	chr4	211400767	GCGAGCGAG
MO17	Mul2	chr4	217229790	GCTTGCCGA
MO17	Mul2	chr5	5197195	GCGTGGGCG
MO17	Mul2	chr5	5199460	GCGTGGGCG
MO17	Mul2	chr5	26466383	AGCCTAGGA
MO17	Mul2	chr5	42849194	AATATGATG
MO17	Mul2	chr5	126213492	CTCGCGGGC
MO17	Mul2	chr5	153237757	GGCATGGGG
MO17	Mul2	chr5	161969989	TTGGCAAGC
MO17	Mul2	chr5	180873325	GTTGCGTGC
MO17	Mul2	chr5	184684568	TGGCCCCAC
MO17	Mul2	chr5	185027058	CAAACATTC
MO17	Mul2	chr5	185079405	GAATGTTTT
MO17	Mul2	chr5	191610797	AATGCAAGG
MO17	Mul2	chr6	2917476	TCCATGATG
MO17	Mul2	chr6	4072269	CTGCTCTCG
MO17	Mul2	chr6	19513671	CAAAAATGG
MO17	Mul2	chr6	31283834	CAGTGGCCG
MO17	Mul2	chr6	59141567	TCAAACAGG
MO17	Mul2	chr6	63914664	CCGTTTTTTT
MO17	Mul2	chr6	92197933	CTTACAAGG
MO17	Mul2	chr6	95593073	TCAAACAGG
MO17	Mul2	chr6	114620777	CCCACCGCC
MO17	Mul2	chr6	117288224	CCAATCATC
MO17	Mul2	chr6	117757951	CCTTGATTT
MO17	Mul2	chr6	121771628	GACCTCAAA
MO17	Mul2	chr6	129097781	GGAACGAAT
MO17	Mul2	chr6	137479179	GGTTCGCCA
MO17	Mul2	chr6	137479186	TGGTTCGCC
MO17	Mul2	chr6	152474926	GATTCAAAT

MO17	Mu12	chr6	157068221	CCTCAAGAA
MO17	Mu12	chr6	157068229	CCTCAAGAA
MO17	Mu12	chr6	169129268	CCCCCACCC
MO17	Mu12	chr6	169241025	CCCCCACCC
MO17	Mu12	chr7	29692026	AGTTACGCC
MO17	Mu12	chr7	30913431	CCAGAACCC
MO17	Mu12	chr7	50179197	GCCCGCGAG
MO17	Mu12	chr7	50182115	GCCCGCGAG
MO17	Mu12	chr7	144119874	GTGGGGGCC
MO17	Mu12	chr7	161229569	ATCTGTCAG
MO17	Mu12	chr7	169729474	CCATTTCCA
MO17	Mu12	chr7	169731084	CCATTTCCA
MO17	Mu12	chr8	5414433	CTCGCGCGC
MO17	Mu12	chr8	100614800	CCATTGTAG
MO17	Mu12	chr8	141273174	ATAGATTGG
MO17	Mu12	chr8	141274171	CTGATTGGG
MO17	Mu12	chr8	148886228	CCTGTTTGA
MO17	Mu12	chr8	148887210	CCTGTTTGA
MO17	Mu12	chr9	514440	TGAGTTGGG
MO17	Mu12	chr9	532640	CCTGAGTTG
MO17	Mu12	chr9	532648	CCTGAGTTG
MO17	Mu12	chr9	4231258	GCACGCAAC
MO17	Mu12	chr9	4231266	GCACGCAAC
MO17	Mu12	chr9	7781359	CCTGAGTTG
MO17	Mu12	chr9	13190529	GGCGGTGGG
MO17	Mu12	chr9	21325864	TCAAACAGG
MO17	Mu12	chr9	21325869	TCAAACAGG
MO17	Mu12	chr9	31200845	TGACATCTC
MO17	Mu12	chr9	65599040	TTTGAGGTC
MO17	Mu12	chr9	65599075	TTAGAGGTC
MO17	Mu12	chr9	80678776	CGAGGAGAG
MO17	Mu12	chr9	94445147	CCGTTTTTTT
MO17	Mu12	chr9	107612907	AAAAGACGG
MO17	Mu12	chr9	120235432	CTCGTGCCC
MO17	Mu12	chr9	129431052	AAAGTCAAG
MO17	Mu12	chr9	136481345	TCAAACAGG
MO17	Mu12	chrUNKNOWN	380784	CAGGGAAAC
MO17	Mu12	chrUNKNOWN	389185	GCGAGCGAG
MO17	Mu12	chrUNKNOWN	713397	GCGAGCGAG
MO17	Mu12	chrUNKNOWN	2802958	ACGAATCTT
MO17	Mu12	chrUNKNOWN	3605870	GGCGACGTA
MO17	Mu12	chrUNKNOWN	7422090	ACCGATAAA
MO17	Mu12	chrUNKNOWN	8423439	CATATGTAC

MO17	Mul2	chrUNKNOWN	10938872	ATACATGCC
MO17	Mul2	chrUNKNOWN	12783520	CAGTGGCCG
W22	Mul-9	chr1	19746434	TTTGAAATG
W22	Mul-9	chr1	19746443	TTTGAAATG
W22	Mul-9	chr1	101026009	CTGTGCGAG
W22	Mul-9	chr1	101060278	CTCGCACAG
W22	Mul-9	chr1	101060286	CTCGCACAG
W22	Mul-9	chr1	264263006	TTAGGTCCG
W22	Mul-9	chr1	264267812	TTAGGTCCG
W22	Mul-9	chr10	10267286	GAAAGAGAG
W22	Mul-9	chr10	129970865	CTGGTAATA
W22	Mul-9	chr10	129970873	CTGGTAATA
W22	Mul-9	chr10	132671325	CCCCTACGG
W22	Mul-9	chr10	132671330	CCCCTACGG
W22	Mul-9	chr10	146912555	CTCGATTTG
W22	Mul-9	chr2	1696519	GTCTCTGTG
W22	Mul-9	chr2	1696527	GTCTCTGTG
W22	Mul-9	chr2	25300688	GAGGCTCTC
W22	Mul-9	chr2	25302603	GAGGCTCTC
W22	Mul-9	chr2	71709108	CTCTCTGAT
W22	Mul-9	chr2	71709116	CTCTCTGAT
W22	Mul-9	chr2	135007660	GGCTGGCGG
W22	Mul-9	chr2	142272069	CATCCAAAC
W22	Mul-9	chr2	158559629	CTCTCTTTC
W22	Mul-9	chr2	194078115	GCCGGGGGC
W22	Mul-9	chr2	194082980	GCCGGGGGC
W22	Mul-9	chr2	214951873	TTAGGTCCG
W22	Mul-9	chr3	170233622	GTCGCCAGC
W22	Mul-9	chr3	170235173	GTCGCCAGC
W22	Mul-9	chr3	230143403	CCCCTGCAG
W22	Mul-9	chr4	159505930	GCCGTGCGA
W22	Mul-9	chr4	209048525	GCTGGCGTC
W22	Mul-9	chr4	209048533	GCTGGCGTC
W22	Mul-9	chr5	13208513	GTCGCCAGC
W22	Mul-9	chr5	13215095	GTCGCCAGC
W22	Mul-9	chr5	116267118	TCACCCAAG
W22	Mul-9	chr5	116268617	TCACCCGAG
W22	Mul-9	chr5	175353387	TTTGACGGT
W22	Mul-9	chr5	175353388	TTGACGGTG
W22	Mul-9	chr5	201460195	GTCGGTCTA
W22	Mul-9	chr5	201460203	GTCGGTCTA
W22	Mul-9	chr6	107992299	CACAAAAAA
W22	Mul-9	chr6	112507608	GTTTCAGAAA

W22	Mul-9	chr6	112507616	G TTCAGAAA
W22	Mul-9	chr8	138633675	G TTGTATTC
W22	Mul-9	chr8	153725735	G TTAGTTGT
W22	Mul-9	chr8	153727357	G TTAGTTGT
W22	Mul-9	chr9	8145105	CAAGACGTG
W22	Mul-9	chr9	8145113	CAAGACGTG
W22	Mul-9	chr9	86968542	ATCAAATCT
W22	Mul-9	chr9	86968550	ATCAAATCT
W22	Mul-9	chr9	140075456	TTCTCAGCC
W22	Mul-9	chr9	140075465	TTCTCAGCC
W22	Mul-9	chrUNKNOWN	13826404	TGCAGTACA
W22	Mul-9	chrUNKNOWN	13829283	TGCAGTACA
W22	Mul0	chr2	76222892	TCGAGAGGG
W22	Mul0	chr2	199398880	G TTGTGTGG
W22	Mul0	chr2	199398888	G TTGTGTGG
W22	Mul0	chr4	40201165	TCGAGCGCG
W22	Mul0	chr4	40201169	TCGGGCGCG
W22	Mul0	chr4	133716929	TCCCCTGCG
W22	Mul0	chr4	133716937	TCCCCTGCG
W22	Mul0	chr4	170887654	GCGGGCGGA
W22	Mul0	chr4	204351539	ATGATGTTG
W22	Mul0	chr5	73323804	GTCAAATC
W22	Mul0	chr5	73327895	GTCAAATC
W22	Mul0	chr8	138633677	GCTGTATTC
W22	Mul0	chr9	10256387	GATGGGGAG
W22	Mul2	chr1	5855090	CCCCTCAGT
W22	Mul2	chr1	9045993	CTAGATTTG
W22	Mul2	chr1	37644610	ACCAAATGG
W22	Mul2	chr1	46120376	CCATTTTTT
W22	Mul2	chr1	65294475	TAACATATC
W22	Mul2	chr1	164914751	CTGCTCTAC
W22	Mul2	chr1	228684862	TGGAAATGG
W22	Mul2	chr1	255428941	GTTTCCCAA
W22	Mul2	chr1	255431232	TTTCCCTTG
W22	Mul2	chr1	259661577	CCATTTTTT
W22	Mul2	chr1	279300802	ATTTATGAC
W22	Mul2	chr1	297180880	GAGAGATGA
W22	Mul2	chr1	297188349	GAGAGATGA
W22	Mul2	chr10	4001312	CCCTCTCCT
W22	Mul2	chr10	9786669	CCATTTTTT
W22	Mul2	chr10	15300760	CTTGCAATG
W22	Mul2	chr10	55963355	CCTCTAGAG
W22	Mul2	chr10	106665024	CCCCATGGC

W22	Mu12	chr10	134125091	CGCCACCGG
W22	Mu12	chr10	138397252	TCCCAGGAT
W22	Mu12	chr10	141276027	TGGTTGACG
W22	Mu12	chr10	141279103	GTGGCTGAC
W22	Mu12	chr2	1207318	CTTTGGATA
W22	Mu12	chr2	4039076	CTCGTGGAG
W22	Mu12	chr2	24982189	GACCTCAAA
W22	Mu12	chr2	25000049	TTTGAGGTC
W22	Mu12	chr2	25001836	CAAAGGGTC
W22	Mu12	chr2	32730341	CAGGGAAAC
W22	Mu12	chr2	37869180	GGGCACGAG
W22	Mu12	chr2	152204163	TGTAGTGCA
W22	Mu12	chr2	169238501	CCCGTGTTG
W22	Mu12	chr2	210074350	ACCTATTCC
W22	Mu12	chr2	210074358	ACCTATTCC
W22	Mu12	chr2	221528287	GGTATACAA
W22	Mu12	chr2	221528295	GGTATACAA
W22	Mu12	chr3	3839648	GCTTGCCGA
W22	Mu12	chr3	3839656	GCTTGCCGA
W22	Mu12	chr3	9282491	ATTTCCCGT
W22	Mu12	chr3	9286569	ATTTCCCGT
W22	Mu12	chr3	54825892	GGACTTGCG
W22	Mu12	chr3	54825897	GGACTTGCG
W22	Mu12	chr3	89795711	CTTCGGAGA
W22	Mu12	chr3	121611818	GGCGTAACT
W22	Mu12	chr3	121613607	GGCGTAACT
W22	Mu12	chr3	156342516	GTCCCCAGC
W22	Mu12	chr3	192256105	CGCCGCGAC
W22	Mu12	chr3	192256113	CGCCGCGAC
W22	Mu12	chr3	216632366	TACTGCAGT
W22	Mu12	chr3	217655664	CCGTTTTTTT
W22	Mu12	chr3	220339229	CTCGTGGAG
W22	Mu12	chr3	220339237	CTCGTGGAG
W22	Mu12	chr4	96634756	GGGCTCAAT
W22	Mu12	chr4	110554888	CAAGATGGG
W22	Mu12	chr4	117222508	ACCGCAGAC
W22	Mu12	chr4	117224174	ACCGCAGAC
W22	Mu12	chr4	152475445	TTCTGCGTT
W22	Mu12	chr4	166495091	GTACATATG
W22	Mu12	chr4	166547003	CATATGTAC
W22	Mu12	chr4	182724999	GTTTTTCAGA
W22	Mu12	chr4	199244475	GGTTTCGGAC
W22	Mu12	chr4	210943904	GAGAGAGAT

W22	Mu12	chr4	210945539	GAGATGTCA
W22	Mu12	chr4	211398529	GCGAGCGAG
W22	Mu12	chr4	211400767	GCGAGCGAG
W22	Mu12	chr4	239406228	GTGAGTGAG
W22	Mu12	chr4	239406230	GTGTGTGAG
W22	Mu12	chr4	240230508	GCGATGCGG
W22	Mu12	chr4	240230516	GCGATGCGG
W22	Mu12	chr4	244752104	GATGAGGAG
W22	Mu12	chr4	244759229	GATGAGGAG
W22	Mu12	chr5	26466383	AGCCTAGGA
W22	Mu12	chr5	26839718	CGCGGGCGG
W22	Mu12	chr5	42849194	AATATGATG
W22	Mu12	chr5	97142862	GCGATGCGG
W22	Mu12	chr5	155255661	GCCTTGGGC
W22	Mu12	chr5	155260687	GCCTTGGGC
W22	Mu12	chr5	161969989	TCGGCAAGC
W22	Mu12	chr5	185027058	CAAACATTC
W22	Mu12	chr5	185079405	GAATGTTTG
W22	Mu12	chr5	191610797	AATGCAAGG
W22	Mu12	chr5	191610805	AATGCAAGG
W22	Mu12	chr5	215629072	AAAAAACGG
W22	Mu12	chr6	63914659	CGTTTTTTTT
W22	Mu12	chr6	92047273	ATGCAGATG
W22	Mu12	chr6	93816795	CAACACGGG
W22	Mu12	chr6	154460191	CTTGTTGGC
W22	Mu12	chr6	158392377	TCTGGAGGC
W22	Mu12	chr7	17586505	TCTAGGTTC
W22	Mu12	chr7	17586511	TCTAGGTTC
W22	Mu12	chr7	29692026	AGTTACGCC
W22	Mu12	chr7	144119871	GTGGGAGCC
W22	Mu12	chr7	159353900	AAAAAATGG
W22	Mu12	chr7	161229569	ATCTGTCAG
W22	Mu12	chr7	169729474	CCATTTCCA
W22	Mu12	chr7	169731084	CCATTTCCA
W22	Mu12	chr8	5414433	CTCGCGCGC
W22	Mu12	chr8	8045837	CCGTTTTTTT
W22	Mu12	chr8	11654079	AAAAAATGG
W22	Mu12	chr8	31356004	CAACACGGG
W22	Mu12	chr8	31356012	CAACACGGG
W22	Mu12	chr8	100614801	CATTGTAGG
W22	Mu12	chr8	116461829	GCTTGCCGA
W22	Mu12	chr8	141273174	GTAGATTGG
W22	Mu12	chr8	141274171	CTGATTGGG

W22	Mu12	chr8	142983538	CCCGTCCCC
W22	Mu12	chr8	142983546	CCCGTCCCC
W22	Mu12	chr8	174147997	GCAAGCTTG
W22	Mu12	chr9	14402800	CCCGTGTTG
W22	Mu12	chr9	14402808	CCCGTGTTG
W22	Mu12	chr9	25697019	CTAATTTTG
W22	Mu12	chr9	37587573	CGTAGTGCA
W22	Mu12	chr9	49227827	CCATTTTTT
W22	Mu12	chr9	89417958	CCGTTTTTT
W22	Mu12	chr9	107612912	AAAAAAACG
W22	Mu12	chr9	130763403	GCAAACCAA
TIL-1	Mu1-9	chr1	23792400	TACTGGAGT
TIL-1	Mu1-9	chr1	59123448	CATGGACAT
TIL-1	Mu1-9	chr1	85714506	ATGTCCATG
TIL-1	Mu1-9	chr1	192534615	CCAATTGGT
TIL-1	Mu1-9	chr1	196193415	GATGGGGAT
TIL-1	Mu1-9	chr1	273709444	ATCTCTGAG
TIL-1	Mu1-9	chr1	273709445	GAGGTCGAA
TIL-1	Mu1-9	chr1	293153277	TTGGATCTG
TIL-1	Mu1-9	chr1	293153283	TTGGATCCG
TIL-1	Mu1-9	chr1	293153285	TTGGATCTG
TIL-1	Mu1-9	chr10	8359341	GCTGGGGAC
TIL-1	Mu1-9	chr10	57817953	TTGGCAGTG
TIL-1	Mu1-9	chr2	135007660	GGCTGGCGG
TIL-1	Mu1-9	chr2	135009766	GGCTGGCGG
TIL-1	Mu1-9	chr2	136896747	CATGGACAT
TIL-1	Mu1-9	chr3	6786961	ACTCCAGTA
TIL-1	Mu1-9	chr3	192453114	AAATGGATG
TIL-1	Mu1-9	chr3	192454287	AAATGGATG
TIL-1	Mu1-9	chr4	127799046	ATGCTGAGG
TIL-1	Mu1-9	chr4	127799053	TATGCTGAG
TIL-1	Mu1-9	chr4	159505930	GCCGTGCGA
TIL-1	Mu1-9	chr4	165969407	GCTTCTTCT
TIL-1	Mu1-9	chr4	212799894	GTCCGGGAG
TIL-1	Mu1-9	chr5	12867393	GCGTGCGTG
TIL-1	Mu1-9	chr5	12867401	GCGTGCGTG
TIL-1	Mu1-9	chr5	113986705	CAAGGACGC
TIL-1	Mu1-9	chr5	162172428	CTACTTTTC
TIL-1	Mu1-9	chr5	162172436	CTACTTTTC
TIL-1	Mu1-9	chr5	163349395	TGCGCCTGG
TIL-1	Mu1-9	chr5	163349403	TGCGCCTGG
TIL-1	Mu1-9	chr5	199583164	CTCGACTGC
TIL-1	Mu1-9	chr5	199583172	CTCGACTGC

TIL-1	Mul-9	chr5	215660910	CCTCCTGTA
TIL-1	Mul-9	chr5	215660918	CCTCCTGTA
TIL-1	Mul-9	chr6	61512868	GCTGGGGAC
TIL-1	Mul-9	chr6	61512872	GCTGGGGAC
TIL-1	Mul-9	chr6	88799046	GGCAGGGAG
TIL-1	Mul-9	chr6	89452091	GTCGCCGTT
TIL-1	Mul-9	chr6	89452099	GTCGCCGAC
TIL-1	Mul-9	chr6	112507608	GTTTCAGAAA
TIL-1	Mul-9	chr6	112507616	GTTTCAGAAA
TIL-1	Mul-9	chr7	163974760	CATGGACAT
TIL-1	Mul-9	chr9	86968542	ATCAAATCT
TIL-1	Mul-9	chr9	86968550	ATCAAATCT
TIL-1	Mul-9	chr9	148332340	CGGACAAAG
TIL-1	Mul0	chr2	199398880	GTTGTGTGG
TIL-1	Mul0	chr3	189105626	GTCTAGAGC
TIL-1	Mul0	chr4	158906485	AGAAGAGGG
TIL-1	Mul0	chr4	158906493	AGAAGAGGG
TIL-1	Mul0	chr5	14699797	CTCCCCAGC
TIL-1	Mul0	chr5	14699805	CTCCCCAGC
TIL-1	Mul0	chr5	70381872	GTTTTTCGG
TIL-1	Mul0	chr5	70386843	GTTTTTCGG
TIL-1	Mul0	chr5	203658329	GCCTGGTGC
TIL-1	Mul0	chr5	203658336	GCCTGGTGC
TIL-1	Mul0	chr5	211716624	ATTTTGC GA
TIL-1	Mul0	chr5	211716631	CATTTTGAG
TIL-1	Mul0	chr7	143685343	CCGAAAAAC
TIL-1	Mul2	chr1	23421157	CTCTTCGTA
TIL-1	Mul2	chr1	24834111	AAAAGAGGG
TIL-1	Mul2	chr1	37644610	ACCAAATGG
TIL-1	Mul2	chr1	104000456	CAAAAATGG
TIL-1	Mul2	chr1	115673838	CCGCGCAGA
TIL-1	Mul2	chr1	148517219	TAAAAAACG
TIL-1	Mul2	chr1	216178602	GATTTAATT
TIL-1	Mul2	chr1	255862376	CTGAAAAC T
TIL-1	Mul2	chr1	259661577	CCATTTTTT
TIL-1	Mul2	chr10	881994	CCCCTCTAG
TIL-1	Mul2	chr10	998234	TAGAGGGGG
TIL-1	Mul2	chr10	4001312	CCCTCTCCT
TIL-1	Mul2	chr10	18130504	TAGAGGGGG
TIL-1	Mul2	chr10	62286122	GGAGGAGGA
TIL-1	Mul2	chr10	135327980	GTCAGGGCT
TIL-1	Mul2	chr10	135329010	CAGGGCTCG
TIL-1	Mul2	chr2	5681848	CTCAAAGCC

TIL-1	Mu12	chr2	5681856	CTCAAAACC
TIL-1	Mu12	chr2	9947891	CTTGGACGA
TIL-1	Mu12	chr2	12840264	CCCATTTTT
TIL-1	Mu12	chr2	24581452	CTCGGTTGC
TIL-1	Mu12	chr2	25000049	TTTGAGGTC
TIL-1	Mu12	chr2	25001836	CAAAGGGTC
TIL-1	Mu12	chr2	41169226	AACGGAAGA
TIL-1	Mu12	chr2	56871254	CCATTTTTT
TIL-1	Mu12	chr2	92129907	TCTGCGCGG
TIL-1	Mu12	chr2	152204163	TGTAGTGCA
TIL-1	Mu12	chr2	166047953	CTTGTGCGC
TIL-1	Mu12	chr2	197215139	CGCGGTGGC
TIL-1	Mu12	chr2	229531941	TAGAGGGGG
TIL-1	Mu12	chr2	229540123	AGAGGGGGG
TIL-1	Mu12	chr3	3839648	GCTTGCCGA
TIL-1	Mu12	chr3	3839656	GCTTGCCGA
TIL-1	Mu12	chr3	44634269	GGTTTTGCA
TIL-1	Mu12	chr3	44634277	GGTTTTGCA
TIL-1	Mu12	chr3	198011936	GGTGGACTG
TIL-1	Mu12	chr3	217655664	CCGTTTTTT
TIL-1	Mu12	chr3	227274385	AAAAAATGG
TIL-1	Mu12	chr4	19135427	TAGAGGGGG
TIL-1	Mu12	chr4	96634756	GGGCTCAAT
TIL-1	Mu12	chr4	117710460	AGCGGTGTG
TIL-1	Mu12	chr4	166495091	GTACATATG
TIL-1	Mu12	chr4	166547003	CATATGTAC
TIL-1	Mu12	chr4	182724999	GTTTTTCAGA
TIL-1	Mu12	chr4	182813239	AGTTTCAGA
TIL-1	Mu12	chr4	182833406	AGTTTCAGA
TIL-1	Mu12	chr4	191316757	TGCACTACG
TIL-1	Mu12	chr4	239406228	GTGAGTGAG
TIL-1	Mu12	chr5	4143111	GTAGTTTTT
TIL-1	Mu12	chr5	23237962	GCCGTGCTC
TIL-1	Mu12	chr5	26466383	AGCCTAGGA
TIL-1	Mu12	chr5	26838263	CGCGGGCGG
TIL-1	Mu12	chr5	42851585	AATATAATG
TIL-1	Mu12	chr5	75952464	AGTTTCAGA
TIL-1	Mu12	chr5	185027058	CAAACATTC
TIL-1	Mu12	chr5	185079405	GAATGTTTG
TIL-1	Mu12	chr5	200452877	TAGAGGGGG
TIL-1	Mu12	chr5	203658329	GCCTGGTGC
TIL-1	Mu12	chr5	203658336	GCCTGGTGC
TIL-1	Mu12	chr5	215629072	AAAAAACGG

TIL-1	Mul2	chr6	2365424	GCAGGTCAA
TIL-1	Mul2	chr6	2365432	GCAGGTCAA
TIL-1	Mul2	chr6	2917476	TCCATGATG
TIL-1	Mul2	chr6	92047273	ATGCAGATG
TIL-1	Mul2	chr6	118306026	GGAGGAGGA
TIL-1	Mul2	chr6	121061543	CTGCGATAT
TIL-1	Mul2	chr6	122067770	TGTTTGGTG
TIL-1	Mul2	chr6	154460191	CTTGTTGGC
TIL-1	Mul2	chr6	161409603	GTGCCGGAG
TIL-1	Mul2	chr6	166433210	CTTGCCATC
TIL-1	Mul2	chr7	27870762	TCGTGAGGA
TIL-1	Mul2	chr7	126146334	CCGTTTTTTT
TIL-1	Mul2	chr7	144119874	GTGGGGGCC
TIL-1	Mul2	chr7	154071387	CGGAGCAGT
TIL-1	Mul2	chr7	161229569	ATCTGTCAG
TIL-1	Mul2	chr8	100614801	CATTGTAGG
TIL-1	Mul2	chr8	141273174	GTAGATTGG
TIL-1	Mul2	chr8	141551809	GTGGGAGAG
TIL-1	Mul2	chr8	141551817	GTGGGAGAG
TIL-1	Mul2	chr8	150001149	GTGAATATG
TIL-1	Mul2	chr8	158670019	AAAAGAGAC
TIL-1	Mul2	chr8	171749899	CCACTCAGA
TIL-1	Mul2	chr9	15351165	AAAAAACGG
TIL-1	Mul2	chr9	37587573	CGTAGTGCA
TIL-1	Mul2	chrUNKNOWN	2134830	CCCCCTCTA
TIL-1	Mul2	chrUNKNOWN	12783520	CAGTGGCCG
TIL-11	Mul-9	chr1	23792400	TACTGGAGT
TIL-11	Mul-9	chr1	33903858	CGTCGCCGC
TIL-11	Mul-9	chr1	33903861	GTCGCCGCC
TIL-11	Mul-9	chr1	143267304	TCAAAGGGG
TIL-11	Mul-9	chr1	150251733	ACTAAGAGC
TIL-11	Mul-9	chr1	150251737	AATGAGAGC
TIL-11	Mul-9	chr1	182238999	CCCCGTGTC
TIL-11	Mul-9	chr1	182239008	CCCCTGTCT
TIL-11	Mul-9	chr1	223805434	GTCTCATCT
TIL-11	Mul-9	chr1	240645665	CCGCCCCAC
TIL-11	Mul-9	chr1	264263006	TTAGGTCGG
TIL-11	Mul-9	chr1	264267812	TTAGGTCGG
TIL-11	Mul-9	chr10	14553777	ATTCCCATC
TIL-11	Mul-9	chr10	14553785	ATTCCCATC
TIL-11	Mul-9	chr10	57825502	TTGGCAGTG
TIL-11	Mul-9	chr2	25300688	GAGGCTCTC
TIL-11	Mul-9	chr2	25302603	GAGGCTCTC

TIL-11	Mul-9	chr2	27958817	GTTGGCTTC
TIL-11	Mul-9	chr2	68252427	GATCTGGAT
TIL-11	Mul-9	chr2	68252435	GATCTGGAT
TIL-11	Mul-9	chr2	126544550	AGCTGCGGC
TIL-11	Mul-9	chr2	133879755	CTCGAGCCG
TIL-11	Mul-9	chr2	184094928	AGGGGAGGG
TIL-11	Mul-9	chr2	184527141	GAGGAGGAG
TIL-11	Mul-9	chr2	214951873	TTAGGTTCGG
TIL-11	Mul-9	chr2	214951881	TTAGGTTCGG
TIL-11	Mul-9	chr2	216885329	GGAAGAGAC
TIL-11	Mul-9	chr3	56931541	GTTTGCCAT
TIL-11	Mul-9	chr3	203236481	TGGTGTGG
TIL-11	Mul-9	chr3	205237044	CGAAGCGGT
TIL-11	Mul-9	chr3	215879987	GGGAGCGGG
TIL-11	Mul-9	chr4	241230661	GGAAAACGA
TIL-11	Mul-9	chr4	241230669	GGAAAACGA
TIL-11	Mul-9	chr5	21457756	GTCCAAGAG
TIL-11	Mul-9	chr5	21457757	GTCCAAGAG
TIL-11	Mul-9	chr5	23137992	GTTTTTTCT
TIL-11	Mul-9	chr5	23138000	GTTTTTTCT
TIL-11	Mul-9	chr5	54748264	GCACTGAAC
TIL-11	Mul-9	chr5	54748272	GCACTGCAC
TIL-11	Mul-9	chr5	67359338	GCAGGGAAC
TIL-11	Mul-9	chr5	86107085	GTCGACAGC
TIL-11	Mul-9	chr5	86107093	GTCGACAGC
TIL-11	Mul-9	chr5	91554460	TCCGGTATT
TIL-11	Mul-9	chr5	91554464	TCCGGTATT
TIL-11	Mul-9	chr5	152008704	CTCAGACGT
TIL-11	Mul-9	chr5	152008713	TCAGACGTT
TIL-11	Mul-9	chr5	175353380	TTGACGGTG
TIL-11	Mul-9	chr5	211716624	ATTTTGCGA
TIL-11	Mul-9	chr5	211716631	CATTTTGAG
TIL-11	Mul-9	chr6	2365368	CAGCCTCCC
TIL-11	Mul-9	chr6	88799046	GGCAGGGAG
TIL-11	Mul-9	chr7	5548985	TCCGGTATT
TIL-11	Mul-9	chr7	48473780	GCGGGAGAG
TIL-11	Mul-9	chr7	48474915	GCGGGAGAG
TIL-11	Mul-9	chr7	101032123	TCCAAGGGG
TIL-11	Mul-9	chr7	101032131	TCCAAGGGG
TIL-11	Mul-9	chr7	147135016	CACGCTGTA
TIL-11	Mul-9	chr8	124888956	ACGGCAAAC
TIL-11	Mul-9	chr8	124962257	ATGGCAAAC
TIL-11	Mul-9	chr8	140344459	CTCCTCCTC

TIL-11	Mul-9	chr8	140606536	TTCTTG TTC
TIL-11	Mul-9	chr8	140606544	TTCTTG TTC
TIL-11	Mul-9	chr8	153725735	GTTAGTTGT
TIL-11	Mul-9	chr8	153727357	GTTAGTTGT
TIL-11	Mul-9	chr8	155441208	GCGGCGAGG
TIL-11	Mul-9	chr8	155441216	GCGGCGAGG
TIL-11	Mul-9	chr8	158889648	TCTGAAGGC
TIL-11	Mul-9	chr9	86968542	ATCAAATCT
TIL-11	Mul0	chr1	199599908	TGTGGAAAC
TIL-11	Mul0	chr3	208243138	CCGCTTCC
TIL-11	Mul0	chr7	32479319	GCCCTACAG
TIL-11	Mul2	chr1	4330648	GAGAGCAGA
TIL-11	Mul2	chr1	4330676	GAGAGCAGA
TIL-11	Mul2	chr1	55607850	TGTGGTAAG
TIL-11	Mul2	chr1	55607855	TGTGGTAAG
TIL-11	Mul2	chr1	164914752	TGCTCTACT
TIL-11	Mul2	chr1	228947668	CACGGAAGT
TIL-11	Mul2	chr1	228947671	CACGGAAGT
TIL-11	Mul2	chr1	241036345	TTCATCAA
TIL-11	Mul2	chr1	268593297	CCGCTGGG
TIL-11	Mul2	chr1	268593361	CCGCTGGG
TIL-11	Mul2	chr1	289072008	ATGGACAGG
TIL-11	Mul2	chr1	289072011	ATGGACAGG
TIL-11	Mul2	chr10	4001312	CCCTCTCCT
TIL-11	Mul2	chr10	119180615	CTCCCTCGT
TIL-11	Mul2	chr10	125204541	CCTCCCAGG
TIL-11	Mul2	chr10	127015035	GTGGGCTTG
TIL-11	Mul2	chr10	127015043	GTGGGCTTG
TIL-11	Mul2	chr2	24982189	GACCTCAA
TIL-11	Mul2	chr2	25000049	TTTGAGGTC
TIL-11	Mul2	chr2	25001836	CAAAGGTC
TIL-11	Mul2	chr2	37681711	CCTCCCAGG
TIL-11	Mul2	chr2	174429588	TCCTCCACA
TIL-11	Mul2	chr2	177932386	GTCTACGAC
TIL-11	Mul2	chr2	219231285	ATTCGTGAA
TIL-11	Mul2	chr2	221889400	CTCGCTCC
TIL-11	Mul2	chr2	221889408	CTCGCTCC
TIL-11	Mul2	chr3	121611818	GGCGTAACT
TIL-11	Mul2	chr3	174677907	GTGGGTATG
TIL-11	Mul2	chr3	174677915	GTGGGTATG
TIL-11	Mul2	chr4	87970072	CCGCTGGG
TIL-11	Mul2	chr4	117224174	GTCTGCGGT
TIL-11	Mul2	chr4	141370454	ATCTCACGG

TIL-11	Mu12	chr4	166495091	GTACATATG
TIL-11	Mu12	chr4	166547003	CATATGTAC
TIL-11	Mu12	chr4	182724995	GTTTTTAGA
TIL-11	Mu12	chr4	239406228	GTGAGTGAG
TIL-11	Mu12	chr4	240230508	GCGATGCGG
TIL-11	Mu12	chr4	244752104	GATGAGGAG
TIL-11	Mu12	chr4	244759229	CTCCTCATC
TIL-11	Mu12	chr5	23237960	GCCGTGCCC
TIL-11	Mu12	chr5	26466383	AGCCTAGGA
TIL-11	Mu12	chr5	26839718	CGCGGGCGG
TIL-11	Mu12	chr5	180873325	GTTGCGTGC
TIL-11	Mu12	chr5	185027058	CAAACATTC
TIL-11	Mu12	chr5	185079405	GAATGTTTG
TIL-11	Mu12	chr5	191610797	AATGCAAGG
TIL-11	Mu12	chr6	81338048	CCCTGCGAG
TIL-11	Mu12	chr6	157068229	CCTCAAGAA
TIL-11	Mu12	chr6	163973601	CTCGGTTCGG
TIL-11	Mu12	chr6	163973609	CTCGGTTCGG
TIL-11	Mu12	chr6	166433210	CTTGCCATC
TIL-11	Mu12	chr7	17586505	TCTAGGTTC
TIL-11	Mu12	chr7	17586511	TCTAGGTTC
TIL-11	Mu12	chr7	80745292	CCGCCGTCT
TIL-11	Mu12	chr7	113563243	CCCAGGCGG
TIL-11	Mu12	chr8	42932444	GACCTCAAA
TIL-11	Mu12	chr8	148886228	CCTGTTTGA
TIL-11	Mu12	chr8	148887210	CCTGTTTGA
TIL-11	Mu12	chr9	4231266	GCACGCAAC
TIL-11	Mu12	chr9	79219366	CCCAGGCGG
TIL-11	Mu12	chr9	79219429	CCCAGGCGG
TIL-14	Mu1-9	chr1	31547006	AGTTCCAAC
TIL-14	Mu1-9	chr1	36633493	GGTGGGTGT
TIL-14	Mu1-9	chr1	69912636	AAGCATATA
TIL-14	Mu1-9	chr1	69912643	CAAGCATAT
TIL-14	Mu1-9	chr1	127706260	GCGTCTCCT
TIL-14	Mu1-9	chr1	127706268	GCGTCTCCT
TIL-14	Mu1-9	chr1	264263006	TTAGGTTCGG
TIL-14	Mu1-9	chr1	264267812	TTAGGTTCGG
TIL-14	Mu1-9	chr1	284730450	GTGTAGCGT
TIL-14	Mu1-9	chr1	284730458	GTGTAGCGC
TIL-14	Mu1-9	chr10	4807989	CCGGCCCAC
TIL-14	Mu1-9	chr10	57817953	TTGGCAGTG
TIL-14	Mu1-9	chr10	57817961	TTGGCAGTG
TIL-14	Mu1-9	chr10	57825502	TTGGCAGTG

TIL-14	Mul-9	chr10	73896107	GTGGGCCCGG
TIL-14	Mul-9	chr10	76529660	GTGGGCCCGG
TIL-14	Mul-9	chr10	84011171	GTGGGCCCGG
TIL-14	Mul-9	chr10	84011179	GTGGGCCCGG
TIL-14	Mul-9	chr10	95549954	CCGGCCCAC
TIL-14	Mul-9	chr10	135931825	CCGGCCCAC
TIL-14	Mul-9	chr10	135940445	CCGGCCCAC
TIL-14	Mul-9	chr10	140658702	CTTTGCTTA
TIL-14	Mul-9	chr2	11182138	GTTTGAGTT
TIL-14	Mul-9	chr2	12001220	TAAGCAAAG
TIL-14	Mul-9	chr2	12001228	TAAGCAAAG
TIL-14	Mul-9	chr2	43144616	CCGGCCCAC
TIL-14	Mul-9	chr2	43153193	GGACCCACG
TIL-14	Mul-9	chr2	135007660	GGCTGGCGG
TIL-14	Mul-9	chr2	135009766	GGCTGGCGG
TIL-14	Mul-9	chr2	165894948	GTGGGCCCGG
TIL-14	Mul-9	chr2	204497124	CCGGCCCAC
TIL-14	Mul-9	chr2	214951873	TTAGGTCGG
TIL-14	Mul-9	chr2	214951881	TTAGGTCGG
TIL-14	Mul-9	chr3	164865943	CTCCTCGGT
TIL-14	Mul-9	chr3	164865951	CTCCTCGGT
TIL-14	Mul-9	chr3	186088298	GTTTGAGTT
TIL-14	Mul-9	chr3	192453114	AAATGGATG
TIL-14	Mul-9	chr3	192454287	AAATGGATG
TIL-14	Mul-9	chr3	230139824	CCCATGCAG
TIL-14	Mul-9	chr3	230143403	CCCCTGCAG
TIL-14	Mul-9	chr4	6946626	AACTCAAAC
TIL-14	Mul-9	chr4	7039704	GTAGGACTG
TIL-14	Mul-9	chr4	7039712	GTAGGACTG
TIL-14	Mul-9	chr4	23486359	GTTTATGCC
TIL-14	Mul-9	chr4	58929004	CGTGGGGGT
TIL-14	Mul-9	chr4	133125649	TGGGCCGGA
TIL-14	Mul-9	chr4	159505930	GCCGTGCGA
TIL-14	Mul-9	chr4	159506805	GCCGTGCGA
TIL-14	Mul-9	chr4	165969407	GCTTCTTCT
TIL-14	Mul-9	chr4	174367455	ATCTATAGG
TIL-14	Mul-9	chr4	241230661	GGAAAACGA
TIL-14	Mul-9	chr4	241230669	GGAAAACGA
TIL-14	Mul-9	chr5	42342232	CCGGCCCAC
TIL-14	Mul-9	chr5	116267117	ATCACCCAA
TIL-14	Mul-9	chr5	116268617	TCACCCGAG
TIL-14	Mul-9	chr5	175353380	TTGACGGTG
TIL-14	Mul-9	chr5	190082484	GTTTGAGTT

TIL-14	Mul-9	chr6	28306795	GCTGCAGGA
TIL-14	Mul-9	chr6	104062636	CTGCAGAGA
TIL-14	Mul-9	chr6	112507608	GTTTCAGAAA
TIL-14	Mul-9	chr6	112507616	GTTTCAGAAA
TIL-14	Mul-9	chr6	159357866	CCGGCCCAC
TIL-14	Mul-9	chr7	139884887	TCCGCCTAT
TIL-14	Mul-9	chr8	4819545	CCGGCCCAC
TIL-14	Mul-9	chr8	4819553	CCGGCCCAC
TIL-14	Mul-9	chr8	71393327	CCGGCCCAC
TIL-14	Mul-9	chr8	137160125	CCC GGCCCA
TIL-14	Mul-9	chr9	78186956	GCGGCCGTG
TIL-14	Mul-9	chr9	78186964	GCGGCCGTG
TIL-14	Mul-9	chr9	86968542	ATCAAATCT
TIL-14	Mul-9	chr9	86968550	ATCAAATCT
TIL-14	Mul-9	chr9	115971623	GTGGGCCGG
TIL-14	Mul-9	chr9	143065860	ACTATAATT
TIL-14	Mul-9	chrUNKNOWN	5341590	ATCAAATCA
TIL-14	Mul-9	chrUNKNOWN	10236078	GTGGGCCGG
TIL-14	Mul0	chr1	282667382	CTCGAAATG
TIL-14	Mul0	chr1	282712869	CATTTTCGAG
TIL-14	Mul0	chr10	24764948	CTTTTTTCT
TIL-14	Mul0	chr10	24764954	CTTTTTTCT
TIL14	Mul0	chr10	149024046	AGGGCACTC
TIL-14	Mul0	chr2	76218121	TCGAGAGGG
TIL-14	Mul0	chr2	76222892	TCGAGATGG
TIL-14	Mul0	chr2	79137485	GGTGGCAAC
TIL-14	Mul0	chr2	79137493	GGTGGCAAC
TIL-14	Mul0	chr2	199398880	GTTGTGTGG
TIL-14	Mul0	chr2	199398888	TTGTGTGGG
TIL-14	Mul0	chr3	42433628	CCCTCTACA
TIL-14	Mul0	chr3	185338367	GAAGTGAAG
TIL-14	Mul0	chr3	185338375	GAAGTGAAG
TIL-14	Mul0	chr3	207584229	AGTGTGCGC
TIL14	Mul0	chr3	207584238	GTGTGCGCG
TIL-14	Mul0	chr4	125145002	CCACTGGCC
TIL-14	Mul0	chr4	125145010	CCACTGGCC
TIL-14	Mul0	chr4	134472412	ATCTGAAGG
TIL-14	Mul0	chr4	134472418	ATCTGAAAG
TIL-14	Mul0	chr6	82267957	GCACAGGGG
TIL14	Mul0	chr6	161830878	GCTCGGTCC
TIL-14	Mul0	chr9	86968542	ATCAAATCT
TIL-14	Mul0	chr9	86968550	ATCAAATCT
TIL-14	Mul0	chr9	133089846	CCTCCCACG

TIL-14	Mul0	chr9	133089853	CCCTCCCAC
TIL-14	Mul2	chr1	145539	ACGTGTGGT
TIL-14	Mul2	chr1	145547	ACGTGTGGT
TIL-14	Mul2	chr1	10975143	CTCTCCTCG
TIL-14	Mul2	chr1	37631584	ACCGAATGG
TIL-14	Mul2	chr1	37644606	ACCGAATGG
TIL-14	Mul2	chr1	104000456	CAAAAATGG
TIL-14	Mul2	chr1	148517219	TAAAAAACG
TIL-14	Mul2	chr1	148517222	TTAAAAAAC
TIL-14	Mul2	chr1	156777148	GTTCAACGG
TIL-14	Mul2	chr1	209635428	AACACAGCC
TIL-14	Mul2	chr1	259661581	CCATTTTTG
TIL-14	Mul2	chr1	293105542	GAAGCAACG
TIL-14	Mul2	chr1	293105549	GAAGCAACG
TIL-14	Mul2	chr1	299438326	CTGCTCTCC
TIL-14	Mul2	chr10	134192589	TCTTCAGCC
TIL-14	Mul2	chr2	9947891	CTTGACGA
TIL-14	Mul2	chr2	25000049	TTTGAGGTC
TIL-14	Mul2	chr2	25001836	CAAAGGGTC
TIL-14	Mul2	chr2	41169226	AACGGAAGA
TIL-14	Mul2	chr2	56871254	CCATTTTTG
TIL-14	Mul2	chr2	166047945	CTTGTGCGC
TIL-14	Mul2	chr2	166047953	CTTGTGCGC
TIL-14	Mul2	chr2	172959624	CTCGGGTCG
TIL-14	Mul2	chr2	172959632	CTCGGGTCG
TIL-14	Mul2	chr2	197519923	CCTTTCATG
TIL-14	Mul2	chr3	3069893	CGAGACAGC
TIL-14	Mul2	chr3	137939804	CACTATGCC
TIL-14	Mul2	chr3	174677915	GTGGGTATG
TIL-14	Mul2	chr3	196793062	CCTTCTCCA
TIL-14	Mul2	chr3	223787656	CCTGTAGGA
TIL-14	Mul2	chr3	230017369	TTCTTCTG
TIL-14	Mul2	chr4	31533656	GATGAGGAG
TIL-14	Mul2	chr4	141370454	ATCTCACGG
TIL-14	Mul2	chr4	166495091	GTACATATG
TIL-14	Mul2	chr4	166547003	CATATGTAC
TIL-14	Mul2	chr4	191316757	TGCACTACG
TIL-14	Mul2	chr4	206328918	CTGTTTTTT
TIL-14	Mul2	chr4	239406228	GTGAGTGAG
TIL-14	Mul2	chr4	244752093	GATGAGGAG
TIL-14	Mul2	chr4	244759229	GATGAGGAG
TIL-14	Mul2	chr5	2804395	CCCTCCACG
TIL-14	Mul2	chr5	3132014	TTCTTTCCG

TIL-14	Mu12	chr5	23270351	TGCTCTGTT
TIL-14	Mu12	chr5	26466383	AGCCTAGGA
TIL-14	Mu12	chr5	26839718	CGCGGGCGG
TIL-14	Mu12	chr5	185027058	CAAACATTC
TIL-14	Mu12	chr5	185079405	GAATGTTTG
TIL-14	Mu12	chr5	191610797	AATGCAAGG
TIL-14	Mu12	chr6	28306795	GCTGTAGGA
TIL-14	Mu12	chr6	121061543	CTGCGATAT
TIL-14	Mu12	chr6	161409603	GTGCCGGAG
TIL-14	Mu12	chr7	168040500	CGTTCCGGG
TIL-14	Mu12	chr8	5414433	CTCGCGCGC
TIL-14	Mu12	chr8	8732207	ACGTGACTG
TIL-14	Mu12	chr8	17473048	AAAAAACAG
TIL-14	Mu12	chr8	56659742	TCTTGCATT
TIL-14	Mu12	chr8	72198358	CAAAAATGG
TIL-14	Mu12	chr8	122200807	AAAAAAACA
TIL-14	Mu12	chr8	139821649	TCCTCTGGC
TIL-14	Mu12	chr8	148886228	CCTGTTTGA
TIL-14	Mu12	chr8	148887210	CCTGTTTGA
TIL-14	Mu12	chr8	153727784	AAAATTTGG
TIL-14	Mu12	chr9	4231266	GCACGCAAC
TIL-14	Mu12	chr9	19060011	GTTATGAGG
TIL-14	Mu12	chr9	24526877	TGTTGCTTG
TIL-14	Mu12	chr9	37587573	CGTAGTGCA
TIL-14	Mu12	chr9	68117808	GGTGGTTGA
TIL-14	Mu12	chr9	143065853	TCTATAAATT
TIL-14	Mu12	chr9	146958032	GGTGTGCTG
TIL-14	Mu12	chr9	147020771	GCTGCAGGA
TIL-14	Mu12	chrUNKNOWN	12783520	CAGTGGCCG
TIL-15	Mu1-9	chr1	31627099	CTTTATACG
TIL-15	Mu1-9	chr1	264168398	AAAGGCTGA
TIL-15	Mu1-9	chr1	264168406	AAAGGCTGA
TIL-15	Mu1-9	chr1	264263006	TTAGGTCCG
TIL-15	Mu1-9	chr1	264267812	TTAGGTCCG
TIL-15	Mu1-9	chr10	2695677	TCCTTTGGC
TIL-15	Mu1-9	chr10	10267286	GAAAGAGAG
TIL-15	Mu1-9	chr10	57817961	TTGGCAGTG
TIL-15	Mu1-9	chr10	119571336	CACCGAAGA
TIL-15	Mu1-9	chr10	135523518	GCTTGCGGA
TIL-15	Mu1-9	chr2	158557737	CTCTCTTTC
TIL-15	Mu1-9	chr2	158559629	CTCTCTTTC
TIL-15	Mu1-9	chr2	214951873	TTAGGTCCG
TIL-15	Mu1-9	chr3	5218885	ACTGGACAG

TIL-15	Mul-9	chr3	54490053	CGTAGCGGG
TIL-15	Mul-9	chr3	192454287	AAATGGATG
TIL-15	Mul-9	chr3	222184435	CCTGCTCAC
TIL-15	Mul-9	chr3	222240693	CCTGCTCAC
TIL-15	Mul-9	chr5	67359338	GCAGGGAAC
TIL-15	Mul-9	chr5	86107093	GTCGACAGC
TIL-15	Mul-9	chr5	95712447	CACCGAAGA
TIL-15	Mul-9	chr5	124606626	ACAGCCATT
TIL-15	Mul-9	chr5	124607034	ACAGCCATT
TIL-15	Mul-9	chr5	168593504	GTGTCCGGC
TIL-15	Mul-9	chr5	174857474	TCTTCGGTG
TIL-15	Mul-9	chr6	28306795	GCTGCAGGA
TIL-15	Mul-9	chr6	47652355	CCACAAATA
TIL-15	Mul-9	chr6	74467317	CCCTGCCAA
TIL-15	Mul-9	chr6	83826441	GCCTCTGTG
TIL-15	Mul-9	chr7	103873034	CTTCAGTAG
TIL-15	Mul-9	chr7	129500559	ATGGCCGAG
TIL-15	Mul-9	chr8	140606536	TTCTTGTTT
TIL-15	Mul-9	chr8	169630728	GTCTCCCAC
TIL-15	Mul-9	chr9	27580335	CGCTCTGTT
TIL-15	Mul-9	chr9	27580343	CACTCTGTT
TIL-15	Mul-9	chr9	28952231	GAAAGAGAG
TIL-15	Mul-9	chr9	34725229	GACGGGAAG
TIL-15	Mul-9	chr9	86968542	ATCAAATCT
TIL-15	Mul-9	chr9	86968550	ATCAAATCT
TIL-15	Mul-9	chrUNKNOWN	13826404	TGCAGTACA
TIL-15	Mul-9	chrUNKNOWN	13829283	TGCAGTACA
TIL-15	Mul0	chr1	24057144	ACCAGACAC
TIL-15	Mul0	chr1	24057152	ACCAGACAC
TIL-15	Mul0	chr1	103305287	GCGGGGCGG
TIL-15	Mul0	chr2	21965511	GTTCGCTTT
TIL-15	Mul0	chr4	133716937	TCCCCTGCG
TIL-15	Mul0	chr4	170882661	TCCGCCCGC
TIL-15	Mul0	chr4	170887658	GCGAGCGGA
TIL-15	Mul0	chr5	11407307	CTGGTGCAG
TIL-15	Mul0	chr5	78496112	CGCGGGATG
TIL-15	Mul0	chr5	132407180	CGCGGGATG
TIL-15	Mul0	chr6	109367787	GTCTCAGCC
TIL-15	Mul0	chr7	129500567	ATGGCCGAG
TIL-15	Mul0	chr8	123909907	CTTTTTTCA
TIL-15	Mul0	chr9	11643467	TGGGCTGGG
TIL-15	Mul0	chr9	11653693	GGGCTGGGA
TIL-15	Mul2	chr1	19513553	CGAGAGCAG

TIL-15	Mu12	chr1	24057144	ACCAGACAC
TIL-15	Mu12	chr1	24057152	ACCAGACAC
TIL-15	Mu12	chr1	37644606	ACCGAATGA
TIL-15	Mu12	chr1	48108886	TCGCATTGT
TIL-15	Mu12	chr1	55607850	TGTGGTAAG
TIL-15	Mu12	chr1	86595530	GTTTCGTTGG
TIL-15	Mu12	chr1	111562669	TCTGTTTTTC
TIL-15	Mu12	chr1	115673838	CCGCGCAGA
TIL-15	Mu12	chr1	150964626	TCGGGGAAC
TIL-15	Mu12	chr1	150964678	TCGGGGAAC
TIL-15	Mu12	chr1	201020716	ATATCGAGG
TIL-15	Mu12	chr1	201421470	ATGATTAGC
TIL-15	Mu12	chr1	216177818	TTCATTACT
TIL-15	Mu12	chr1	239257924	CAAAAAAAC
TIL-15	Mu12	chr1	259661577	CCATTTTTTT
TIL-15	Mu12	chr1	268593292	CCGCTGGG
TIL-15	Mu12	chr10	4001312	CCCTCTCCT
TIL-15	Mu12	chr10	9345105	GTTTCGTTGG
TIL-15	Mu12	chr10	15300760	CTTGCAATG
TIL-15	Mu12	chr10	15308429	CTTGCAATG
TIL-15	Mu12	chr10	30284887	CATCATATC
TIL-15	Mu12	chr10	35483010	ACGGCAGCC
TIL-15	Mu12	chr10	40781053	AATATGATG
TIL-15	Mu12	chr10	64912929	CCAACGAAC
TIL-15	Mu12	chr10	70933873	GTTTCAAAC
TIL-15	Mu12	chr10	70933881	GTTTCAAAC
TIL-15	Mu12	chr10	79444984	CCAACGGAC
TIL-15	Mu12	chr10	99668137	GTTTCGTTGG
TIL-15	Mu12	chr10	101696709	AAAAAACGG
TIL-15	Mu12	chr10	102160009	GCCTCAGCC
TIL-15	Mu12	chr10	102160017	ACCTCAGCC
TIL-15	Mu12	chr10	102798787	CCAACGAAC
TIL-15	Mu12	chr10	103073179	AAAAAAGG
TIL-15	Mu12	chr10	119180615	CTCCCTCGT
TIL-15	Mu12	chr10	140369582	CCAACGAAC
TIL-15	Mu12	chr10	144276123	TACTTCATC
TIL-15	Mu12	chr10	144276125	GGTGATATG
TIL-15	Mu12	chr10	146725851	TCTCGAGAC
TIL-15	Mu12	chr10	146725852	CTCTCGAGA
TIL-15	Mu12	chr2	9947888	CTCCCTGGA
TIL-15	Mu12	chr2	14415088	CGTTTCGTT
TIL-15	Mu12	chr2	19241199	CCCAAGTAT
TIL-15	Mu12	chr2	19241206	CCCAAGTA

TIL-15	Mu12	chr2	24581452	CTCGGTTGC
TIL-15	Mu12	chr2	24982189	GACCTCAAA
TIL-15	Mu12	chr2	25000049	TTTGAGGTC
TIL-15	Mu12	chr2	32307444	CAATGCGAA
TIL-15	Mu12	chr2	37869180	GGGCACGAG
TIL-15	Mu12	chr2	39450649	GGCGACGAT
TIL-15	Mu12	chr2	39450657	GACGACGAT
TIL-15	Mu12	chr2	44473557	CTCGCCCTC
TIL-15	Mu12	chr2	92129907	TCTGCGCGG
TIL-15	Mu12	chr2	138425824	ATCTGTGTG
TIL-15	Mu12	chr2	152204164	CCGTAGTGC
TIL-15	Mu12	chr2	164986733	GCCTGTTCGT
TIL-15	Mu12	chr2	176017855	GCGGTATGA
TIL-15	Mu12	chr2	188598484	AAATTATTG
TIL-15	Mu12	chr2	197519923	CCTTTCATG
TIL-15	Mu12	chr2	197525159	CCTTTCATG
TIL-15	Mu12	chr2	207958804	GTACAGAAC
TIL-15	Mu12	chr2	207958827	GTACAGAAC
TIL-15	Mu12	chr2	212502671	GGCCCACGC
TIL-15	Mu12	chr2	212502677	GGCCCACGC
TIL-15	Mu12	chr2	230681917	ATCTTCCAA
TIL-15	Mu12	chr2	230681925	ATCTTCCAA
TIL-15	Mu12	chr3	13961881	CAACGAACG
TIL-15	Mu12	chr3	15862117	GGCTACAGC
TIL-15	Mu12	chr3	54490053	GTAGCGGGG
TIL-15	Mu12	chr3	89795711	CTTCAGAGA
TIL-15	Mu12	chr3	107202921	CCAGTTCTT
TIL-15	Mu12	chr3	122798122	CACCGGGTG
TIL-15	Mu12	chr3	122798130	CACCGGGTG
TIL-15	Mu12	chr3	123120622	GCTCTTGCC
TIL-15	Mu12	chr3	123120628	TGCTCTTGC
TIL-15	Mu12	chr3	131246208	TCTCCACAC
TIL-15	Mu12	chr3	131246216	TCTCCACAC
TIL-15	Mu12	chr3	137939804	CACTATGCC
TIL-15	Mu12	chr3	156342516	GTCCCCAGC
TIL-15	Mu12	chr3	156383673	GTCCCCAGC
TIL-15	Mu12	chr3	174677907	GTGGGTATG
TIL-15	Mu12	chr3	174677915	GTGGGTATG
TIL-15	Mu12	chr3	216962792	CCAACGAAC
TIL-15	Mu12	chr3	217655664	CCGTTTTTTT
TIL-15	Mu12	chr4	30057147	ACCTGACGG
TIL-15	Mu12	chr4	30057160	ACGTGACGG
TIL-15	Mu12	chr4	36278332	ACTTCGCCT

TIL-15	Mu12	chr4	43099274	CAACTTCAG
TIL-15	Mu12	chr4	65877958	TAAATTATT
TIL-15	Mu12	chr4	67680114	GTTTAGACT
TIL-15	Mu12	chr4	67680404	GTTTAGACT
TIL-15	Mu12	chr4	71147569	CCCCACACC
TIL-15	Mu12	chr4	96634756	GGGCTCAAT
TIL-15	Mu12	chr4	161135534	CCTCGTCGG
TIL-15	Mu12	chr4	166495091	GTACATATG
TIL-15	Mu12	chr4	168526010	TGGTAATGC
TIL-15	Mu12	chr4	172693620	TCTACGTAG
TIL-15	Mu12	chr4	182724999	GTTTTTCAGA
TIL-15	Mu12	chr4	191316757	TGCACTACG
TIL-15	Mu12	chr4	200868608	ACGACAGCT
TIL-15	Mu12	chr4	239406228	GTGAGTGAG
TIL-15	Mu12	chr5	26466385	AACCTAGGA
TIL-15	Mu12	chr5	26838263	CGCGGGCGG
TIL-15	Mu12	chr5	26839718	CGCGGGCGG
TIL-15	Mu12	chr5	42851585	AATATGATG
TIL-15	Mu12	chr5	64749197	GTCGCACTG
TIL-15	Mu12	chr5	100266817	CCAACGAAC
TIL-15	Mu12	chr5	142950413	AATAATTTA
TIL-15	Mu12	chr5	159638069	CGTTTCGTTG
TIL-15	Mu12	chr5	185027058	CAAACATTC
TIL-15	Mu12	chr5	185079405	GAATGTTTG
TIL-15	Mu12	chr5	191610797	AATGCAAGG
TIL-15	Mu12	chr5	203749479	TTCGTCGGC
TIL-15	Mu12	chr5	203763309	TTCGTCGGC
TIL-15	Mu12	chr5	214442515	TTGTGGAGA
TIL-15	Mu12	chr5	214578191	TCCGCCGGC
TIL-15	Mu12	chr5	215629072	AAAAAACGG
TIL-15	Mu12	chr6	3564348	AATAATTTA
TIL-15	Mu12	chr6	22394708	CCGTTTTTTT
TIL-15	Mu12	chr6	22394712	CGTTTTTTTA
TIL-15	Mu12	chr6	28306795	GCTGCAGGA
TIL-15	Mu12	chr6	55872876	TCCCCGCC
TIL-15	Mu12	chr6	59179011	GCTACGGGG
TIL-15	Mu12	chr6	92842968	TGTAGTGCA
TIL-15	Mu12	chr6	109240327	ATCTAAAGT
TIL-15	Mu12	chr6	114703271	TGGAGAAGG
TIL-15	Mu12	chr6	121061537	GCGGTATGA
TIL-15	Mu12	chr6	146135776	CCAACGAAC
TIL-15	Mu12	chr6	164674718	AAGCCATCG
TIL-15	Mu12	chr6	164674726	ATCGGGGGC

TIL-15	Mu12	chr6	169241024	TCCCCACC
TIL-15	Mu12	chr7	95770434	CCAACGAAC
TIL-15	Mu12	chr7	113002964	CTTCGCATT
TIL-15	Mu12	chr7	126146334	CCGTTTTTTT
TIL-15	Mu12	chr7	126270335	AATAATTTA
TIL-15	Mu12	chr7	136322570	CGCGGAAGG
TIL-15	Mu12	chr7	144119874	GTGGGGGCC
TIL-15	Mu12	chr7	161229569	ATCTGTCAG
TIL-15	Mu12	chr7	167493431	AACATTAGA
TIL-15	Mu12	chr7	169729473	TCCATTTCC
TIL-15	Mu12	chr8	5414433	CTCGCGCGC
TIL-15	Mu12	chr8	8045837	CCGTTTTTTT
TIL-15	Mu12	chr8	17473053	AAAAAAACA
TIL-15	Mu12	chr8	55561241	TAAATTATT
TIL-15	Mu12	chr8	68787675	ACCAGAGAG
TIL-15	Mu12	chr8	104254931	GTTCGTTGG
TIL-15	Mu12	chr8	120021601	CGAGACGGC
TIL-15	Mu12	chr8	141273174	GTAGATTGG
TIL-15	Mu12	chr8	141274171	CTGATTGGG
TIL-15	Mu12	chr8	148887210	CCTGTTTGA
TIL-15	Mu12	chr8	158654007	CCAACGAAC
TIL-15	Mu12	chr8	162533913	AATAATTTA
TIL-15	Mu12	chr8	163197198	GGTCTGTGG
TIL-15	Mu12	chr9	7199139	CTTTTCTTG
TIL-15	Mu12	chr9	7509789	CATGTGAGT
TIL-15	Mu12	chr9	7509796	ACATGTGAG
TIL-15	Mu12	chr9	15061435	GCGAGCGTC
TIL-15	Mu12	chr9	16219735	CTGAACAGG
TIL-15	Mu12	chr9	37587573	CGTAGTGCA
TIL-15	Mu12	chr9	52218933	CCAACGAAC
TIL-15	Mu12	chr9	89417958	CCGTTTTTTT
TIL-15	Mu12	chr9	107612912	CAAAAAAAC
TIL-15	Mu12	chr9	112265159	AATAATTTA
TIL-15	Mu12	chr9	122725864	ACGCTCGCG
TIL-15	Mu12	chrUNKNOWN	1206141	GTTCGTTGG
TIL-15	Mu12	chrUNKNOWN	3949219	GTTCGTTGG
TIL-15	Mu12	chrUNKNOWN	4432770	GTTCGTTGG
TIL-15	Mu12	chrUNKNOWN	12783520	CAGTGCCG
TIL-15	Mu12	chrUNKNOWN	13989818	CCAACGAAC
TIL-17	Mu1-9	chr1	12908801	AGTGGTGTG
TIL-17	Mu1-9	chr1	12908809	AGTGGTGTG
TIL-17	Mu1-9	chr1	166720093	CTCTTTTTT
TIL-17	Mu1-9	chr1	192534615	CCAATTGGT

TIL-17	Mul-9	chr1	215947275	GTCGGCTGG
TIL-17	Mul-9	chr1	286507980	CTTCCCGTC
TIL-17	Mul-9	chr1	286507988	CTTCCCGTC
TIL-17	Mul-9	chr10	1528766	CATACCAAA
TIL-17	Mul-9	chr10	26092417	CTAGTTTTA
TIL-17	Mul-9	chr10	95816317	CCCTTGAT
TIL-17	Mul-9	chr2	170371447	TCATTTCCGG
TIL-17	Mul-9	chr2	222626068	AACTGCATA
TIL-17	Mul-9	chr2	222626073	AACTGCATA
TIL-17	Mul-9	chr3	17667046	ATATACTGG
TIL-17	Mul-9	chr3	17667054	ATATACTGG
TIL-17	Mul-9	chr3	156476232	GACACAGGT
TIL-17	Mul-9	chr3	162086773	GTCTATGTT
TIL-17	Mul-9	chr3	186538356	GTTGGAGGA
TIL-17	Mul-9	chr3	186538364	GTTGGAGGA
TIL-17	Mul-9	chr4	204148219	CCCCTTGGA
TIL-17	Mul-9	chr4	205456456	ATCGCTAGA
TIL-17	Mul-9	chr4	245028283	TTCTAAGGC
TIL-17	Mul-9	chr4	245262746	GGCGCAGCC
TIL-17	Mul-9	chr4	245262752	GGCGCAGCC
TIL-17	Mul-9	chr5	30710208	ATCGCTAGA
TIL-17	Mul-9	chr5	73645935	TCCGGTGGG
TIL-17	Mul-9	chr5	124607034	ACAGCCATT
TIL-17	Mul-9	chr5	211716624	ATTTTGC GA
TIL-17	Mul-9	chr5	215710584	CCTACCGAA
TIL-17	Mul-9	chr6	89452091	GTCGCCGAT
TIL-17	Mul-9	chr6	89452099	GTCGCCGAC
TIL-17	Mul-9	chr7	4969417	CCAGCCGAC
TIL-17	Mul-9	chr7	48473780	GCGGGAGAG
TIL-17	Mul-9	chr7	48474915	GCGGGAGAG
TIL-17	Mul-9	chr7	101032123	TCCAAGGGG
TIL-17	Mul-9	chr7	101032131	TCCAAGGGG
TIL-17	Mul-9	chr7	129476513	GGAGAGAAG
TIL-17	Mul-9	chr7	129476521	GGAGAGAAG
TIL-17	Mul-9	chr7	151077094	CACGCTCGC
TIL-17	Mul-9	chr7	151077102	CACGCTCGC
TIL-17	Mul-9	chr8	13135449	TCTAGCGAT
TIL-17	Mul-9	chr8	84671868	TGTGTGTTT
TIL-17	Mul-9	chr8	140606536	TTCTTGTTT
TIL-17	Mul-9	chr8	140606544	TTCTTGTTT
TIL-17	Mul-9	chr9	1964225	AACACACAC
TIL-17	Mul-9	chr9	86968542	ATCAAATCT
TIL-17	Mul-9	chr9	86968550	ATCAAATCT

TIL-17	Mu1-9	chr9	98364784	CTCCATGTT
TIL-17	Mu1-9	chr9	98364792	CTCCGTGTT
TIL-17	Mu1-9	chr9	119937508	GCGGGACGC
TIL-17	Mu1-9	chr9	119937512	GCGGGACGC
TIL-17	Mu1-9	chr9	134489929	TCCAAGGGG
TIL-17	Mu1-9	chr9	140075465	TTCTCAGCC
TIL-17	Mu1-9	chrUNKNOWN	1099618	AGACGGGAA
TIL-17	Mu1-9	chrUNKNOWN	2559941	TCTAGCGAT
TIL-17	Mu10	chr1	17669190	GTTTGTGCGC
TIL-17	Mu10	chr1	117819615	GGCTCCCGG
TIL-17	Mu10	chr1	248504111	CTGGCCGTG
TIL-17	Mu10	chr1	282667382	CTCGAAATG
TIL-17	Mu10	chr1	282712869	CATTTTCGAG
TIL-17	Mu10	chr10	24764948	CTTTTTTCT
TIL-17	Mu10	chr10	24764954	CTTTTTTCT
TIL-17	Mu10	chr10	26666847	GTTTATGAA
TIL-17	Mu10	chr10	26666849	TTTATGAAA
TIL17	Mu10	chr10	26765521	TTTATGAAA
TIL-17	Mu10	chr10	146725798	GCTCCCTGG
TIL-17	Mu10	chr2	199398880	GTTGTGTGG
TIL-17	Mu10	chr2	199398888	GTTGTGTGG
TIL-17	Mu10	chr3	21938454	ATCCACATC
TIL-17	Mu10	chr3	21938460	ATCCACATC
TIL-17	Mu10	chr4	39099270	TAGAGAGAA
TIL-17	Mu10	chr4	42133990	GTACAGCAC
TIL-17	Mu10	chr4	241703022	GGGTGAGAT
TIL-17	Mu10	chr5	14699797	CTCCCCAGC
TIL-17	Mu10	chr5	14699805	CTCCCCAGC
TIL-17	Mu10	chr5	23032174	ACCACCGGC
TIL-17	Mu10	chr5	23032182	ACCACCGGC
TIL-17	Mu10	chr5	100132261	CTCCCCAGC
TIL-17	Mu10	chr5	211716624	ATTTTGC GA
TIL-17	Mu10	chr5	211716631	CATTTT GAG
TIL-17	Mu10	chr6	128755403	GTACAGCAC
TIL-17	Mu10	chr7	48473773	CCGGGAGAG
TIL-17	Mu10	chr7	48474915	GCGGGAGAG
TIL17	Mu10	chr7	68128989	CACGGCCAG
TIL-17	Mu10	chr7	115146272	GCGTGGTGG
TIL-17	Mu10	chr8	38522071	TCCAGCCTC
TIL-17	Mu10	chr8	86898952	AGGCGACAG
TIL-17	Mu10	chr8	138362068	TTCTAGTTT
TIL-17	Mu12	chr1	10975143	CTCTCCTCG
TIL-17	Mu12	chr1	37644610	ACCAAATGG

TIL-17	Mu12	chr1	55607850	TGTGGTAAG
TIL-17	Mu12	chr1	55607855	TGTGGTAAG
TIL-17	Mu12	chr1	92449217	CCCGTAGCC
TIL-17	Mu12	chr1	153632582	GGCTACGGG
TIL-17	Mu12	chr1	166720101	CTCTTTTTT
TIL-17	Mu12	chr1	180238452	GGCTACGGG
TIL-17	Mu12	chr1	252512309	CCCGTAGCC
TIL-17	Mu12	chr1	255428941	GTTTCCCAA
TIL-17	Mu12	chr1	263848328	ATCGCCTCT
TIL-17	Mu12	chr1	299438326	CTGCTCTCC
TIL-17	Mu12	chr10	2848	GGCTACGGG
TIL-17	Mu12	chr10	1732767	GGCTACGGG
TIL-17	Mu12	chr10	3931832	CCCCTCTCC
TIL-17	Mu12	chr10	4001312	CCCTCTCCT
TIL-17	Mu12	chr10	5757837	CCCGTAGCC
TIL-17	Mu12	chr10	11711685	GGCTACGGG
TIL-17	Mu12	chr10	11776899	GGCTATGGG
TIL-17	Mu12	chr10	15300760	CTTGCAATG
TIL-17	Mu12	chr10	15308429	CTTGCAATG
TIL-17	Mu12	chr10	16208189	CTCGTCGGT
TIL-17	Mu12	chr10	17390707	CCCTTCTCTC
TIL-17	Mu12	chr10	17968533	GGCTACGGG
TIL-17	Mu12	chr10	23393883	GGCCACGGG
TIL-17	Mu12	chr10	24948354	CCCGTAGCC
TIL-17	Mu12	chr10	27092751	CCCGTAGCC
TIL-17	Mu12	chr10	30556629	CCGCTGCGC
TIL-17	Mu12	chr10	31269599	CTTACCACA
TIL-17	Mu12	chr10	31883694	CCCCTCTCT
TIL-17	Mu12	chr10	35473684	CGGCAGCCA
TIL-17	Mu12	chr10	35483010	ACGGCAGCC
TIL-17	Mu12	chr10	40595711	AATATGATG
TIL-17	Mu12	chr10	40595719	AATATGATG
TIL-17	Mu12	chr10	41262391	GGCTACGGG
TIL-17	Mu12	chr10	42227109	CCAGTAGCC
TIL-17	Mu12	chr10	44114838	GGAGGCGTC
TIL-17	Mu12	chr10	44491043	CCCGTAGCC
TIL-17	Mu12	chr10	45432395	CATCATATT
TIL-17	Mu12	chr10	57813012	GGCAGGGAT
TIL-17	Mu12	chr10	59359085	GGCTACGGG
TIL-17	Mu12	chr10	61467640	GAGGAATTG
TIL-17	Mu12	chr10	65410065	CCCGTAGCC
TIL-17	Mu12	chr10	68226252	CCCGTAGCC
TIL-17	Mu12	chr10	71749471	GGCTACGGG

TIL-17	Mu12	chr10	88193727	CCCGTAGCC
TIL-17	Mu12	chr10	93904468	GGCTACGGG
TIL-17	Mu12	chr10	98444777	CCCGTAGCC
TIL-17	Mu12	chr10	109818012	CCTCCCGTC
TIL-17	Mu12	chr10	116479548	CTCAGCATG
TIL-17	Mu12	chr10	116479556	CTCGGCATG
TIL-17	Mu12	chr10	123395285	GGCTACGGG
TIL-17	Mu12	chr10	133273075	CCCGTAGCC
TIL-17	Mu12	chr10	146557512	GGCTACGGG
TIL-17	Mu12	chr10	146557520	GGCTACGGG
TIL-17	Mu12	chr10	146586003	GGCTACGGG
TIL-17	Mu12	chr10	147129698	GACGGGAGG
TIL-17	Mu12	chr10	147129735	GACGGGAGG
TIL-17	Mu12	chr2	496212	CTCGGCATT
TIL-17	Mu12	chr2	1089430	TCCTTCCCC
TIL-17	Mu12	chr2	24581453	TCGGTTGCG
TIL-17	Mu12	chr2	25000044	GACCCTTTG
TIL-17	Mu12	chr2	37681407	GCACTAATG
TIL-17	Mu12	chr2	37869180	GGGCACGAG
TIL-17	Mu12	chr2	46312927	CCCGTAGCC
TIL-17	Mu12	chr2	63309331	GTGGATCTG
TIL-17	Mu12	chr2	65572626	GTCAGAGGC
TIL-17	Mu12	chr2	107385876	TCCTCTTCC
TIL-17	Mu12	chr2	107385884	TCCTCTTCC
TIL-17	Mu12	chr2	113503509	CTCGGCATG
TIL-17	Mu12	chr2	117876096	GGAAACAAG
TIL-17	Mu12	chr2	149547189	TCCATATGG
TIL-17	Mu12	chr2	149548163	TCCATATGG
TIL-17	Mu12	chr2	152204163	TGTAGTGCA
TIL-17	Mu12	chr2	166840850	TGCAGGGTG
TIL-17	Mu12	chr2	172205740	CAGCGGAGC
TIL-17	Mu12	chr2	197215141	TCGCGGGGC
TIL-17	Mu12	chr2	203293320	GGCTACGGG
TIL-17	Mu12	chr3	1763267	CGTGCGGTC
TIL-17	Mu12	chr3	1763275	CGTGCGGTC
TIL-17	Mu12	chr3	16026824	CCCGTAGCC
TIL-17	Mu12	chr3	16221042	GGCTACAGC
TIL-17	Mu12	chr3	21821458	CTACCCGTA
TIL-17	Mu12	chr3	36137635	GTTAAGGAG
TIL-17	Mu12	chr3	161858390	ACACTAGAC
TIL-17	Mu12	chr3	162086769	CGTCTATGT
TIL-17	Mu12	chr3	162086773	GTCTATGTT
TIL-17	Mu12	chr3	184864664	CTAGGCGAG

TIL-17	Mu12	chr3	184864672	CTAGGCGAG
TIL-17	Mu12	chr3	199343657	GGCTACGGG
TIL-17	Mu12	chr3	210661448	CCCGTAGCC
TIL-17	Mu12	chr4	11294640	GTCGAGCGG
TIL-17	Mu12	chr4	64300124	CTCGGCATG
TIL-17	Mu12	chr4	67680114	GTTTAGACT
TIL-17	Mu12	chr4	67680404	GTTTAGACT
TIL-17	Mu12	chr4	96634756	GGGCTCAAT
TIL-17	Mu12	chr4	113085139	AGCCTGAAG
TIL-17	Mu12	chr4	136075548	CCCCAACCC
TIL-17	Mu12	chr4	136075556	CCCCAACCC
TIL-17	Mu12	chr4	161135527	CTCGTCGGT
TIL-17	Mu12	chr4	161135535	CTCGTCGGT
TIL-17	Mu12	chr4	166495091	GTACATATG
TIL-17	Mu12	chr4	166547002	CATATGTAT
TIL-17	Mu12	chr4	168526003	GGTAATGCA
TIL-17	Mu12	chr4	168526011	GGTAATGCA
TIL-17	Mu12	chr4	182724996	CAGAAGGTC
TIL-17	Mu12	chr4	182724999	GTTTTTCAGA
TIL-17	Mu12	chr4	191316757	TGCACTACG
TIL-17	Mu12	chr4	200868607	CACGACAGC
TIL-17	Mu12	chr4	239406228	GTGAGTGAG
TIL-17	Mu12	chr5	8517544	CTGCTACTC
TIL-17	Mu12	chr5	26466383	AGCCTAGGA
TIL-17	Mu12	chr5	26838263	CGCGGGCGG
TIL-17	Mu12	chr5	42849194	AATATGATG
TIL-17	Mu12	chr5	42851585	AATATGATG
TIL-17	Mu12	chr5	64749197	TGTCGCACT
TIL-17	Mu12	chr5	132724116	CACCCTGAC
TIL-17	Mu12	chr5	167153492	CCAGAGGGA
TIL-17	Mu12	chr5	185027058	CAAACATTC
TIL-17	Mu12	chr5	185079405	GAATGTTTT
TIL-17	Mu12	chr5	191610797	AATGCAAGG
TIL-17	Mu12	chr5	207526903	CTATGCGGA
TIL-17	Mu12	chr5	214442521	GCTCGCGGG
TIL-17	Mu12	chr5	214578190	CTCCGCCGG
TIL-17	Mu12	chr6	2575151	GTTTTCCAA
TIL-17	Mu12	chr6	2917476	TCCATGATG
TIL-17	Mu12	chr6	13851597	GGCTACGGG
TIL-17	Mu12	chr6	13851605	GGATACGGG
TIL-17	Mu12	chr6	38435508	CCCGAGGCC
TIL-17	Mu12	chr6	53962988	ATGAAGACC
TIL-17	Mu12	chr6	55872875	ATCCCCGCC

TIL-17	Mu12	chr6	62418458	CATCATATT
TIL-17	Mu12	chr6	74383151	CCCTCTCCT
TIL-17	Mu12	chr6	77087974	AATATGATG
TIL-17	Mu12	chr6	78114239	CCCGTAGCC
TIL-17	Mu12	chr6	78155916	CCCGTAGCC
TIL-17	Mu12	chr6	89940991	GGCTACGGG
TIL-17	Mu12	chr6	92197928	CCTTGCAAG
TIL-17	Mu12	chr6	92842968	CGTAGTGCA
TIL-17	Mu12	chr6	99963634	GTGGATCTG
TIL-17	Mu12	chr6	100137700	CAGCTCAAT
TIL-17	Mu12	chr6	100137708	CAGCTCAAT
TIL-17	Mu12	chr6	106449118	CCCGTAGCC
TIL-17	Mu12	chr6	107182865	CCCGTAGCC
TIL-17	Mu12	chr6	109240325	GTAATGTGT
TIL-17	Mu12	chr6	109240327	ATCTAATGT
TIL-17	Mu12	chr6	110826082	GGCTACGGG
TIL-17	Mu12	chr6	143020500	GGAAGGGAT
TIL-17	Mu12	chr6	149531955	GAGTAGCAG
TIL-17	Mu12	chr6	157788113	CGCCCCGAT
TIL-17	Mu12	chr6	158541306	ATCTGCTCA
TIL-17	Mu12	chr6	166433210	CTTGCCATC
TIL-17	Mu12	chr6	169129268	CCCCCACCC
TIL-17	Mu12	chr6	169241025	CCCCCACCC
TIL-17	Mu12	chr7	15575142	TGAACAGGA
TIL-17	Mu12	chr7	15575481	TGAACAGGA
TIL-17	Mu12	chr7	29508617	CTCGGCATG
TIL-17	Mu12	chr7	29913742	GTCAAAGGT
TIL-17	Mu12	chr7	51499769	CTCGGCATG
TIL-17	Mu12	chr7	51751905	CATGCCGAG
TIL-17	Mu12	chr7	51751913	CATGCCGAG
TIL-17	Mu12	chr7	136322569	CCGCGGAAG
TIL-17	Mu12	chr7	144119874	GTGGGGCCA
TIL-17	Mu12	chr7	151005031	ACGGCAAGA
TIL-17	Mu12	chr7	161229569	ATCTGTCAG
TIL-17	Mu12	chr7	167493430	CAACATTAG
TIL-17	Mu12	chr7	167493438	CAACATTAG
TIL-17	Mu12	chr7	169668702	CTAAAAGAG
TIL-17	Mu12	chr7	169668703	ACTAAAAGA
TIL-17	Mu12	chr7	169729474	CCATTTCCA
TIL-17	Mu12	chr8	5414433	CTCGCGCGC
TIL-17	Mu12	chr8	8995040	TCCATTTCA
TIL-17	Mu12	chr8	37023109	CCCGTAGCC
TIL-17	Mu12	chr8	44535993	CCCGTAGCC

TIL-17	Mu12	chr8	66089811	CATCATATT
TIL-17	Mu12	chr8	92169214	CTCGGCATG
TIL-17	Mu12	chr8	109095975	GGCTACGGG
TIL-17	Mu12	chr8	120021601	CGAGACGGC
TIL-17	Mu12	chr9	7000884	CCCGTAGCC
TIL-17	Mu12	chr9	9497336	GCTACGGGG
TIL-17	Mu12	chr9	14452982	GGCTACGGG
TIL-17	Mu12	chr9	16219735	TGAACAGGA
TIL-17	Mu12	chr9	22666174	TCTCTCTCT
TIL-17	Mu12	chr9	30376224	GACGCCACG
TIL-17	Mu12	chr9	37204160	GGCTACGGG
TIL-17	Mu12	chr9	37587573	CGTAGTGCA
TIL-17	Mu12	chr9	40524602	CATCCCTGC
TIL-17	Mu12	chr9	52945708	CTCGGCACG
TIL-17	Mu12	chr9	62651198	ACTAAAAGA
TIL-17	Mu12	chr9	63431838	CCGCTCGAC
TIL-17	Mu12	chr9	74188523	CCGTAGCCT
TIL-17	Mu12	chr9	78735749	CTCGGCATG
TIL-17	Mu12	chr9	78735757	CTCGGCATG
TIL-17	Mu12	chr9	80678772	TCGGGGAGA
TIL-17	Mu12	chr9	85510106	CCCGTAGCC
TIL-17	Mu12	chr9	95994917	CCCGTAGCC
TIL-17	Mu12	chr9	98334525	GGCTACGGG
TIL-17	Mu12	chr9	115623561	GGCTACGGG
TIL-17	Mu12	chr9	120688928	CCCGTAGCC
TIL-17	Mu12	chr9	130377493	CTCTCTCTT
TIL-17	Mu12	chr9	139170075	GATCCCTGA
TIL-17	Mu12	chr9	140112790	GGCTACGGG
TIL-17	Mu12	chr9	146113969	TCCTGTTCA
TIL-17	Mu12	chr9	147125385	TCTCTCTCT
TIL-17	Mu12	chr9	147125393	TCTCTCTCT
TIL-17	Mu12	chrUNKNOWN	756223	GGCTATGGG
TIL-17	Mu12	chrUNKNOWN	833180	GGCTACGGG
TIL-17	Mu12	chrUNKNOWN	1239802	GGCTACGGG
TIL-17	Mu12	chrUNKNOWN	3164384	GGCTACGGG
TIL-17	Mu12	chrUNKNOWN	6262680	CTCGTAGCC
TIL-17	Mu12	chrUNKNOWN	6656498	ATTGAGCTC
TIL-17	Mu12	chrUNKNOWN	8287600	GGCTACGGG
TIL-17	Mu12	chrUNKNOWN	12184565	CCCGTAGCC
TIL-17	Mu12	chrUNKNOWN	12184573	CCCGTAGCC
TIL-17	Mu12	chrUNKNOWN	12783520	CAGTGGCCG

LIST OF REFERENCES

- Alleman M, Freeling M** (1986) The Mu transposable elements of maize: evidence for transposition and copy number regulation during development. *Genetics* **112**: 107-119
- Alonso JM, Stepanova AN, Leisse TJ, Kim CJ, Chen H, Shinn P, Stevenson DK, Zimmerman J, Barajas P, Cheuk R, et al.** (2003) Genome-wide insertional mutagenesis of *Arabidopsis thaliana*. *Science* **301**: 653-657
- Anderson CT, Carroll A, Akhmetova L, Somerville C** (2010) Real-time imaging of cellulose reorientation during cell wall expansion in *Arabidopsis* roots. *Plant Physiol* **152**: 787-796
- Arabidopsis Genome Initiative** (2000) Analysis of the genome sequence of the flowering plant *Arabidopsis thaliana*. *Nature* **14**: 796-815
- Arioli T, Peng L, Betzner AS, Burn J, Wittke W, Herth W, Camilleri C, Höfte H, Plazinski J, Birch R, et al.** (1998) Molecular analysis of cellulose biosynthesis in *Arabidopsis*. *Science* **279**: 717-720
- Bacic A, Stone BA** (1980) A (1→3)- and (1→4)-linked β -D-glucan in the endosperm cell walls of wheat. *Carbohydr Res* **82**: 372-387
- Backues SK, Konopka CA, McMichael CM, Bednarek SY** (2007) Bridging the divide between cytokinesis and cell expansion. *Curr Opin Plant Biol* **10**: 607-615
- Bai L, Singh M, Pitt L, Sweeney M, Brutnell TP** (2007) Generating novel allelic variation through Activator insertional mutagenesis in maize. *Genetics* **175**: 981-992
- Barker F, Thompson DV, Talbot DR, Swanson J, Bennetzen JL** (1984) Nucleotide sequence of the maize transposable element Mu1. *Nucleic Acids Res* **12**: 5955-5967
- Bednarek SY, Falbel TG** (2002) Membrane trafficking during plant cytokinesis. *Traffic* **3**: 621-629
- Bensen RJ, Johal GS, Crane VC, Tossberg JT, Schnable PS, Meely RB, Briggs SP** (1995) Cloning and characterization of the maize An1 gene. *Plant Cell* **7**: 75-84
- Bernal AJ, Jensen JK, Harholt J, Sørensen S, Møller I, Blaukopf C, Johansen B, de Lotto R, Pauly M, Schelle HV, et al.** (2007) Disruption of *ATCSLD5* results in reduced growth, reduced xylan and homogalacturonan synthase activity and altered xylan occurrence in *Arabidopsis*. *Plant J* **52**: 791-802
- Bernal AJ, Yoo C-M, Mutwil M, Jensen JK, Hou G, Blaukopf C, Sørensen S, Blancaflor EB, Scheller HV, Willats WGT** (2008) Functional analysis of the cellulose synthase-like genes *CSLD1*, *CSLD2*, and *CSLD4* in tip-growing *Arabidopsis* cells. *Plant Physiol* **148**: 1238-1253
- Bonetta DT, Facette M, Raab TK, Somerville CR** (2002) Genetic dissection of plant cell-wall biosynthesis. *Biochem Soc Tran* **30**: 298-301
- Brutnell TP** (2002) Transposon tagging in maize. *Funct Integr Genomics* **2**: 4-12
- Brutnell TP, Conrad LJ** (2003) Transposon tagging using Activator (Ac) in maize. *Methods Mol Biol* **23**: 157-176

- Buckeridge MS, Rayon C, Urbanowicz B, Tine MAS, Carpita N** (2004) Mixed linkage (1→3),(1→4)-β-D-Glucans of grasses. *Cereal Chem* **81**: 115-127
- Burton RA, Gibeaut DM, Bacic A, Findlay K, Roberts K, Hamilton A, Baulcombe DC, Fincher GB** (2000) Virus-induced silencing of a plant cellulose synthase gene. *Plant Cell* **12**: 691-705
- Burton RA, Shirley NJ, King BJ, Harvey AJ, Fincher GB** (2004) The Cesa gene family of barley. Quantitative analysis of transcripts reveals two groups of co-expressed genes. *Plant Physiol* **134**: 224-236
- Burton RA, Wilson SM, Hrmova M, Harvey AJ, Shirley NJ, Medhurst A, Stone BA, Newbigin EJ, Bacic A, Fincher GB** (2006) Cellulose Synthase-Like *Cs/F* genes mediate the synthesis of cell wall (1,3;1,4)-β-D-glucans. *Science* **311**: 1940-1942
- Campbell JA, Davies GH, Bulone V, Henrissat B** (1997) A classification of nucleotide-diphospho-sugar glycosyltransferases based on amino acid sequence similarities. *Biochem. J* **326**: 929-939
- Carpita NC** (1984) Cell wall development in maize coleoptiles. *Plant Physiol* **76**: 202-212
- Carpita NC, Gibeaut DM** (1993) Structural models of primary cell walls in flowering plants: consistency of molecular structure with the physical properties of walls during growth. *Plant J* **3**: 1-30.
- Carpita NC** (1996) Structure and biogenesis of the cell walls of grasses. *Annu Rev Plant Mol Biol* **47**: 445-476
- Carpita NC, Defernez M, Findlay K, Wells B, Shoue DA, Catchpole G, Wilson RH, McCann MC** (2001) Cell wall architecture of the elongating maize coleoptile. *Plant Physiol* **127**: 551-565
- Carpita NC, McCann M** (2002) The functions of cell wall polysaccharides in composition and architecture revealed through mutations. *Plant Soil* **247**: 71-80
- Carpita NC, McCann MC** (2008) Maize and sorghum: genetic resources for the bioenergy grasses. *Trends Plant Sci* **13**: 415-420
- Chaffey N, Barlow P** (2002) Myosin, microtubules, and microfilaments: co-operation between cytoskeletal components during cambial cell division and secondary vascular differentiation in trees. *Planta* **214**: 526-536
- Chandler VL, Hardeman KJ** (1992) The *Mu* elements of *Zea mays*. *Adv Genet* **30**: 77-122
- Chomet P, Lisch D, Hardeman DJ, Chandler VL, Freeling M** (1991) Identification of a regulatory transposon that controls the Mutator transposable element system in maize. *Genetics* **129**: 261-270
- Clancy M, Hannah LC** (2002) Splicing of the maize *Sh1* first intron is essential for enhancement on gene expression, and a T-rich motif increases expression without affecting splicing. *Plant Physiol* **130**: 918-929
- Cleary AL, Smith LG** (1998) The *Tangled1* gene is required for spatial control of cytoskeletal arrays associated with cell division during maize leaf development. *Plant Cell* **10**: 1875-1888

- Cocuron JC, Lerouxel O, Drakakaki G, Alonso AP, Leipman AH, Keegstra K, Raikhel N, Wilkerson CG** (2007) A gene from the cellulose synthase-like C family encodes a β -1,4 glucan synthase. *Proc Natl Acad Sci USA* **104**: 8550-8555
- Cole RA, Fowler JE** (2006) Polarized growth: maintaining focus on the tip. *Curr Opin Plant Biol* **9**: 579-588
- Cosgrove DJ** (2005) Growth of the plant cell wall. *Nat Rev Mol Cell Biol* **6**: 850-861
- Coutinho PM, Henrissat B** (1999) Carbohydrate-active enzymes server at URL: <http://afmb.cnrs-mrs.fr/CAZY/index.html>
- Coutinho PM, Stam M, Blanc E, and Henrissat B** (2003) Why are there so many carbohydrate-active enzyme-related genes in plants? *Trends Plant Sci* **8**: 563-565
- Cresse AD, Hulbert SH, Brown WE, Lucas JR, Bennetzen JL** (1995) Mu1-related transposable elements of maize preferentially insert into low copy number DNA. *Genetics* **140**: 315-324
- Crowell EF, Bischoff V, Desprez T, Rolland A, Stierhof Y-D, Scumacher K, Gonneau M, Hofte H, Vernhetes S** (2009) Pausing of Golgi bodies on microtubules regulates secretion of cellulose synthase complexes in Arabidopsis. *Plant Cell* **21**: 1141-1154
- Deeks MJ, Cyrckova F, Machesky LM, Mikitova V, Ketelaar T, Zarsky V, Davies B, Hussey PJ** (2005) Arabidopsis group Ie formins localize to specific cell membrane domains, interact with actin-binding proteins and cause defects in cell expansion upon aberrant expression. *New Phytol* **168**: 529-540
- Delmer DP, Stone BA** (1988) Biosynthesis of plant cell walls. In: Priess J (ed) *The biochemistry of plants*. Academic Press Inc., New York, pp 373–421
- Delmer DP** (1999) Cellulose biosynthesis: exciting times for a difficult field of study. *Annu Rev Plant Physiol Plant Mol Biol* **50**: 245-276
- Derbyshire P, Findlay K, McCann MC, Roberts K** (2007) Cell elongation in Arabidopsis hypocotyls involves dynamic changes in cell wall thickness. *J Exp Bot* **58**: 2079-2089
- Dhont S, Vanhaeren H, Van Loo D, Cnudde V, Inzé D** (2010) Plant structure visualization by high-resolution X-ray computed tomography. *Trends Plant Sci* **15**: 419-422
- Dhonukshe P, Baluška F, Schlicht M, Hlavacka A, Šamaj J, Friml J, Gadella WJ** (2006) Endocytosis of cell surface material mediates cell plate formation during plant cytokinesis. *Dev Cell* **10**: 137-150
- Dhugga KS, Barreiro R, Whitten B, Stecca K, Hazebroek J, Randhawa GS, Dolan M, Kinney AJ, Tomes D, Nichols S, Anderson P** (2004) Guar seed β -mannan synthase is a member of the cellulose synthase super gene family. *Science* **303**: 363-366
- Dietrich CR, Cui F, Packila ML, Li J, Ashlock DA, Nikolau BJ, Schnable PS** (2002) Maize Mu transposons are targeted to the 5' untranslated region of the *gl8* gene and sequences flanking Mu target-site duplications exhibit nonrandom nucleotide composition throughout the genome. *Genetics* **160**: 697-716

- Doblin MS, De Melis L, Newbigin E, Bacic A, Read SM** (2001) Pollen tubes of *Nicotiana glauca* express two genes from different β -glucan synthase families. *Plant Physiol* **125**: 2040-2052
- Doblin MS, Pettolino FA, Wilson SM, Campbell R, Burton RA, Fincher GB, Newbigin E, Bacic A** (2009) A barley *cellulose synthase-like CSLH* gene mediates (1,3;1,4)- β -D-glucan synthesis in transgenic *Arabidopsis*. *Proc Natl Acad Sci USA* **106**: 5996-6001
- Doebley J** (2004) The genetics of maize evolution. *Annu Rev Genet* **38**: 37-59
- Duvick DN** (2005) The contribution of breeding to yield advances in maize (*Zea mays* L.). *Adv Agron* **86**: 83-145
- Edwards M, Dea ICM, Bulpin PV, Reid JSG** (1985) Xyloglucan (amyloid) mobilization in the cotyledons of *Topaeolum-majus* L seeds following germination. *Planta* **163**: 133-140
- Eveland AL, McCarty DR, Koch KE** (2008) Transcript profiling by 3'-untranslated region sequencing resolves expression of gene families. *Plant Physiol* **146**: 32-44
- Farrokhi N, Burton RA, Brownfield L, Hrmova M, Wilson SM, Bacic A, Fincher GB** (2006) Plant cell wall biosynthesis: genetic, biochemical and functional genomics approaches to the identification of key genes. *Plant Biotech J* **4**: 145-167
- Favery B, Ryan E, Foreman J, Linstead P, Boudonck K, Steer M, Shaw P, Dolan L** (2001) KOJAK encodes a cellulose synthase-like protein required for root hair cell morphogenesis in *Arabidopsis*. *Genes Dev* **15**: 79-87
- Fernandes J, Dong QF, Schneider B, Morrow DJ, Nan GL, Brendel V, Walbot V** (2004) Genome-wide mutagenesis of *Zea mays* L. using RescueMu transposons. *Genome Biol* **5**: R82
- Fincher GB** (2009) Revolutionary times in our understanding of cell wall biosynthesis and remodeling in the grasses. *Plant Physiol* **149**: 27-37
- Fukunaga K, Hill J, Vigouroux Y, Matsuoka Y, Sanchez JG, Liu K, Buckler ES, Doebley J** (2005) Genetic diversity and population structure of teosinte. *Genetics* **169**: 2241-2254
- František B, Salaj J, Mathur J, Braun M, Jasper F, Šamaj J, Chua N-H, Barlow W, Volkman D** (2000) Root hair formation: F-actin-dependent tip growth is initiated by local assembly of profiling-supported F-actin meshworks accumulated within expansin-enriched bulges. *Dev Biol* **227**: 618-632
- Gallagher K, Smith LG** (1999) Discordia mutations specifically misorient asymmetric cell divisions during development of the maize leaf epidermis. *Development* **126**: 4623-4633
- Hershberger RJ, Warren CA, Walbot V** (1991) Mutator activity in maize correlates with the presence and expression of the Mu transposable element Mu9. *Proc Natl Acad Sci USA* **88**: 10198-10202

- Hildebrand T, Ruesegger P** (1997) A new method for the model-independent assessment of thickness in three-dimensional images. *J Microsc* **185**: 67-75
- Holland N, Holland D, Helentjaris T, Dhugga K, Xoconostle-Cazares B, Delmer DP** (2000) A comparative analysis of the plant cellulose synthase (*CesA*) gene family. *Plant Physiol* **123**: 1313-1323
- Hong Z, Delauney AJ, Verma DPS** (2001) A cell plate-specific callose synthase and its interaction with phragmoplastin. *Plant Cell* **13**: 755-768
- Ilyama K, Lam TBT, Stone BA** (1990) Phenolic acid bridges between polysaccharides and lignin. *Phytochemistry* **29**: 733-737
- Ingouff M, Fitz Gerald JN, Guerin C, Robert H, Sorensen MB, Van Damme D, Geelen D, Blanchoin L, Berger F** (2005) Plant formin AtFH5 is an evolutionarily conserved actin nucleator involved in cytokinesis. *Nat Cell Biol* **7**: 374-380
- International Human Genome Sequencing Consortium, Lander ES, Linton LM, Birren B, Nusbaum C, Zody MC, Baldwin J, Devon K, Dewar K, Doyle M, et al.** (2001) Initial sequencing and analysis of the human genome. *Nature* **409**: 860-921
- Jarvis MC, Forsyth W, Duncan HJ** (1988) A survey of the pectic content of nonlignified monocot cell walls. *Plant Physiol* **88**: 309-314
- Jarvis MC** (1994) Structure and properties of pectin gels in plant cell walls. *Plant Cell Environ* **7**: 153-164
- Jeong YM, Mun JH, Kim H, Lee SY, Kim SG** (2007) An upstream region in the first intron of petunia actin-depolymerizing factor 1 affects tissue-specific expression in transgenic *Arabidopsis thaliana*. *Plant J* **50**: 230-239
- Jin SY, Chen HZ** (2007) Near-infrared analysis of the chemical composition of rice straw. *Indust Crops Prod* **26**: 207-211
- Jung HG, Casler MD** (2006) Maize stem tissues: impact of development on cell wall degradability. *Crop Sci* **46**: 1801-1809
- Keegstra K, Walton J** (2006) Plant science: β -glucans – brewer's bane, dietician's delight. *Science* **311**: 1872-1873
- Kidwell MG, Lisch DR** (2000) Transposable elements and host genome evolution. *Trends Ecol Evol* **15**: 95-99
- Kim CM, Park SH, Je BI, Park SH, Park SJ, Piao, HL, Eun MY, Dolan L, Han C-D** (2007) *OsCSLD1*, a cellulose synthase-like D1 gene, is required for root hair morphogenesis in rice. *Plant Physiol* **143**: 1220-1230
- Kim JB, Olek AT, Carpita NC** (2000) Plasma membrane and cell wall exo-B-D glucanases in developing maize coleoptiles. *Plant Physiol*. **123**: 471-485
- Kimura S, Laosinchai W, Itoh T, Cui X, Linder CR, Brown RM** (1999) Immunogold labeling of rosette terminal cellulose-synthesizing complexes in the vascular plant *Vigna angularis*. *Plant Cell* **11**: 2075-2085

- Kolkman JM, Conrad LJ, Farmer PR, Hardeman K, Ahern KR, Lewis PE, Sawers RJH, Lebejko S, Chomet P, Brutnell TP** (2005) Distribution of Activator (Ac) throughout the maize genome for use in regional mutagenesis. *Genetics* **169**: 981-995
- Kurek I, Kawagoe Y, Jacob-Wilk D, Doblin M, Delmer D** (2002) Dimerization of cotton fiber cellulose synthase catalytic subunits occurs via oxidation of the zinc-binding domains. *Proc Natl Acad Sci USA* **99**: 11109–11114
- Larkin MA, Blackshields G, Brown NP, Chenna R, McGettigan PA, McWilliam H, Valentin F, Wallace IM, Wilm A, Lopez R, et al.** (2007) Clustal W and Clustal X version 2.0. *Bioinformatics* **23**: 2947-2948
- Lee M, Sharopova N, Beavis WD, Grant D, Katt M, Blair DL, Hallauer AR** (2002) Expanding the genetic map of maize with the intermated B73 x Mo17 (IBM) population. *Plant Mol Biol* **48**: 453-461
- Letunic I, Doerks T, Bork P** (2009) SMART 6: recent updates and new developments. *Nucleic Acids Res (Database issue)*: D229-232
- Li M, Xiong G, Li R, Cui J, Tang D, Zhang B, Pauly M, Cheng Z, Zhou Y** (2009) Rice cellulose synthase-like D4 is essential for normal cell-wall biosynthesis and plant growth. *Plant J* **60**: 1055-1069
- Liepman AH, Wilkerson C, Keegstra K** (2005). Expression of cellulose synthase-like (Csl) genes in insect cells reveals that Csl/A family members encode mannan synthases. *Proc Natl Acad Sci USA* **102**: 2221-2226
- Lippman ZB, Zamir D** (2007) Heterosis: revisiting the magic. *Trends Genet* **23**: 60-66
- Lisch D, Chomet P, Freeling M** (1995) Genetic characterization of the Mutator system in maize: behavior and regulation of Mu transposons in a minimal line. *Genetics* **139**: 1777-1796
- Lisch D** (2002) Mutator transposons. *Trends Plant Sci* **7**: 498-504
- Liu S, Yeh C-T, Ji T, Ying K, Wu H, Tan HM, Fu Y, Nettleton D, Schnable PS** (2009) Mu transposon insertion sites and meiotic recombination events co-localize with epigenetic marks for open chromatin across the maize genome. *PLoS Genetics* (10.1371/journal.pgen.1000733)
- Lukowitz W, Mayer U, Jürgens G** (1996) Cytokinesis in the Arabidopsis embryo involves the syntaxin-related KNOLLE gene product. *Cell* **84**: 61-71
- Mohanty A, Luo A, DeBlasio S, Ling, X, Yang Y, Tuthill DE, Williams KE, Hill D, Zadrozny T, Chan A, Sylvester AW, Jackson D** (2009) Advancing cell biology and functional genomics in maize using fluorescent protein-tagged lines. *Plant Physiol* **149**: 601-605
- Lynch MA, Staehelin LA** (1995) Immunocytochemical localization of cell-wall polysaccharides in the root-tip of *Avena sativa*. *Protoplasma* **188**: 115-127
- Lynd LR, Wyman CE, Gerngross TU** (1999) Biocommodity engineering. *Biotechnol Prog* **15**: 777-793

- Margulies M, Egholm M, Altman WE, Attiya S, Bader JS, Bemben LA, Berka J, Baverman MS, Chen YJ, Chen Z, et al.** (2005) Genome sequencing in microfabricated high-density picolitre reactors. *Nature* **437**: 376-380
- Matsuoka Y, Vigouroux Y, Goodman MM, Sanchez JG, Buckler E, Doebley J** (2002) A single domestication for maize shown by multilocus microsatellite genotyping. *Proc Natl Acad Sci USA* **99**: 6080-6084
- May BP, Liu H, Vollbrecht E, Senior L, Rabinowicz PD, Roh D, Pan X, Stein L, Freeling M, Alexander D, Mertienssen R** (2003) Maize-targeted mutagenesis: a knockout resource for maize. *Proc Natl Acad Sci USA* **101**: 14349-14354
- McCann MC, Wells B, Roberts K** (1990) Direct visualization of the crosslinks in the primary cell wall. *J Cell Sci* **96**: 323-334
- McCann MC, Roberts K** (1991) Architecture of the primary cell wall. In *The Cytoskeletal Basis of Plant Growth and Form*. C.W. Lloyd, ed. Academic Press: London. pgs. 109-129
- McCann MC, Roberts K** (1994) Changes in cell wall architecture during cell elongation. *J Exp Bot* **45**: 1683-1691
- Manfield IW, Orfila C, McCartney L, Harholt J, Bernal AJ, Scheller HV, Gilmartin PM, Mikkelsen JD, Knox JP, Willats WGT** (2004) Novel cell wall architecture of isoxaben-habituated *Arabidopsis* suspension-cultured cells: global transcript profiling and cellular analysis. *Plant Journal* **40**: 260-275
- McCarty DR, Carson CB, Stinard PS, Robertson DS** (1989) Molecular analysis of viviparous-1: an abscisic acid-insensitive mutant of maize. *Plant Cell* **1**: 523-532
- McCarty DR, Settles AM, Suzuki M, Tan BC, Latshaw S, Porch T, Robin K, Baier J, Avigne W, Lai J, et al.** (2005) Steady-state transposon mutagenesis in inbred maize. *Plant J* **44**: 52-61
- McCarty DR, Meeley RB** (2009) Transposon Resources for forward and reverse genetics in maize. In JL Bennetzen, S Hake, eds, *Handbook of Maize*. Springer, New York, pp 561-584
- McClintock B** (1947) Chromosome organization and gene expression. *Cold Spring Harb Symp Quant Biol* **16**: 13-47
- Meeley RB, Briggs SP** (1995) Reverse genetics for maize. *Maize Genet Coop Newsl* **69**: 67-82
- Meier H, Reid JSG** (1982) Reverse polysaccharides other than starch in higher plants. In *Encyclopedia of Plant Physiology*, Vol. 13. A.F.A. Loewu W. Tanner, eds. Springer-Verlag: Berlin. pgs. 418-471
- Mellerowicz EJ, Baucher M, Sundberg B, Boerjan W** (2001) Unravelling cell wall formation in the woody dictyo stem. *Plant Mol Biol* **47**: 239-274
- Miyata T, Yasunaga T, Nishida T** (1980) Nucleotide sequence divergence and functional constraint in mRNA evolution. *Proc Natl Acad Sci USA* **77**: 7328-7332
- Molchan TM, Valster AH, Hepler PK** (2002) Actomyosin promotes cell plate alignment and late lateral expansion in *Tradescantia* stamen hair cells. *Planta* **214**: 683-693

- Molendijk AJ, Bischoff F, Rajendrakumar CS, Friml J, Braun M, Gilroy S, Palme K** (2001) *Arabidopsis thaliana* Rop GTPases are localized to tips of root hairs and control polar growth EMBO J **20**: 2779-2788
- Moullia B** (2000) Leaves as shell structures: double curvature, auto-stresses, and minimal mechanical energy constraints on leaf rolling in grasses. J Plant Growth Regul **19**: 19-30
- Mueller SC, Brown RM** (1980) Evidence for an intramembrane component associated with a cellulose microfibril-synthesizing complex in higher plants. J Cell Biol **84**: 315-326
- Nairn CJ, Haselkorn T** (2005) Three loblolly pine *CesA* genes expressed in developing xylem are orthologous to secondary cell wall *CesA* genes of angiosperms. New Phytol **166**: 907-915
- Nam J, Mysore KS, Zheng C, Knue MK, Matthysse AG, Gelvin SB** (1999) Identification of T-DNA tagged *Arabidopsis* mutants that are resistant to transformation by *Agrobacterium* Mol Gen Genet **261**: 429-438
- Natera SHA, Ford KL, Cassin AM, Patterson JH, Newbigin EJ, Bacic A** (2008) Analysis of the *Oryza sativa* plasma membrane proteome using combined protein and peptide fractionation approaches in conjunction with mass spectrometry. Proteome Res **7**: 1159-1187
- Nemeth C, Freeman J, Jones HD, Sparks C, Pellny TK, Wilkinson MD, Dunwell J, Anderson AM, Aman A, Guillon F, et al.** (2010) Down-regulation of the CSLF6 gene results in decreased (1,3;1,4)- β -D-glucan in endosperm of wheat. Plant Physiol **152**: 1209-1218
- Okamoto H, Hirochika H** (2001) Silencing of transposable elements in plants. Trends Plant Sci **6**: 527-534
- Orfila C, Sorensen SO, Harholt J, Geshi N, Crombie H, Truong HN, Reid JS, Knox JP, Scheller HV** (2005) *QUASIMODO1* is expressed in vascular tissue of *Arabidopsis thaliana* inflorescence stems, and affects homogalacturonan and xylan biosynthesis. Planta **222**: 613-622
- Park S, Baker JO, Himmel ME, Parillaz PA, Johnson DK** (2010) Cellulose crystallinity index: measurement techniques and their impact on interpreting cellulose performance. Biotech Biofuels **3**: 10
- Pauly M, Keegstra K** (2008) Cell-wall carbohydrates and their modification as a resource for biofuels. Plant J **54**: 559-568
- Pear JR, Kawagoe Y, Schreckengost WE, Delmer DP, Stalker DM** (1996) Higher plants contain homologs of the bacterial *celA* genes encoding the catalytic subunit of cellulose synthase. Proc Natl Acad Sci USA **93**: 12637-12642
- Penning BW, Hunter CT III, Tayengwa R, Eveland AL, Dugard CK, Olek AT, Vermerris W, Koch KE, McCarty DR, Davis MF, et al.** (2009) Genetic resources for maize cell wall biology. Plant Physiol **151**: 1-29
- Persson S, Caffall KH, Freshour G, Hilley MT, Bauer S, Poindexter P, Hahn MG, Hohnen D, Somerville C** (2007) The *Arabidopsis irregular xylem8* mutant is

- deficient in glucuronoxylan and homogalacturonan, which are essential for secondary cell wall integrity. *Plant Cell* **19**: 237-255
- Peterson RL, Farquhar ML** (1996) Root hairs: specialized tubular cells extending root surfaces. *Bot Rev* **62**: 1-40
- Pilling E, Höfte H** (2003) Feedback from the wall. *Curr Opin Plant Biol* **6**: 611-616
- Popper ZA, and Fry SC** (2003) Primary cell wall composition of bryophytes and charophytes. *Annals Botany* **91**: 1-12
- Raizada MN, Walbot V** (2000) The late developmental pattern of Mu transposon excision is conferred by a cauliflower mosaic virus 35S-driven MURA cDNA in transgenic maize. *Plant Cell* **12**: 5-22
- Ragauskas AJ, Williams CK, Davison BH, Britovsek G, Cairney J, Eckert CA, Frederick WJ, Hallet JP, Leak DJ, Liotta CL, et al.** (2006) The path forward for biofuels and biomaterials. *Science* **311**: 484-489
- Rebollo R, Horard B, Hubert B, Vieira C** (2010) Jumping genes and epigenetics: Towards new species. *Gene* **454**: 1-7
- Redgwell RJ, Selvendran RR** (1986) Structural features of cell-wall polysaccharides in onion *Allium cepa*. *Carbohydr Res* **157**: 183-199
- Reid JSG** (1993) Seed storage polysaccharides: models for the study of cell wall matrix biosynthesis and turnover. *J Cell Biochem Suppl* **17**: 9-15
- Reiter W-D** (2002) Biosynthesis and properties of the plant cell wall. *Curr Opin Plant Biol* **5**: 536-42
- Reynolds JO, Eisses JF, Sylvester AW** (1998) Balancing division and expansion during maize leaf morphogenesis: analysis of the mutant, *warty-1*. *Dev* **125**: 259-268
- Richmond T** (2000) Higher plant cellulose synthases. *Genome Biol* **1**: reviews3001.1-reviews3001.6
- Richmond TA, Somerville CR** (2000) The cellulose synthase superfamily. *Plant Physiol* **124**: 495-498
- Richmond TA, Somerville CR** (2001) Integrative approaches to determining Csl function. *Plant Mol Biol* **47**: 131-143
- Roberts AW, Bushoven JT** (2007) The cellulose synthase (*CESA*) gene superfamily of the moss *Physcomitrella patens*. *Plant Mol Biol* **63**: 207-219
- Robertson DS** (1978) Characterization of a mutator system in maize. *Mut Res* **51**: 21-28
- Rose AB, Elfersi T, Parra G, Korf I** (2008) Promoter-proximal introns in *Arabidopsis thaliana* are enriched in dispersed signals that elevate gene expression. *Plant Cell* **20**: 543-551
- Rudall PJ, Caddick LR** (1994) Investigation of the presence of phenolic compounds in monocotyledonous cell walls, using UV fluorescence microscopy. *Ann Bot* **74**: 483-491

- Sabba RP, Vaughn KC** (1999) Herbicides that inhibit cellulose biosynthesis. *Weed Sci* **47**: 757-763
- Samuels AL, Giddings TH, Staehelin LA** (1995) Cytokinesis in tobacco BY-2 and root tip cells: a new model of cell plate formation in higher plants. *J Cell Biol* **130**: 1345-1357
- Samuga A, Joshi CP** (2004) Cloning and characterization of cellulose synthase-like gene, PtCSLD2 from developing xylem of aspen trees. *Physiol Plant* **120**: 631-641
- Sandhu AP, Randhawa GS, Dhugga KS** (2009) Plant cell wall matrix polysaccharide biosynthesis. *Mol Plant* **2**: 840-850
- Saxena IM, Brown RM, Fevre M, Geremia RA, Henrissat B** (1995) Multidomain architecture of β -glycosyl transferases: implications for mechanism of action. *J Bacteriol* **177**: 1419-1424
- Schnable P, Peterson PA, Saedler H** (1989) The *bz-rcy* allele of the Cy transposable element system of *Zea mays* contains a Mu-like element insertion. *Mol Gen Genet* **217**: 459-463
- Schnable PS, Ware D, Fulton RS, Stein JC, Wei F, Pasternak S, Liang C, Zhang J, Fulton L, Graves TA, et al.** (2009) The B73 maize genome: complexity, diversity, and dynamics. *Science* **326**: 1112-1115
- Scheible W-R, Pauly M** (2004) Glycosyltransferases and cell wall biosynthesis: novel players and insights. *Curr Opin Plant Biol* **7**:285-95
- Schubert C** (2006) Can biofuels finally take center stage? *Nat Biotech* **24**: 777-784
- Schultz J, Milpetz F, Bork P, Ponting CP** (1998) SMART, a simple modular architecture research tool: identification of signaling domains. *Proc Natl Acad Sci USA* **95**: 5857-5864
- Settles AM, Latshaw S, McCarty DR** (2004) Molecular analysis of high-copy insertion sites in maize. *Nucleic Acids Res* **32**: e54
- Settles AM, Holding DR, Tan BC, Latshaw SP, Liu J, Suzuki M, Li L, O'Brien BA, Fajardo DS, Wroclawska E, et al.** (2007) Sequence-indexed mutations in maize using the UniformMu transposon-tagging population. *BMC Genomics* **8**: 116
- Shapiro J** (1979) Molecular model for the transposition and replication of bacteriophage Mu and other transposable elements. *Proc Natl Acad Sci USA* **76**: 1933-1937
- Slotkin RK, Freeling M, Lisch D** (2003) Mu killer causes the heritable inactivation of the Mutator family of transposable elements in *Zea mays*. *Genetics* **165**: 781-797
- Smith AM, Heisler LE, St. Onge RP, Farias-Hesson E, Wallace IM, Bodeau J, Harris AN, Perry KM, Giaever G, Pourmand N, Nislow C** (2010) Highly-multiplexed barcode sequencing: an efficient method for parallel analysis of pooled samples. *Nuc Acids Res* **38**: e142
- Smith BG, Harris PJ** (1999) The polysaccharide composition of Poales cell walls: Poaceae cell walls are not unique. *Biochem System Ecol* **27**: 33-53

- Smith LG, Hake S, Sylvester AW** (1996) The *tangled-1* mutation alters cell division orientations throughout maize leaf development without altering leaf shape. *Development* **122**: 481-489
- Smith LG, Gerttula SM, Han S, Levy J** (2001) TANGLED1: a microtubule binding protein required for the spatial control of cytokinesis in maize. *J Cell Biol* **152**: 231-236
- Somerville C** (2006) Cellulose synthesis in higher plants. *Annu Rev Cell Dev Biol* **22**: 53-78
- Spitzer C, Schellmann S, Sabovljevic A, Shahriari M, Keshavaiah C, Bechtold N, Herzog M, Müller S, Hanisch F-G, Hülskamp M** (2006) The Arabidopsis *elc* mutant reveals functions of an ESCRT component in cytokinesis. *Development* **133**: 4679-4689
- Springer NM, Stupar RM** (2007) Allelic variation and heterosis in maize: How do two halves make more than a whole? *Genome Res* **17**: 264-275
- Springer NM, Ying K, Fu Y, Ji T, Yeh C-T, Jia Y, Wu W, Richmond T, Kitzman J, Rosenbaum H, et al.** (2009) Maize inbreds exhibit high levels of copy number variation (CNV) and presence/absence variation (PAV) in genome content. *PLoS Genetics* (10.1371/journal.pgen.1000734)
- Staehein LA, Hepler PK** (1996) Cytokinesis in higher plants. *Cell* **84**: 821-824
- Steppe K, Cnudde V, Girard C, Lemeur R, Cnudde J-P, Jacobs P** (2004) Use of X-ray computed microtomography for non-invasive determination of wood anatomical characteristics. *J Struct Biol* **148**: 11-21
- Sticklen MB** (2008) Plant genetic engineering for biofuel production: towards affordable cellulosic ethanol. *Nat Rev Gen* **9**: 433-443
- Sun JX, Sun XF, Zhao H, Sun RC** (2004) Isolation and characterization of cellulose from sugarcane bagasse. *Polymer Degradation and Stability* **84**: 331-339
- Suzuki S, Li Laigeng L, Sun Y-H, Chiang VL** (2006) The cellulose synthase gene superfamily and biochemical functions of xylem-specific cellulose synthase-like genes in *Populus trichocarpa*. *Plant Physiol* **142**: 1233-1245
- Sylvester AW, Cande WZ, Freeling M** (1990) Division and differentiation during normal and *liguleless-1* maize leaf development. *Development* **110**: 985-1000
- Sylvester AW** (2000) Division decisions and the spatial regulation of cytokinesis. *Curr Opin Plant Biol* **3**: 58-66
- Szymanski DB** (2009) Plant cells taking shape: new insights into cytoplasmic control. *Curr Opin Plant Biol* **12**: 735-744
- Szymanski DB, Cosgrove DJ** (2009) Dynamic coordination of cytoskeletal and cell wall systems during plant cell morphogenesis. *Curr Biol* **19**: R800-R811
- Takeda T, Furuta Y, Awano T, Mizuno K, Mitsuishi Y, Hayashi T** (2002) Supresión and acceleration of cell elongation by integration of xyloglucans in pea stem segments. *Proc Nat Acad Sci USA* **99**: 9055-90660

- Tamura K, Dudley J, Nei M, Kumar S** (2007) MEGA4: molecular evolutionary genetics analysis (MEGA) software version 4.0. *Mol Biol Evol* **24**: 1596-1599
- Van Erp H, Walton JD** (2009) Regulation of the cellulose synthase-like gene family by light in the maize mesocotyl. *Planta* **229**: 885-897
- Vogel J** (2008) Unique aspects of the grass cell wall. *Curr Opin Plant Biol* **11**: 301-307
- Vollbrecht E, Duvick J, Schares JP, Ahern KR, Deewatthanawong P, Xu L, Conrad LJ, Kikuchi K, Kubinec TA, Hall BD, et al.** (2010) Genome-wide distribution of transposed Dissociation elements in maize. *Plant Cell* **22**: 1667-1685
- Walbot V** (2000) Saturation mutagenesis using maize transposons. *Curr Opin Plant Biol* **3**: 103-107
- Walker KL, Smith LG** (2002) Investigation of the role of cell-cell interactions in division plane determination during maize leaf development through mosaic analysis of the *tangled* mutation. *Development* **129**: 3219-3226
- Wang X, Cnops G, Vanderhaeghen R, De Block S, Van Montagu M, Van Lijsebettens M** (2001) *AtCSLD3*, a cellulose synthase-like gene important for root hair growth in Arabidopsis. *Plant Physiol* **126**: 575-586
- Wei F, Coe E, Nelson W, Bharti AK, Engler F, Butler E, Kim HR, Goicoechea LJ, Mingsheng C, Seunghye L, et al.** (2007) Physical and genetic structure of the maize genome reflects its complex evolutionary history. *PLoS Genetics* (10.1371/journal.pgen.0030123)
- Weil CF, Monde R-A** (2007) Getting the point - mutations in maize. *Crop Sci* **47**: S60-S67
- Wessler SR** (2001) Plant transposable elements: a hard act to follow. *Plant Physiol* **125**: 149-151
- Willats WGT, McCartney L, Mackie W, Knox PJ** (2001) Pectin: cell biology and prospects for functional analysis. *Plant Mol Biol* **47**: 9-23
- Wilson SM, Burton RA, Doblin MS, Stone BA, Newbignin EJ, Fincher GB, Bacic A** (2006) Temporal and spatial appearance of wall polysaccharides during cellularization of barley (*Hordeum vulgare*) endosperm. *Planta* **224**: 655-667
- Xu J, Scheres B** (2005) Cell polarity: ROPing the ends together. *Curr Opin Plant Biol* **8**: 613-618
- Yin Y, Huang J, Xu Y** (2009) The cellulose synthase superfamily in fully sequenced plants and algae. *BMC Plant Biol* **9**: 99
- Yong W, Link B, O'Malley R, Tewari J, Hunter CT, Lu C-A, Li X, Bleeker AB, Koch KE, McCann MC, et al.** (2005) Genomics of plant cell wall biogenesis. *Planta* **221**: 747-751
- Yu J, Hu S, Wang J, Wong GK-S, Li S, Liu B, Deng Y, Dai L, Zhou Y, Zhang X, et al.** (2002) A draft sequence of the rice genome (*Oryza sativa* L. ssp. *indica*). *Science* **296**: 79-92

- Yu JM, Holland JB, McMullen MD, Buckler ES** (2008) Genetic design and statistical power of nested association mapping in maize. *Genetics* **178**: 539-551
- Zeng W, Keegstra K** (2008) *AtCSLD2* is an integral Golgi membrane protein with its N-terminus facing the cytosol. *Planta* **228**: 823-838
- Zhang B, Deng L, Qian Q, Xiong G, Zeng D, Li R, Guo L, Li J, Zhou Y** (2009) A missense mutation in the transmembrane domain of *CESA4* affects protein abundance in the plasma membrane and results in abnormal cell wall biosynthesis in rice. *Plant Mol Biol* **71**: 509-524
- Zhong R, Ye Z-H** (2007) Regulation of cell wall biosynthesis. *Curr Opin Plant Biol* **10**: 564-572
- Zhu YM, Nam J, Humara JM, Mysore KS, Lee LY, Cao H, Valentine L, Li J, Kaiser AD, Kopecky AL, et al.** (2003) Identification of *Arabidopsis* rat mutants. *Plant Physiol* **132**: 494-505

BIOGRAPHICAL SKETCH

Charles (Chip) Hunter grew up in Panama City, Florida before moving to Gainesville to attend the University of Florida, as both an undergraduate and graduate student. He majored in microbiology and cell science, and minored in plant molecular and cellular biology in the College of Agriculture and Life Sciences. He graduated Cum Laude, and joined the Plant Molecular and Cellular Biology program as a doctoral student in 2004. He was awarded the prestigious American Society of Plant Biology-Pioneer Hi-Bred International Graduate Student Prize in 2008 for conducting the most agriculturally-relevant graduate research in the United States. He has conducted research under the guidance of Dr. Karen Koch in the Department of Horticultural Sciences, where his experiments have focused on establishing roles for cell wall biosynthetic enzymes in maize, identifying related maize mutants, and in testing contributions by Mu transposable elements to diversity in maize and its wild ancestor teosinte.